

Aus der Medizinische Klinik und Poliklinik I
Klinikum der Ludwig-Maximilians-Universität München



Dissertation

zum Erwerb des Doctor of Philosophy (Ph.D.)

an der Medizinischen Fakultät der

Ludwig-Maximilians-Universität München

***Investigating Neutrophil-driven Thrombopoiesis in
Cardiovascular/Inflammatory Diseases: Intermittent Hypoxia and
Myocardial Infarction***

vorgelegt von:
Shaza El Nemr

aus:
Nahle / Libanon

Jahr:
2024

Mit Genehmigung der Medizinischen Fakultät der
Ludwig-Maximilians-Universität München

Erstes Gutachten von: Priv. Doz. Dr. Tobias Petzold

Zweites Gutachten von: Prof. Dr. Markus Sperandio

Drittes Gutachten von: Priv. Doz. Dr. Philipp Freiherr von Hundelshausen

Viertes Gutachtes: Prof. Dr. Markus Rehberg

Dekan: **Prof. Dr. med. Thomas Gudermann**

Datum der Verteidigung:

16.07.2024

To my FAMILY.

Some of the described results in this thesis have been published in the following publications:

Petzold T, Zhang Z, Ballesteros I, Saleh I, Polzin A, Thienel M, Liu L, Ul Ain Q, Weber C, Kilani B, Mertsch P, Götschke J, Cremer S, Lorenz M, Ishikawa-Ankerhold H, Raatz E, **El-Nemr S**, Görlach A, Marhuenda E, Pircher J, Stegner D, Gieger C, Schmidt-Supprian M, Almendros I, Kelm M, Schulz C, Hidalgo A, Massberg S (2022). Neutrophil “plucking” on megakaryocytes drives platelet production and boosts cardiovascular disease. *Immunity*. <https://doi.org/doi:10.1016/j.immuni.2022.10.001>

In addition, the results presented in this thesis about hypoxia have been assembled into a manuscript for submission with my name as a first co-author.

Table of Contents

| | |
|---|-----------|
| <i>List of Abbreviations</i> | 9 |
| <i>Table of Figures</i> | 12 |
| <i>List of Tables</i> | 14 |
| <i>Abstract</i> | 15 |
| 1. Introduction | 17 |
| 1.1 <i>Megakaryopoiesis and thrombopoiesis</i> | 17 |
| 1.2 <i>Platelet compartments and functions</i> | 18 |
| 1.2.1 Mature platelets | 18 |
| 1.2.2 Immature reticulated platelets (RPs) | 19 |
| 1.3 <i>Neutrophils or polymorphonuclear leukocytes</i> | 20 |
| 1.3.1. Neutrophil role in cardiovascular conditions: intermittent hypoxia and myocardial infarction | 21 |
| 1.3.2 Interactions between megakaryocytes and neutrophils..... | 21 |
| 1.4 <i>Platelets and neutrophils interplay in thromboinflammation and beyond in myocardial infarction and obstructive sleep apnea</i> | 22 |
| 1.5 <i>Intermittent hypoxia and myocardial infarction</i> | 25 |
| 1.5.1 Role of Intermittent hypoxia in obstructive sleep apnea | 25 |
| 1.5.2 Obstructive sleep apnea prevalence and diagnostic index | 27 |
| 1.5.3 CPAP or continuous positive airway pressure treatment | 28 |
| 1.5.4 Myocardial infarction and STEMI | 29 |
| 1.6 <i>Correlation of myocardial infarction and sleep apnea</i> | 30 |
| 1.7 <i>Aims of the study</i> | 31 |
| 2. Materials and Reagents | 32 |
| 2.1 <i>Antibodies</i> | 32 |
| 2.2 <i>Reagents and chemicals</i> | 33 |
| 2.3 <i>Assays</i> | 34 |
| 2.4 <i>Machines and equipment</i> | 35 |
| 2.5 <i>Software</i> | 35 |

| | |
|---|-----------|
| 3. Methods | 36 |
| 3.1 <i>Human general practices and methodology</i> | 36 |
| 3.1.1 Obstructive sleep apnea human samples | 36 |
| 3.1.2 Flow chamber assay on collagen | 36 |
| 3.1.3 Plaque preparation and flow chamber | 37 |
| 3.1.4 Human whole blood freezing | 37 |
| 3.1.5 Sorting of neutrophils from frozen whole blood | 38 |
| 3.1.6 FlowSOM clustering methodology and tSNE analysis | 38 |
| 3.1.7 Quantification and imaging of human RPs | 38 |
| 3.2 <i>Mice general practices and methodology</i> | 39 |
| 3.2.1 Mice strains and ethics | 39 |
| 3.2.2 Anesthesia | 39 |
| 3.2.3 Mice models | 40 |
| 3.2.4 Intravital live imaging using multiphoton microscopy | 41 |
| 3.2.5 Whole-mount bone imaging using confocal microscopy | 41 |
| 3.2.6 Neutrophil adoptive transfer | 42 |
| 3.2.7 Lung tissue staining and confocal imaging | 42 |
| 3.2.8 Bone marrow (BM) and lung cell isolation | 43 |
| 3.2.9 Flow cytometry and cell quantification | 43 |
| 3.2.10 Quantification of murine platelets and RPs | 43 |
| 3.2.11 Measurement of platelet lifespan | 44 |
| 3.2.12 BM cytokine profiling in mice | 44 |
| 3.2.13 LFA-1 antibody blocking experiment | 44 |
| 3.2.14 Tail bleeding assay | 45 |
| 3.3 <i>Further experiments</i> | 45 |
| 3.3.1 Measurements of blood count | 45 |
| 3.3.2 Calculation of ROS | 45 |
| 3.3.3 CXCR4 quantification | 46 |
| 3.4 <i>Statistical analysis</i> | 46 |
| 3.5 <i>Clinical characteristics of human samples</i> | 47 |
| 4. Results | 49 |
| 4.1 <i>Obstructive sleep apnea and intermittent hypoxia</i> | 49 |
| 4.1.1 PDW, MPV, and platelet immature fraction are boosted with the severity of OSA | 49 |
| 4.1.2 Thrombus formation is driven by RPs under arterial flow conditions | 50 |

| | |
|---|-----------|
| 4.1.3 Platelet activation markers are highly expressed in OSA patients..... | 52 |
| 4.1.4 Activation markers are elevated on immature platelet fraction | 53 |
| 4.1.5 Augmented neutrophil counts are associated with increased platelet number | 54 |
| 4.1.6 ROS level is boosted in circulating neutrophils under OSA..... | 55 |
| 4.1.7 CXCR4 expression on neutrophils is enhanced in OSA..... | 56 |
| 4.1.8 Characterization of intermittent hypoxic murine chamber | 57 |
| 4.1.9 Thrombopoiesis is increased in mice exposed to IH | 59 |
| 4.1.10 Confocal imaging of BM shows larger megakaryocytes in IH mice..... | 60 |
| 4.1.11 MK comparison in BM and lung | 61 |
| 4.1.12 ICAM-1 expression on lung arterial endothelium is higher in IH mice..... | 62 |
| 4.1.13 MKs and neutrophils closely cooperate to increase thrombopoiesis under IH..... | 63 |
| 4.1.14 Cytokine profiling in BM is characterized under IH condition | 64 |
| 4.1.15 Neutrophil-derived ROS level and CXCR4 expression in murine blood are amplified under IH | 66 |
| 4.1.16 Neutrophil CXCR4 are critical mediators of increased platelet production..... | 67 |
| 4.1.17 LFA-1 neutrophil mobilization to places of inflammation increases platelet production under IH..... | 68 |
| 4.1.18 Genetic ablation of neutrophil CXCR4 attenuates thrombus formation in IH mice | 69 |
| 4.1.19 Tail bleeding assay reflects impaired hemostasis in hypoxic mice | 70 |
| 4.1.20 Intermittent hypoxia after 21 days exposure..... | 71 |
| 4.1.21 CPAP therapy reduces RPs related to thrombogenicity in OSA patients | 73 |
| 4.1.22 CPAP therapy decreases the thrombotic risk in OSA patients | 74 |
| 4.1.23 CPAP therapy decreases platelet reactivity in OSA..... | 75 |
| 4.1.24 Neutrophils from untreated OSA patients are characterized by upregulation of mitochondrial proteins..... | 76 |
| <i>4.2 Myocardial infarction/ischemia-reperfusion (MI/IR) murine model and STEMI patients</i> | <i>79</i> |
| 4.2.1 MI/IR murine model is established to translate the responses in patients | 79 |
| 4.2.2 Studying MI/IR model at different time points highlights the temporal dynamics of the injury on megakaryocytes..... | 80 |
| 4.2.3 Thrombopoiesis is increased in ischemia-reperfusion myocardial infarction | 82 |
| 4.2.4 Transferred neutrophils preferentially localize around BM MKs of MI | 83 |
| 4.2.5 Direct engagement of neutrophils at PPL budding sites drives thrombopoiesis in MI..... | 84 |
| 4.2.6 Myocardial ischemia-reperfusion amplifies ROS production and CXCR4 on neutrophils..... | 85 |
| 4.2.7 Genetic ablation of neutrophil CXCR4 decreases platelet production after MI/IR injury | 86 |
| 4.2.8 CXCR4 neutrophil-driven thrombopoiesis drives exaggerated arterial thrombus formation in MI..... | 87 |

| | |
|--|------------|
| 4.2.9 RPs counts and neutrophil CXCR4 expression increase in ST-elevation myocardial infarction patients | 88 |
| 5. Discussion | 90 |
| 5.1 Intermittent hypoxia and myocardial infarction enhance the production of mature and immature platelets..... | 90 |
| 5.2 Plucking neutrophils on proplatelet-forming megakaryocytes triggers thrombopoiesis and boosts thrombotic risk..... | 90 |
| 5.3 Characterization of the BM cytokine profile following intermittent hypoxia | 91 |
| 5.4 Reticulated platelets are better prognostic markers than controversial platelet indices (PDW and MPV) in OSA and MI..... | 92 |
| 5.5 Hyperactive reticulated platelets act as prothrombogenic drivers in IH and MI..... | 93 |
| 5.6 Excessive production of neutrophil-derived ROS may lead to severe cardiovascular outcomes | 95 |
| 5.7 Targeting neutrophil-driven thrombopoiesis diminishes platelet overproduction and thrombus burden | 95 |
| 5.8 CPAP therapy alleviates the thrombotic risk of intermittent hypoxia | 97 |
| 5.9 Limitations of this study | 99 |
| 6. Conclusion and Future Work | 100 |
| Bibliography | 102 |
| Acknowledgment | 118 |
| Affidavit..... | 120 |
| Confirmation of congruency..... | 121 |

List of Abbreviations

| | |
|------------------|--|
| 3D | 3-dimensional |
| AASM | American academy of sleep medicine |
| ACD | Acid citrate dextrose |
| AF | Alexa Fluor |
| AHI | Apnea-hypopnea index |
| AMI | Acute myocardial infarction |
| APC | Allophycocyanin |
| AUC | Area under the curve |
| BM | Bone marrow |
| BSA | Bovine serum albumin |
| BT | Body temperature |
| BV | Brilliant violet |
| CABG | Coronary artery bypass grafting |
| CAD | Coronary artery disease |
| CART | Cocaine- and amphetamine-regulated transcript |
| CIH | Chronic intermittent hypoxia |
| CNS | Central nervous system |
| CPAP | Continuous positive airway pressure |
| CV | Cardiovascular |
| CXCL12 | C-X-C motif chemokine-12 |
| CXCR4 | C-X-C motif chemokine receptor-4 |
| Cy | Cyanine |
| DAPI | 4',6-diamidino-2-phenylindole |
| DCFDA | Dichlorodihydrofluorescein diacetate |
| DMEM | Dulbecco's Modified Eagle Medium |
| DMSO | Dimethylsulfoxide |
| DNA | Deoxyribonucleic acid |
| DPBS | Dulbecco's phosphate buffered saline |
| ECG | Electrocardiogram |
| FACS | Fluorescence-activated cell sorting |
| FBS | Fetal bovine serum |
| FiO ₂ | Fraction of inspired oxygen |
| FITC | Fluorescein isothiocyanate |
| GOBP | Gene ontology biological process |
| GOCC | Gene ontology cellular component |
| GOMF | Gene ontology molecular function |
| GP | Glycoprotein |
| HEPES | 4-(2-hydroxyethyl)-1-piperazineethanesulfonic acid |
| HHU | Heinrich-Heine university |
| HIF1- α | Hypoxia inducible factor 1 subunit alpha |
| HSAT | Home sleep apnea test |

| | |
|-------------------|---|
| HSCs | Hematopoietic stem cells |
| i.p. | Intraperitoneally |
| I/R | Ischemia/reperfusion |
| ICAM-1 | Intercellular adhesion molecule-1 |
| IH | Intermittent hypoxia |
| IL | Interleukin |
| JAK2 | Janus kinase 2 |
| LAD | Left anterior descending |
| LFA-1 | Leukocyte function associated antigen-1 |
| LMU | Ludwig Maximilian University |
| LYMPH | Lymphocyte |
| MAPK | Mitogen-activated protein kinase |
| Mcl-1 | Myeloid cell leukemia-1 |
| MFI | Mean Fluorescent Intensity |
| MgCl ₂ | Magnesiumchloride |
| MI | Myocardial infarction |
| MK | Megakaryocyte |
| MMF | Medetomidine- Midazolam- Fentanyl |
| MMP-9 | Matrix metalloproteinase-9 |
| MONO | Monocyte |
| MPV | Mean platelet volume |
| mRNA | Messenger ribonucleic acid |
| NADPH | Nicotinamide adenine dinucleotide phosphate |
| nCPAP | Nasal continuous positive airway pressure |
| NET | Neutrophil extracellular traps |
| NEUT | Neutrophil |
| NF-κB | Nuclear factor-κB |
| NF2L2 | Nuclear factor-erythroid-derived 2-like 2 |
| NO | Nitric Oxide |
| NOX | NADPH-oxidase |
| ns | Not significant |
| OCT | Optical cutting temperature |
| OPO | Optical parametric oscillator |
| OSA | Obstructive sleep apnea |
| OSAS | Obstructive sleep apnea syndrome |
| PAI-1 | Plasminogen activator inhibitor-1 |
| PB | Pacific blue |
| PBS | Phosphate-buffered saline |
| PCI | Percutaneous coronary intervention |
| PD1-L2 | Programmed death 1 ligand 2 |
| PDW | Platelet distribution width |
| PE | Phycoerythrin |
| PF4 | Platelet factor 4 |
| PFA | Paraformaldehyde |

| | |
|-----------------|---|
| PI3K-Akt | Phosphoinositide 3 kinase |
| PMA | Phorbol 12-myristate 13-acetate |
| PMN | Polymorphonuclear leukocytes |
| PMP | Platelet-derived microparticles |
| PO ₂ | Partial pressure of oxygen |
| POMC | Peptides proopiomelanocortin |
| Pop | Population |
| PPL | Proplatelet |
| PSG | Polysomnography |
| PSGL1 | P-selectin glycoprotein ligand 1 |
| RAGE | Receptor for advanced-glycation end-products |
| RBC | Red blood cells |
| RNS | Reactive nitrogen species |
| ROS | Reactive oxygen species |
| RP | Reticulated platelet |
| RPMI | Roswell park memorial institute medium |
| RT | Room temperature |
| Rt-PCR | Real-time polymerase chain reaction |
| SD | Standard deviation |
| SDF-1 | Stromal cell-derived factor-1 |
| SEM | Standard error of the mean |
| SKF | Kollagen reagens horm suspension |
| SN | Nervous system |
| STATs | Signal transducers and transcription activators |
| STEMI | ST-elevation myocardial infarction |
| TAT | Thrombin-antithrombin |
| Ti:sa | Ti:sapphire laser |
| TNF- α | Tumor necrosis factor |
| TO | Thiazole orange |
| TPO | Thrombopoietin |
| VEGF-A | Vascular endothelial growth factor-A |
| vWF | Von Willebrand Factor |
| WBC | White blood cells |
| XOX | Xanthine oxidase |

Table of Figures

| | |
|---|----|
| Figure 1. Descriptive illustration showing neutrophil-driven platelet production. | 15 |
| Figure 1.1. This figurative scheme presents the cytokines promoting megakaryopoiesis and thrombopoiesis; generated using PowerPoint (modified from [13]). | 18 |
| Figure 1.2. Reticulated platelets (RPs) are increased in unhealthy populations and are considered prognostic predictors in patients with adverse events (modified from [15]). | 20 |
| Figure 1.3. Platelet and neutrophil mediation under inflammatory conditions. | 23 |
| Figure 1.4. Scheme illustrating the role of platelets as crucial effectors in hypoxia and myocardial infarction. | 24 |
| Figure 1.5. ROS is a significant contributor to intermittent hypoxia encouraging sympathetic activation, and inflammation along with vascular morbidities in obstructive sleep apnea syndrome. | 26 |
| Figure 1.6. This diagram compares healthy individuals' physical and cellular processes versus patients with OSA, highlighting the most notable differences. | 27 |
| Figure 1.7. A representative Scheme of CPAP machine. | 28 |
| Figure 1.8. Scheme of ST-elevation myocardial infarction (STEMI) of myocardial infarct and illustrative scheme of blood clotting during myocardial infarction presented using PowerPoint. | 29 |
| Figure 4.1. Effects of OSA on platelet compartments. | 50 |
| Figure 4.2. Platelet aggregation and accumulation of OSA blood. | 51 |
| Figure 4.3. Extensive flow cytometric platelet markers evaluation. | 53 |
| Figure 4.4. Activation markers on platelet and RP fractions. | 54 |
| Figure 4.5. Correlation of neutrophil and platelet counts in OSA patients. | 55 |
| Figure 4.6. Circulating neutrophils increase ROS levels under OSA. | 55 |
| Figure 4.7. CXCR4 expression is significantly higher in severe OSA patients. | 56 |
| Figure 4.8. Establishing and characterization of IH at different time points. | 58 |
| Figure 4.9. Flow cytometry measurements of mice under normoxia and hypoxia. | 59 |
| Figure 4.10. MKs in hypoxia mice have greater diameters under hypoxia. | 61 |
| Figure 4.11. Murine BM and lung confocal imaging of MKs under normoxia and hypoxia. | 62 |
| Figure 4.12. ICAM-1 is significantly expressed in the lung endothelium of IH mice. | 63 |
| Figure 4.13. The interaction between MKs and neutrophils is visualized using two-photon imaging in normoxia and hypoxia mice. | 64 |
| Figure 4.14. BM cytokine is quantified in normoxia and hypoxia mice. | 65 |
| Figure 4.15. IH increases the level of neutrophil-derived ROS and CXCR4 expression. | 66 |
| Figure 4.16. Measurements of Mrp8-Cre/CXCR4 ^{fl/fl} mice under normoxia and hypoxia. | 67 |
| Figure 4.17. LFA-1 blockage lowers platelet and RP production in hypoxic mice. | 69 |
| Figure 4.18. Abrogation of neutrophil CXCR4 reduces the thrombotic risk in IH mice. | 70 |

| | |
|--|----|
| Figure 4.19. Tail bleeding assay shows reduced bleeding time in hypoxic mice. | 71 |
| Figure 4.20. Measurements in mice after 3 weeks of IH exposure. | 73 |
| Figure 4.21. Flow cytometry measurements of OSA patients pre and post-CPAP therapy..... | 74 |
| Figure 4.22. CPAP therapy minimizes platelet adhesion and aggregate generation in OSA. | 75 |
| Figure 4.23. tSNE and flowSOM measurements of platelet markers pre and post-therapy. | 76 |
| Figure 4.24. Functional enrichment analysis of sorted neutrophils in OSA pre- and post-therapy. | 78 |
| Figure 4.25. Establishing of MI after 1-hour ischemia-reperfusion and characterization. | 80 |
| Figure 4.26. Characterizing the established MI/IR model at different time points. | 81 |
| Figure 4.27. Platelet and RP counts are amplified in MI/IR murine models..... | 82 |
| Figure 4.28. Close MK-neutrophil interaction following adoptive neutrophil transfer. | 84 |
| Figure 4.29. Augmented thrombopoiesis and MK-neutrophil interaction are visualized under MI. | 85 |
| Figure 4.30. Neutrophil-derived ROS and CXCR4 expression augment in MI/IR. | 86 |
| Figure 4.31. Ablation of neutrophil CXCR4 affects platelet production after MI/IR injury..... | 87 |
| Figure 4.32. Arterial thrombosis burden is corrected by abrogated neutrophil CXCR4 in MI/IR mice. | 88 |
| Figure 4.33. Measurements of platelets, RPs, and CXCR4 in STEMI patients. | 89 |

List of Tables

| | |
|---|----|
| Table 1. A table summarizing the severity classification of OSA. | 28 |
| Table 2. Antibodies used in this thesis. | 32 |
| Table 3. Reagents and chemicals used in this thesis..... | 33 |
| Table 4. Assays and items used in this project..... | 34 |
| Table 5. Machines and equipment used in this project. | 35 |
| Table 6. Software used in this project. | 35 |
| Table 7. Clinical descriptions of OSA patients and controls (healthy individuals) recruited in this study project..... | 47 |
| Table 8. Clinical characteristics of OSA patients pre- & post-therapy recruited in this study (n=9 per group). | 48 |

Abstract

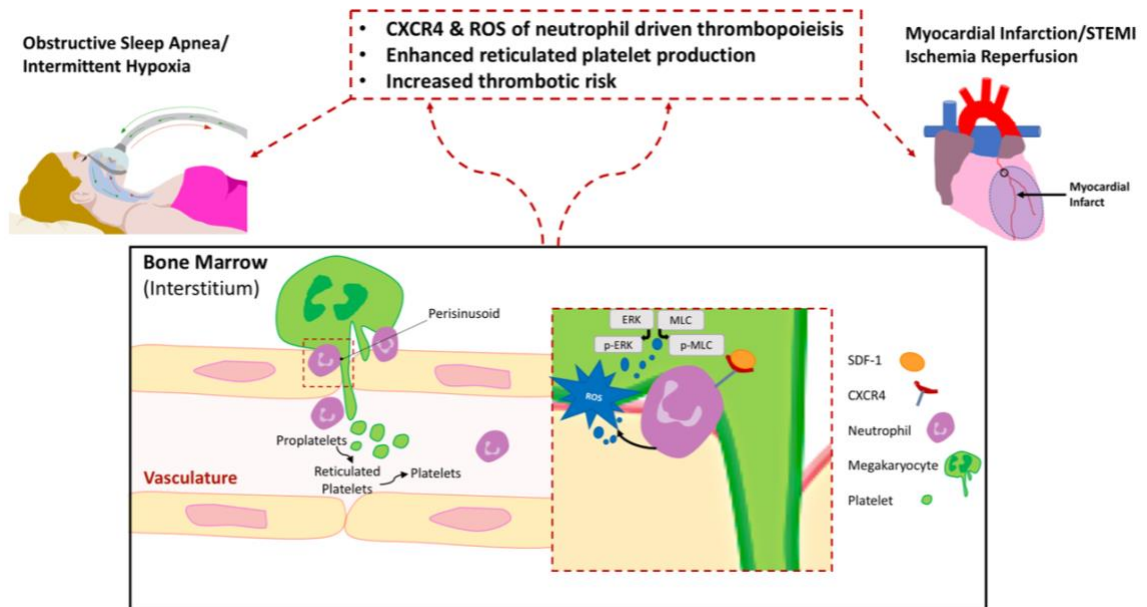


Figure 1. Descriptive illustration showing neutrophil-driven platelet production.

This scheme summarizes this research project by elucidating an augmented reticulated platelet release into the vasculature from megakaryocytes which are in close proximity to neutrophils. The interaction between megakaryocytes and neutrophils is through CXC4/SDF-1 pathway triggering the generation of reactive oxygen species (ROS); which will result in an increase of thrombus burden in cardiovascular inflammatory diseases including myocardial infarction and intermittent hypoxia. This illustrative scheme is generated using PowerPoint.

Neutrophils' engagement in platelet production augments the risk of thrombotic problems. Yet, little is known about the biological interactions between the platelet progenitors named megakaryocytes and neutrophils in bone marrow (BM), undergoing cardiovascular complications. Obstructive sleep apnea (OSA) is a prevalent sleep-associated respiratory disease that is linked to patient morbidity along with an enhanced risk of cardiovascular morbidity such as myocardial infarction (MI). Specifically, how BM interactions influence adverse thromboinflammatory effects driving thrombotic complications in OSA and MI remains elusive.

To investigate the role of neutrophils in enhancing thrombopoiesis under inflammatory cardiovascular disease conditions, murine models of myocardial ischemia-reperfusion and

intermittent hypoxia were established. Hypoxia followed by reoxygenation is associated with myocardial ischemia-reperfusion damage; nevertheless, the precise processes are not completely elucidated. In this study, it was demonstrated that direct megakaryocyte-neutrophil interactions in BM regulate thrombopoiesis. Murine models as well as ST-elevation myocardial infarction (STEMI) and OSA patients showed an increased amount of prothrombotic immature reticulated platelets in the vasculature, which may lead to enhanced thrombus formation. Indeed, reticulated platelet activation, number, and aggregation are enhanced under intermittent hypoxia in mice and OSA patients. Both investigated intermittent hypoxia and myocardial infarction conditions boosted the levels of neutrophil-derived CXCR4 and ROS. In addition, this project showed that continuous positive airway pressure therapy for OSA patients can reduce excess production of platelets and activity along with lowering the level of ROS and CXCR4 expression on circulating neutrophils.

It is important to highlight that gaining a comprehensive understanding of neutrophil functions in cardiovascular diseases can lead to the development of effective therapeutic strategies targeting neutrophil dysfunction, number, and impact. The findings of this research project advance our understanding of the cellular architecture within the BM niche. Additionally, this study uncovers the role of young immature platelets and neutrophil-derived ROS and CXCR4 to highlight the importance of immune cells in thrombopoiesis. In conclusion, this study guides us toward estimating the function of immature platelets as crucial players in the immune gamut involved in cardiovascular events and subsequently examines the potential mechanisms in which they influence cardiovascular disease. Targeting neutrophil-driven thrombopoiesis can be a promising approach to overcome platelet overproduction and thereby prevent thrombotic complications in OSA and MI.

1. Introduction

1.1 Megakaryopoiesis and thrombopoiesis

Hematopoietic stem cells (HSCs) will undergo differentiation into megakaryocytes (MKs) through thrombopoietin (TPO) induction [1]. It was discovered in 1994 that c-MPL which is MK specific receptor, stimulates the development as well as the growth of MKs from the precursors of HSCs [2,3]. MK differentiation is driven by the binding of TPO to c-MPL resulting in the activation of cytosolic tyrosine kinases including JAK2 (Janus kinase 2) by autophosphorylation of c-MPL itself. This phosphorylation results in recruiting a wide range of effectors like signal transducers and transcription activators (STATs), mitogen-activated protein (MAP) kinase, and phosphoinositide3 kinase-Akt as well as ERK1/2 pathways [4,5]. Other cytokines (Fig. 1.1) namely IL-3, IL-6, and IL-11 along with erythropoietin collaborate with TPO in fostering megakaryopoiesis; particularly SCF (stem cell factor) promoting the proliferation of MK colony [6]. Yet, the growth factor G-CSF restrains the formation of MK colonies stimulated by EPO, IL-6, or TPO but not that activated by IL-3 [7].

MKs experience endomitosis, a process involving DNA replication without subsequent cell division, developing accumulated polyploid DNA content from $2n$ to $128n$ [8,9]. Thrombopoiesis occurs mainly in the bone marrow where perisinusoidal located mature MKs, recognized as platelet progenitors, release cytoplasmic ligations known as proplatelets (PPLs) that enter the vasculature and differentiate into mature platelets [10]. During physiological stress or inflammatory state, platelet count can increase. It was hypothesized that CCL5 (RANTES) might regulate the generation of platelets by attaching to its CCR5 receptor on megakaryocytes [11] (Fig. 1.1). In addition, acute inflammatory conditions transiently elevated IL-1 α (Interleukin 1 α) leads to cell programming, MK rupture to induce enhanced thrombopoiesis and platelet release [12] (Fig. 1.1). Despite the great progress in research, many mechanisms and factors which lead to MK fragmentation to generate platelets remains unknown.

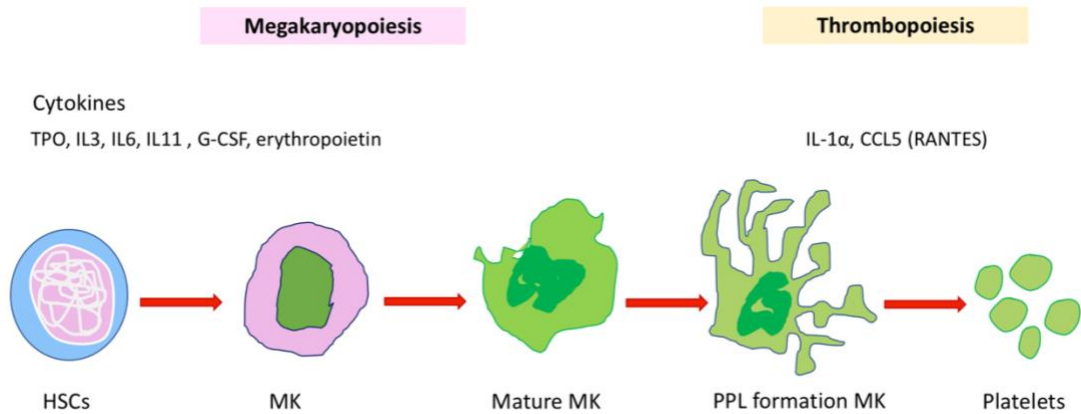


Figure 1.1. This figurative scheme presents the cytokines promoting megakaryopoiesis and thrombopoiesis; generated using PowerPoint (modified from [13]).

TPO: Thrombopoietin, IL: Interleukin, G-CSF: Growth factor, HSCs: Hematopoietic stem cells, MK: Megakaryocyte, PPL: Proplatelet.

1.2 Platelet compartments and functions

Platelet subpopulations are considered a prevalent topic in science. The dynamic nature of platelet characteristics in health and diseases differs because of the different platelet biochemical, physical, and functional variations.

1.2.1 Mature platelets

In 1906, James Homer Wright confined himself to a brief statement about his opinion of the origin of platelets and was the first to identify marrow megakaryocyte as the progenitor cell of blood platelets which were formerly called the “dust of the blood” [14]. Megakaryocytes continuously produce platelets circulating in the blood, which are described as small anucleated blood cells (with a diameter of 2 to 4 μm) [15]. Platelets are characterized by 7-10 days lifespan in the human circulation [16] to keep a constant platelet count per microliter of whole blood of 150,000-400,000; along with a shorter lifespan (4-5 days) in murine blood [17] before being eliminated by liver and spleen [18–20].

Researchers were convinced previously, that platelets are specialized cells that function only to block bleeding and diminish blood vessel injury by forming a clot that seals the wound and

prevents blood loss. Indeed, platelets are the protectors helping in inflammation, attacking microbial interlopers, and alerting immune cells. Platelets can also release chemicals like serotonin helping in liver regeneration after injury and shaping the neonatal vascular system [21].

Platelets are associated not only with hemostasis and arterial thrombosis but also with other physiological and pathophysiological processes like cancer progression and immune response to infection [19,22,23]. Platelets are considered promising targets to advance future clinical therapeutics against a wide range of diseases including infection, and cancer [23]. Consequently, dissecting the distinct biological features and the role of platelets in other inflammatory diseases would be an asset to clarify their functions and effectively target them in the clinic.

1.2.2 Immature reticulated platelets (RPs)

Platelets are heterogeneous varying extensively with regard to their RNA content, size, and thrombogenicity [22]. RPs are freshly liberated platelets from MKs into the circulation. Despite its limitations, a dye termed thiazole orange dye (TO) appears to bind to ribonucleic acid in RPs and enriches its fluorescence signal [24]. RPs are considered larger and contain more RNA in comparison to more mature platelet compartments.

Recently, RPs have gained growing interest since their prothrombotic profile was further studied with the association of major adverse events in various pathological settings [20]. In comparison to older platelets, RPs exhibit a considerably higher thrombogenicity and are known to have a detrimental increase in patients with cardiovascular diseases such as acute myocardial infarction [25]. The RPs' influence on the response of antiplatelet treatment and the association of RPs with coronary artery disease (CAD) as well as the subsequent clinical consequences have been the focus of studies [26] (Fig. 1.2). It has been reported that elevated RPs correlate with a lack of adequate response to antiplatelet treatment, aspirin along with specific P2Y₁₂ receptor inhibitors as illustrated in Fig. 1.2 [20]. Further exploration of RPs may enhance patient risk assessment, early diagnosis of diseases, and mostly cardiovascular therapies. Yet, the precise pathways underlying the elevated RP level remain unclear. Despite a

wide range of hypotheses proposed, no sincere causality has been found. Therefore, it is important to highlight RPs' function in shaping thrombo-inflammatory complications.

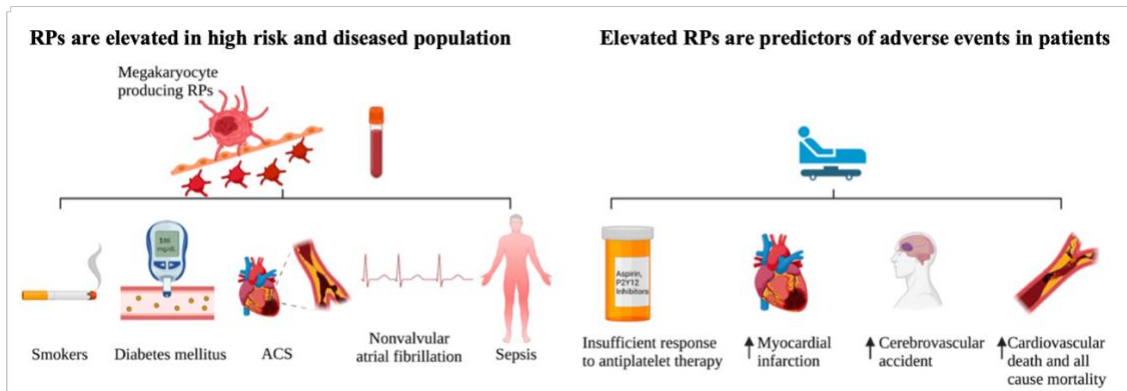


Figure 1.2. Reticulated platelets (RPs) are increased in unhealthy populations and are considered prognostic predictors in patients with adverse events (modified from [15]). ACS: Acute coronary syndrome.

1.3 Neutrophils or polymorphonuclear leukocytes

Neutrophils, alternatively referred to as multi-lobed leukocytes, represent the most abundant myeloid leukocytes in humans [27–29]. Once matured, neutrophils are retained in BM for up to 4-6 days by interacting with the CXCL12/SDF-1 (stromal-derived factor 1) and its recognized receptor CXCR4 on neutrophils [30–32]. To leave BM, neutrophils enter the vasculature by migration through the sinusoidal endothelium [33] and circulate in the bloodstream for less than 1 day under physiological conditions [34]. The increased production rate of neutrophils and their short life span necessitate their elimination from circulation by constitutive apoptosis to maintain homeostasis [34]. Neutrophils are very crucial players and defenders because they eliminate invaders via chemotaxis and consequent phagocytosis by Kupffer cells [35]. Typically, neutrophils are quickly mobilized to sites of infection and inflammation where they engulf invading microbes and employ NADPH oxidase-derived ROS (reactive oxygen species), proteases, and antimicrobial peptides working together to generate a decidedly fatal environment of intraphagosomes [34,36]. It has been presented that ROS levels were altered in models of cardiovascular diseases, hypertension, atherosclerosis, and heart failure [37]. Moreover, oxidative stress was also found to be enhanced in ischemic myocardial syndromes [38].

1.3.1. Neutrophil role in cardiovascular conditions: intermittent hypoxia and myocardial infarction

Patients encountering cardiovascular and breathing morbidities, and obstructive sleep apnea (described by recurring episodes of intermittent hypoxia (IH)), have extended survival of neutrophils provoking sustained inflammation which induces tissue damage and dysfunction [39]. ERK and P38MAPKs (mitogen-activated protein kinases) regulate apoptosis in neutrophils; particularly expression of myeloid cell leukemia 1 (Mcl-1, a member of BCL2 family) can be controlled through ERK pathway [39,40]. A novel regulatory role affecting neutrophil survival via ERK1/2 pathway was underlined in sleep apnea patients and IH [39]. Compared to normoxia and controls, IH stimulated the phosphorylation of ERK1/2 pathway and p38MAPKs to inhibit the translocation of Bax to mitochondria as well as to attenuate the stability of Bax/Mcl-1; promoting the viability of neutrophils under conditions of IH and OSA [39]. It was also observed that p38MAPK is activated after ischemia and this activation was maintained by the ensuing reperfusion [41]. Moreover, ERK1/2 is abnormally expressed in I/R (ischemia-reperfusion) injury and MAPK-ERK1/2 pathway has been described to both exacerbate and protect against myocardial I/R [42]. Despite recent advances in exploring the characteristics and functions of neutrophils, numerous approaches remain unclear and necessitate additional investigation by refining existing models to understand the key mechanism of neutrophil-mediated cardiovascular diseases and hypoxic conditions.

1.3.2 Interactions between megakaryocytes and neutrophils

Within the bone marrow, MKs exist in a milieu of close contiguity to various hematopoietic cells and immunocytes, mainly neutrophils. Nevertheless, to date, the functional significance of the direct or indirect interaction of MK-leukocytes (neutrophils) and its impact on platelet production remains poorly understood. It was revealed by Itkin and his colleagues (2016) that MKs residing within the BM and releasing platelets via perisinusoidal niche, communicate with neutrophils to stipulate neutrophil entry and exit from the circulation to BM where metabolic parameters like ROS are regulated [43]. Moreover, Boisset et al. (2018) explored a network of cellular interactions in BM and discovered a crucial preferential cell interaction of mature neutrophils and MKs inside the BM environment [44]. Interestingly, it was observed that neutrophils are engulfed by BM MKs described in a phenomenon of emperipolesis [45,46];

which strengthens the suggestion of a close connection between MKs and neutrophils. Emperipolesis is intensified in models of murine inflammation associated with enhanced platelet production [46]. However, our understanding of the biological significance behind the interactions between neutrophils and MKs within the BM is limited; predominantly how these interactions contribute to thromboinflammatory concerns that may drive thrombotic risk.

1.4 Platelets and neutrophils interplay in thromboinflammation and beyond in myocardial infarction and obstructive sleep apnea

Despite the advancement in treating cardiovascular diseases, efficacious clinical management remains an arduous challenge in alleviating the effect of thromboinflammation under these conditions [47]. Thromboinflammation is clinically manifested as superficial thrombophlebitis which is characterized by inflammation of superficial veins and thrombosis [47,48]. Yet, it can be more precarious to develop in the microvasculature milieu of damaged tissues [47,48]. Various disorders such as I/R can lead to the development of microvascular thrombosis associated with thrombotic and inflammatory complications [47,48].

Studies have recently deciphered the platelet association in inflammatory progressions including infections and ischemic stroke, along with their involvement in the pathobiology of diverse thromboinflammatory morbidities [47]. Patients with OSA and its main component IH frequently suffer from comorbidities that are directly correlated to risk factors for platelet activation, endothelial damage, and atherosclerosis [49]. The dysregulation in the endothelial vasculature may majorly contribute to thromboinflammation; which is manifested by platelet activation, disruption of the coagulation activity in addition to an amplified leukocyte induction into vasculature, primarily neutrophils [47,48].

Platelets use complicated mediators to arbitrate numerous functions from intuiting the danger to repairing the infected tissue. When activated, platelets release a range of cytokines such as IL-1, CD154 (CD40L), TNF- α (tumor necrosis factor- α), CXCL1, CXCL5, and CXCL12 that trigger inflammation including leukocyte migration, phagocytosis, and ROS production [50–52]. Researchers gained interest in investigating the pathological relationship between platelets and neutrophils in thromboinflammation. Under infection and inflammation, activated

platelets assist in neutrophils trafficking across vessel walls and regulate their recruitment to the inflamed sites [23]. Upon activation, P-selectin is largely present on platelets to mediate the adhesion of stimulated platelets to cells expressing P-selectin glycoprotein ligand 1 (PSGL-1) mainly neutrophils; resulting in integrin activation particularly beta 2-integrin MAC-1 as well as lymphocyte function-associated antigen-1 (LFA-1) on leukocyte membrane [50,53]. Rearrangement of forms of α IIb β 3 (a platelet integrin) facilitates binding to fibrinogen and consequently the aggregation of platelets [49,54]. Neutrophils need MAC-1 to adhere firmly to platelets and to facilitate their recruitment and relocation over accumulated platelets at thrombogenic places [53,55]. Activated platelets produce chemokines like platelet factor-4 (PF4 or CXCL4), NAP-2 (or CXCL7), IL-8 (CXCL8), CCL3 (MIP-1 α), and RANTES (CCL5), which promote inflammation by recruiting leukocytes via their chemotactic activity as illustrated below (Fig. 1.3) [50–52].

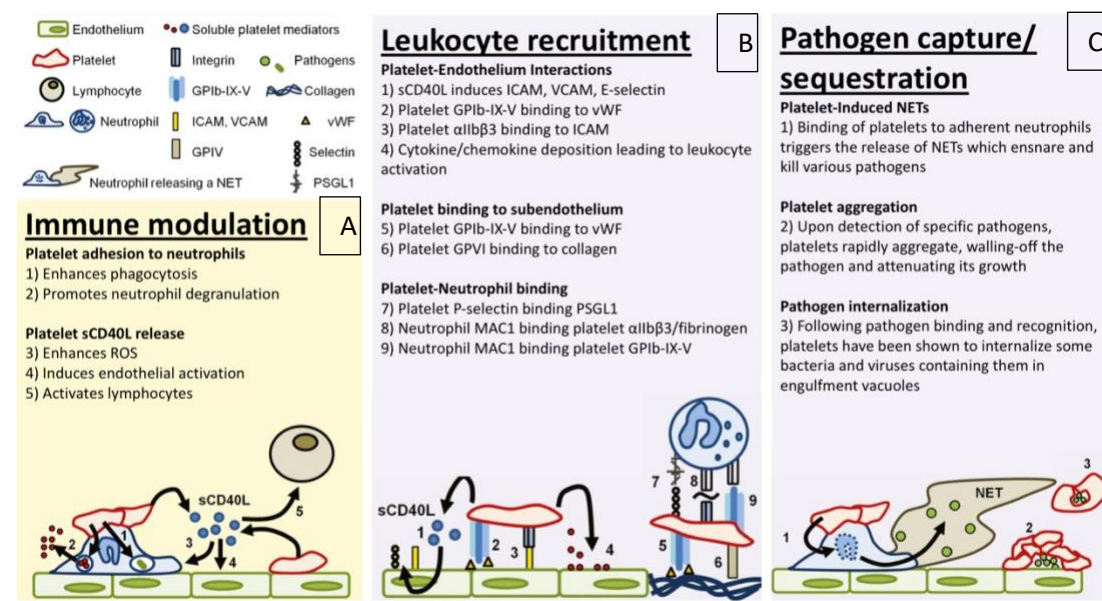


Figure 1.3. Platelet and neutrophil mediation under inflammatory conditions.

Under inflammation, platelets play an important role in (A) immune modulation of neutrophil function, (B) neutrophil adhesion to the subendothelium to release cytokines and chemokines activating neutrophils, and (C) pathogen capturing and sequestration by inducing NETs engulfing the pathogen by platelet aggregates and consequently directly internalize the pathogen. Adapted and modified from [52].

sCD40L: soluble CD40L, vWF: von-Willebrand factor, PSGL1: P-selectin glycoprotein ligand 1, NET: Neutrophil extracellular traps, GP: Glycoprotein.

Platelet-derived microparticles ((PMP or proplatelets (PPL)) circulate increasingly during sustained platelet stimulation. In addition, these PPL deliver RANTES into the inflamed

endothelium triggering monocyte recruitment in inflammation and atherosclerosis [56]. RANTES which is a main chemokine in atherogenesis was found to have an enhanced expression in the vascular wall of mice exposed to IH [57]. Impairment of the homeostasis in OSA vasculature is caused by IH, elevated oxidative stress, and increased concentration of inflammatory lipids and cytokines in circulation. Persistent activation of platelets results in the continuous presence of proatherogenic/inflammatory affluences resulting in the formation of atherosclerosis and thromboembolism which are the endpoints of myocardial infarction as presented in Fig. 1.4 [49].

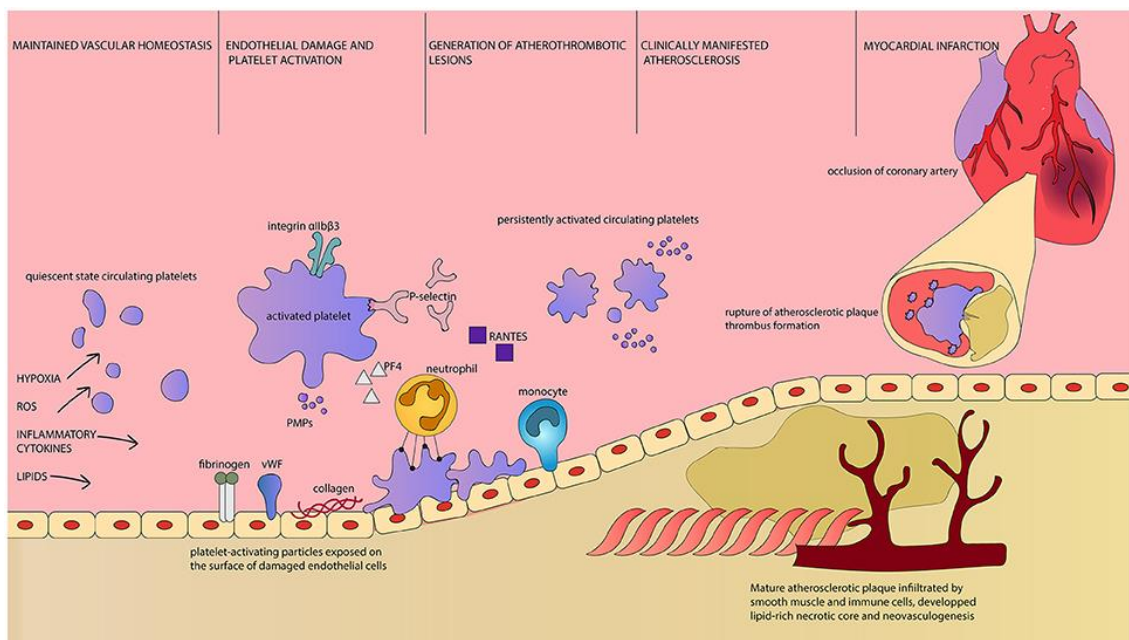


Figure 1.4. Scheme illustrating the role of platelets as crucial effectors in hypoxia and myocardial infarction.

IH, ROS, lipids, and inflammatory cytokines disrupt vascular homeostasis in patients with OSA. Whereas endothelial damage happens, platelet activation takes place by upregulation of PMPs and bioactive substances. P-selectin is released from the surface of platelets to help in the mobilization of leukocytes and the attachment of neutrophils and platelets in addition to the aggregation of platelets. Platelets-derived RANTES on endothelial cells permit the arrest and infiltration of monocytes. Interaction of platelet-neutrophil is mostly dependent on PF4 and P-selectin along with GP1 β α and CD40L, and their ligands. Persistent activation of platelets develops atherosclerotic plaques which upon rupture lead to thrombus formation and occlusion of major arteries; resulting in radical consequences. Reprinted from [49].

1.5 Intermittent hypoxia and myocardial infarction

1.5.1 Role of Intermittent hypoxia in obstructive sleep apnea

Hypoxia is outlined when the body is exposed to environments with different patterns of low oxygen. Hypoxia can be continuous or intermittent, depending on the pattern and length of oxygen exposure [58–60]. These features influence the pathological and physiological reactions to hypoxia, albeit the underlying pathways and mechanisms are unknown. Continuous hypoxia as that experienced in high altitude regions, happens when levels of oxygen decrease from 21% of oxygen (normal atmospheric levels) to oxygen values oscillating mostly between 8% and 12% [59]. Sustained or continuous hypoxia arises in patients with cystic fibrosis and advanced lung diseases such as chronic obstructive pulmonary disease [61–63]. IH happens when oxygen levels fall for only concise periods. IH has been exposed in individuals suffering from sleep apnea; particularly OSA, a predominant sleep disorder involving variable episodes when breathing rates slow or cease [59].

IH is linked with increased ROS production causing the induction of oxidative stress to generate mitochondrial dysfunction and to stimulate XO (xanthine oxidase), NOX (NADPH oxidase), and uncoupling of NOS (nitric oxide synthase); the series of events explained are presented in Fig. 1.5 based on [64–67]. ROS interacts with NO (nitric oxide) to decrease NO bioavailability, which enhances inflammation, hypertension, endothelial dysfunction, atherosclerosis, and hypercoagulability [66]. The ROS-dependent upregulation of endothelin 1 and angiotensin II quantities as long as the sympathetic activation leads to hypertension [66,67]. In parallel, ROS promotes a wide range of transcription factors, like HIF1 α (hypoxia-inducible factor-1 α) and nuclear factors such as NF2L2 as well as NF- κ B which regulates numerous inflammatory processes; resulting in endothelial dysfunction, atherosclerosis, and cerebro/cardio-vascular morbidities [66,68]. Nevertheless, ROS-dependent upregulation of NF2L2 and HIF1 α plays a role in protecting and counteracting some of the detrimental consequences caused by ROS [65,66]. OSA conditions and co-morbidities such as obesity, diabetes mellitus and hyperlipidemia are also affected by ROS and result in inflammation [64,65].

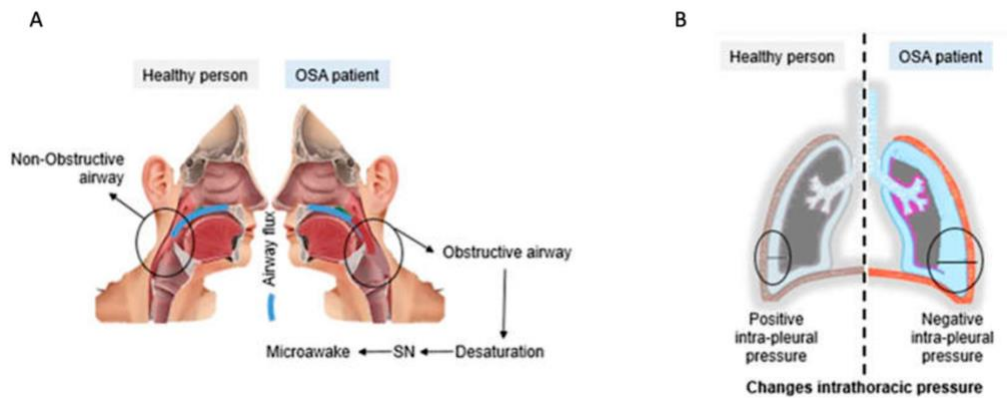


Figure 1.6. This diagram compares healthy individuals' physical and cellular processes versus patients with OSA, highlighting the most notable differences.

A) Blocked airway inlet in OSA patient causing a blockage which results in a reduction of oxygen levels in the blood and triggers the nervous system (SN) causing awakenings during sleep. B) The blockade of breathing airways in an OSA subject causes a difference in intrathoracic pressure compared to a healthy person; reprinted from [73].

1.5.2 Obstructive sleep apnea prevalence and diagnostic index

OSA is found in both genders at different ages, mostly persons aged between 30 and 69 years worldwide [69,70]. OSA prevalence augmented with time and was described to increase to 37% in men and 50% in women [70]. Despite known risk factors and comorbid conditions, OSA is often underestimated and goes undiagnosed [74]. Indeed, the American academy of sleep medicine (AASM) reported that around 29 million individuals in the US, which accounts for 12% of the adult population, are affected by OSA [75]. Surprisingly, 80% of these individuals have not been diagnosed which will lead to medical and financial consequences [75]. It is difficult to have awareness of related health risks associated with OSA due to the failure to connect sleep apnea with its critical comorbidities such as augmented levels of cardiovascular diseases, accidents, and diabetes [75]. OSA patients may be asymptomatic or symptomatic by complaining of fatigue, excessive daytime sleepiness, depression, or memory problems [76,77]. Notably, not only symptomatic but also asymptomatic patients may be associated with distinct cardiovascular risk profiles; which needs to be more considered [78]. Apnea-hypopnea index (AHI) is the diagnostic foremost metric for OSA with the cutoff value of five or more events per hour; calculating the average number of apneas and hypopneas per hour of sleep [69,79]. If the AHI is at least 5 and complemented by exorbitant sleepiness during the day hours, it is considered an OSA syndrome (OSAS) [80–82]. Notably, sleep apnea detected in a

sleep recording with the absence of symptoms is commonly not considered to be OSAS unless AHI is ≥ 15 events/h of sleep [66,83]. OSA severity characterization is summarized in the below Table 1 [84,85].

Table 1. A table summarizing the severity classification of OSA.
h: hour.

| Apnea – Hypopnea Index (AHI) | |
|------------------------------|------------------------------|
| Mild | AHI of 5-15 events/h |
| Moderate | AHI of 15-30 events/h |
| Severe | AHI of more than 30 events/h |

1.5.3 CPAP or continuous positive airway pressure treatment

The frontline care for OSA is a CPAP device (Fig. 1.7), which has been shown to decrease daytime sleepiness in OSA patients by splinting the upper airway passages open to recover patency during sleep [86,87]. Nasal CPAP apparatus therapy is a machine constituted of an air pump coupled to either a nose or face mask. This equipment unlocks the air passage in the throat and inhibits the collapse of soft tissues from collapsing and obstructing the respiratory passage [88]. The CPAP is considered the favored course of therapy for moderate-to-severe OSA having an approximately 75% success rate [88].

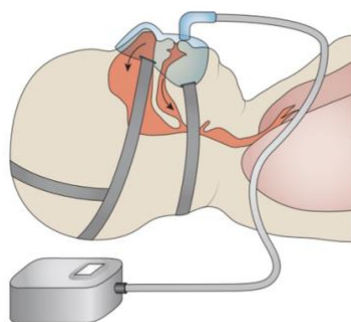


Figure 1.7. A representative Scheme of CPAP machine.

CPAP works on delivering continuous pressure during inhalation and exhalation for sleep apneic patients; reprinted from [66].

Despite the high efficacy of CPAP to reverse the occlusion of the respiratory passage in OSA, the patient's obedience is humble due to the annoyance of nasal mucosa from the nasal flow of air, poor retention, xerostomia, and the noise of the pump [88]. Adherence is described by the use of CPAP for a minimum of 4 hours at night and it was reported that the non-adherence of OSA patients ranges between 46-83% [89]. Additional treatments for sleep apnea are needed for patients who cannot tolerate or refuse to use CPAP; involving weight loss, dental appliances, operation, or electrical stimulation of the upper airway [90]. Despite its well-acknowledged application, there is a scarcity of publications concentrating on examining the molecular pathways that CPAP therapy would influence in OSA patients; which will be addressed in this project.

1.5.4 Myocardial infarction and STEMI

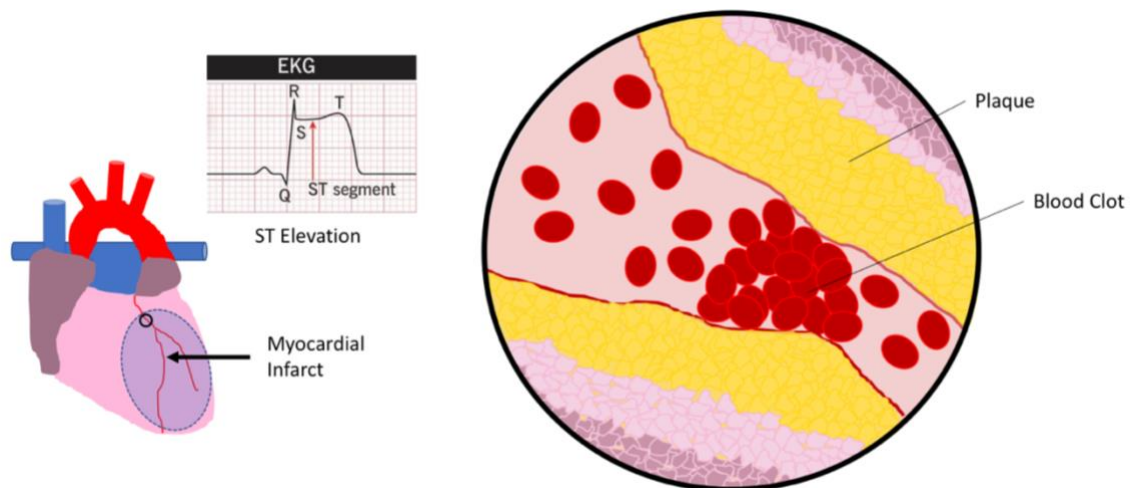


Figure 1.8. Scheme of ST-elevation myocardial infarction (STEMI) of myocardial infarct and illustrative scheme of blood clotting during myocardial infarction presented using PowerPoint.

Myocardial infarction (MI) is a life-threatening morbidity caused by a sudden reduction in blood flow as the occurrence of thrombotic occlusion of the coronary artery is constricted by atherosclerosis [91]; illustrated in Fig. 1.8 MI is termed when ischemia in the heart following imbalanced perfusion results in cardiomyocyte cell death [92]. Despite the rescuing function of reperfusion to the myocardium following STEMI; restoring coronary blood circulation to the ischemic tissue may provoke cardiac myocyte cell death and myocardial injury by a process termed myocardial reperfusion injury [93]. To date, scientists failed to find an effective treatment for plummeting this injury and decreasing MI size in STEMI patients. Reperfusion

injury is triggered by different multifaceted mechanisms comprising the ROS formation [94,95], abrupted metabolic pathways [95], microvascular and endothelial cell dysfunction [96,97], impairments in intracellular calcium handling [95], and stimulation of neutrophils [92] and platelets [98]. Particularly, it remains ambiguous how these mechanisms contribute to promoting adverse inflammatory complications that ultimately result in thrombotic problems under I/R conditions and possibly hypoxia-reoxygenation conditions.

1.6 Correlation of myocardial infarction and sleep apnea

OSA was studied as a concomitant risk factor of chronic arterial hypertension [99] including all cardiovascular morbidities [100]. For instance, OSA patients may be accompanied by systemic hypertension [72,99], pulmonary embolism [101], deep vein thrombosis, and stroke [102,103]. In OSA patients, the occurrence of fatal and non-fatal heart attacks and strokes increased [104]. Most importantly, OSA has been associated with MI [105,106].

Despite that several studies on both humans and animals suggested a significant correlation of OSA and IH cycles to comorbidities and even mortality, additional research is required to explore the effects of short and long-term hypoxia on the progression of cardiovascular diseases. The cyclical fluctuations of hypoxia with periods of reoxygenation are, therefore, analogous to ischemia-reperfusion; contributing to an amplified ROS levels [107]. Hypoxemia in sleep apnea may induce nocturnal cardiac ischemia and increase myocardial ischemic events [108]. It was demonstrated that patients with nocturnal onset of myocardial infarction may be highly correlated with having OSA. These results suggested that OSA may be a trigger and an induction for myocardial infarction [109]. Although CPAP stipulates alterable benefits in the various groups of OSA patients, it seems reasonable for an immediate intervention with CPAP therapy to maximize functional revival and reduce residual damage [107]. Future investigations should focus on the consequences of OSA CPAP treatment to prevent nocturnal cardiac events and avoid the initiation of MI. Additional studies are required to accentuate the relation between OSA and MI and the biomolecular mechanisms behind the serious cardiovascular outcomes in both conditions.

1.7 Aims of the study

Neutrophils and platelets are reported as vastly abundant cells in blood supporting immune defense and hemostasis; nevertheless, their concomitant interaction has been observed in various cardiovascular diseases instigating thrombotic problems. This study appraised the current knowledge of the contribution of neutrophils to thrombopoiesis and its clinical significance as it drives thrombotic implications in OSA and MI patients. Repeated apnea caused by hypoxic events in OSA is considered to be similar to hypoxia-reperfusion injury in MI; leading to the initiation of metabolic and molecular changes [64]. Although various mechanisms are attributed to this damage; yet, it is mainly validated by the enhanced production of oxidative stress in OSA leukocytes [64,110,111]. Subsequently, this project will further elaborate on these findings in OSA and MI to elucidate the underlying mechanisms helping to further understand the connection behind the hypoxic/ischemic and reperfusion/reoxygenation events and highlighting possibilities to find a possible key target in optimizing current therapies in thrombotic cardiovascular diseases.

To achieve these aims, this project is endeavored:

- to explore thrombopoiesis in BM and to understand the mechanisms behind the enhanced platelet production at the site of injury in OSA and MI.
- to unravel the hyperactivity and enhanced function of mature and immature platelets.
- to trigger in-vivo the thrombus formation in murine models of IH and I/R and ex-vivo in blood of OSA and STEMI patients.
- to comprehend the role of neutrophils in BM by studying their relation to oxidative stress and CXCR4 expression.
- to investigate the function of CPAP therapy and explore its impact on thrombopoiesis and thrombus burden.

2. Materials and Reagents

2.1 Antibodies

Table 2. Antibodies used in this thesis.

| Antibodies | Fluorophore | Supplier | Catalog Number |
|--|-----------------|------------------|----------------|
| anti-mouse CD3 complex (clone 17A2) | FITC | BD Bioscience | 555274 |
| anti-human/mouse CD45R (B220) (clone RA3-6B2) | PE-Cy5 | eBioscience™ | 15-045282 |
| anti-mouse CD115 (clone AFS98) | PE | Biologend | 135506 |
| anti-mouse Ly-6G/Ly-6C (GR-1) | PB | Biologend | 108430 |
| Dead Cell stain Sytox™ Blue | BV421 | Invitrogen™ | S34857 |
| anti-mouse NK1.1 (clone PK136) | BV650 | BD Bioscience | 564143 |
| anti-mouse Siglec-F CD170 (clone E50-2440) | BV480 | BD Bioscience | 746668 |
| anti-mouse CD45 (clone I3/2.3) | BV605 | BD Bioscience | 567459 |
| eBioscience™ Fixable Viability Dye eFluor™ 780 | APC-Cy7 (AF750) | Thermofisher | 65-0865-14 |
| anti-mouse Ly6G (clone 1A8) | BV421 (PB) | Biologend | 127627 |
| anti-mouse CXCR4 CD184 (clone 2B11) | PE | eBioscience™ | REF 12-9991-82 |
| anti-mouse/human CD11b(clone M1/70) | BV650 | Biologend | 101239 |
| anti-mouse I-A/I-E (MHC class II) | APC 647 | Biologend | 107618 |
| anti-mouse CD62L (clone MEL-14) | BV510 | Biologend | 104441 |
| anti-mouse TLR4 CD284 | AF488 | FisherScientific | Code 15372080 |
| anti-mouse LFA-1 (CD11a/CD18) | PerCP-Cy5.5 | Biologend | 141008 |
| anti-mouse CD49d | BV480 | BD Bioscience | 746526 |
| anti-mouse CD18 | BV605 | BD Bioscience | 744481 |
| anti-mouse CD41 | BV605 | Biologend | 133921 |
| anti-mouse/rat CD42b | APC | Biologend | 148506 |
| anti-mouse/rat CD29 Beta1 Integrin | PB | Biologend | 102224 |
| anti-mouse CD61 B3intergrin GPIIa | BV650 | BD Biosciences | 740473 |
| anti-mouse CD154 CD40L | PerCP-Cy5.5 | Biologend | 106514 |
| anti-mouse GPVI | FITC | emfret | M011-1 |
| anti-mouse/rat CD62p | PE-Cy7 | Biologend | 148310 |
| anti-mouse CD63 | APC-Cy7 | Biologend | 143907 |
| anti-mouse Integrin alphaIIbbeta3 JON/A | PE | emfret | M023-2 |
| anti-mouse/rat CD42d | APC | Biologend | 148506 |
| Anti-mouse CD41 | FITC | Biologend | 133904 |
| anti-mouse Ly6G | PB | Biologend | 127612 |
| anti-mouse CD184 (CXCR4) | PE | eBioscience™ | 12-991-82 |
| anti-mouse Ly6G (clone 1A8) | PE | Biologend | 127608 |
| anti-mouse GPIX | AF488 | P0p6 derivative | Stegner Lab |
| anti-mouse CD41a (clone MWReg30) | PE | eBioscience™ | 13-0411-82 |

| | | | |
|--|----------------|----------------|------------|
| Streptavidin eFluor 450 | - | eBioscience™ | 48-4317-82 |
| Streptavidin | PE | eBioscience™ | 12-4317-87 |
| anti-mouse CD144 Biotin VE-cadherin (clone eBioBV13) | - | eBioscience™ | 13-1441-82 |
| anti-mouse rat CD31 (clone 13.3) | - | BD Biosciences | 550274 |
| anti-mouse rat CD54/ICAM-1 (clone YN1/1.7.4) | FITC | Biolegend | 116106 |
| Purified anti-mouse CD11a (clone M17/4) | - | Biolegend | 101101 |
| anti-human CD184 (CXCR4) (clone 12G5) | PE | Biolegend | 306506 |
| anti-human CD16 (clone 3G8) | FITC | Biolegend | 302006 |
| anti-human CD16 | BV421 | BD Bioscience | 562874 |
| anti-Human Platelet GPVI (clone HY101) | BV421 | BD Bioscience | 743941 |
| anti-human CD62P (P-Selectin) (clone AK4) | AF700 | Biolegend | 304932 |
| anti-human CD42b (clone HIP1) | BV650 | BD Bioscience | 303926 |
| anti-human CD154 (clone 24-31) | BV510 | Biolegend | 310830 |
| anti-human CD61 (clone VI-PL2) | PE-Dazzle™ 594 | Biolegend | 336426 |
| anti-human CD29 (clone MAR4) | PE | BD Bioscience | 557332 |
| anti-human CD41 (clone HIP8) | PE/Cy5 | Biolegend | 303708 |
| anti-human CD11b (clone ICRF44) | PE | Biolegend | 301306 |
| anti-human CD41/CD61 (clone PAC-1) | AF647 (APC) | Biolegend | 362806 |
| anti-human CD63 (clone H5C6) | APC/Cy7 | Biolegend | 353046 |
| Mouse IgG2a, K isotype Control (clone MOPC-173) | - | Biolegend | 400212 |

2.2 Reagents and chemicals

Table 3. Reagents and chemicals used in this thesis.

| Reagents and Chemicals | Supplier | Catalog Number |
|------------------------------------|---------------|-------------------|
| Qtracker705 Vascular labels | Thermo Fisher | Q21061MP |
| Instant adhesive 910 Metal Bonding | Permabond | GJ1705 |
| Recombinant mouse thrombopoietin | Immunotools | 12343615 |
| Sytox™ Blue Dead Cell Stain | Invitrogen™ | S34857 |
| DAPI | SIGMA | 10236276001 |
| Hoechst 33342 | invitrogen | H3570 Lot# 40801A |
| 10% Normal Goat Serum | invitrogen | 50062Z |
| DNase I | Sigma | D4527 |
| Dispase | Gibco™ | 17105-041 |
| Collagenase D | Roche | 11088882001 |
| Penicillin/Streptomycin | Gibco™ | 15140122 |
| DMEM F12 | Gibco™ | 11320033 |
| Tween-20 | SIGMA | Lot# SLCH9711 |

| | | |
|---|---------------------|---------------------------|
| Triton™ X-100 | SIGMA | Lot# SLCJ6163 T8787 |
| Paraformaldehyde | SIGMA | Lot# SCLCH9711 P1379 |
| MgCl ₂ | Roth | 2189.2 |
| Saponin | Roth | Art.-Nr. 4185.1 |
| Propidium Iodide-FluoroPure™ Grade | Invitrogen | P21493 |
| Pure Link RNase A | Invitrogen | Lot# 2364671 |
| U46619 | Cayman | 16450 |
| Thrombin | Chrono-Log | P/N386 |
| Phorbol 12-myristate 13-acetate | Sigma-Aldrich | P8139 |
| Thiazole Orange | Sigma-Aldrich | 390062 |
| 2',_7_'Dichlorodihydrofluorescein diacetate | Sigma-Aldrich | D6883 |
| EZ-Link™ Sulfo-NHS-Biotin | Thermo Fisher | 27217 |
| BD FACST™ Lysing Solution | BD Biosciences | REF 349202 Lot# 2034961 |
| RPMI-1640 Medium | SIGMA | Lot# RNBK3072 |
| DPBS with calcium and magnesium | Sigma-Aldrich | D8662 |
| FBS Superior | Biosell | BS.S0615 |
| PBS 10x without calcium and magnesium | Life Technologies | 70013-065 |
| DMSO | Roth | A994.2 |
| Heparin-Natrium 25000 | ratiopharm | - |
| HEPES buffer solution 100ml | Sigma | 83264 |
| Glucose | Merck Chemicals | 346351 |
| Collagen | Sigma-Aldrich | CAS 102382 |
| Kollagenreagens Horm | Takeda Austria GmbH | REF 1130630 Lot# 11893864 |
| Rhodamine 6G | Sigma-Aldrich | CAS 989-38-8 |
| Calcium Chloride dihydrate | Merck | CAS 102382 |

2.3 Assays

Table 4. Assays and items used in this project.

| Commercial Assays/Items | Supplier | Catalog Number |
|--|--------------------|-----------------------|
| Collagen 15u-Slide VI | Ibidi | 80661 |
| Plaque 15 sticky-Slide I ^{0.2} Luer | Ibidi | 80168 |
| Coverslips for sticky-Slides | Ibidi | 10812 |
| Proteome Profiler Mouse XL Cytokine Array | R&D systems | ARY028 |
| Neutrophil Isolation Kit, mouse | Miltenyi Biotec | 130-097-658 |
| Mr. Frosty™ Freezing Container | Thermo Scientific™ | 5100-0001 |

2.4 Machines and equipment

Table 5. Machines and equipment used in this project.

| Machines and Equipment | Supplier | Model |
|--------------------------------------|----------------------------|------------------------------------|
| BD LSR Fortessa | BD-BectonDickinson | LSRFortessa |
| BD FACS Melody | BD-BectonDickinson | FACSMelody |
| Zeiss Axio Imager M2 Epifluorescence | Carl Zeiss | Axio Imager2 |
| Zeiss LSM 880 Confocal | Carl Zeiss | LSM 880 with Airyscan |
| TriM Scope II-Two-Photon Microscopy | LaVision Biotech | TriM Scope |
| SimpliAmp Thermal Cycler | Thermal Fischer Scientific | - |
| PCR Detection System | BioRad | MyIQ Single Color Real-Time Cycler |
| AMERSHAM Image Quant 800 | Cytiva | 29399481 |
| AxioObserver | Zeiss | Axio Observer |

2.5 Software

Table 6. Software used in this project.

| Software and algorithms | Distributor |
|--------------------------------|------------------------------|
| FlowJo | Treestar |
| tSNE | FlowJo plugin |
| FlowSOM | FlowJo plugin |
| IMARIS | Bitplane |
| ImageJ/FIJI | National Institute of Health |
| Prism | Graphpad |
| PowerPoint | Microsoft MS |

3. Methods

3.1 Human general practices and methodology

3.1.1 Obstructive sleep apnea human samples

OSA patients who were referred to the breathing disorder ambulance at the LMU (Ludwig Maximilian University) in the city center of Munich, were prospectively screened for the study before undergoing polysomnography screening. Post-patients were recruited three months after initiation of CPAP therapy. Blood samples were taken by venous puncture and were collected in citrate tubes (provided by Sarstedt) at approximately the same time every Friday. Patients diagnosed with OSA which is described with $AHI \geq 5$ obstructive sleep events per hour and free of recognized conditions affecting the thrombotic profile of patients were eligible for the study. Control subjects were recruited from the co-workers through advertising. Control subjects were healthy subjects who were not receiving any medications or not having any known disease. Some of the control subjects (n=9) had a normal physical examination and laboratory tests and underwent polysomnography to exclude the presence of sleep-disordered breathing. The LMU Committee on human research approved the study by the SNORE ("Retikuläre Thrombozyten als neuer potentieller Biomarker bei Schlafbezogenen Atemstörungen"). Written informed consent was agreed upon by all study participants.

3.1.2 Flow chamber assay on collagen

Collagen mixture was first prepared of collagen in SKF (Kollagen Reagens Horm Suspension) in 1:3 dilution. Afterward, flow chambers' slides were covered with 250 $\mu\text{g/ml}$ collagen at 37°C for one hour and then rinsed with PBS (phosphate-buffer saline). Subsequently, 1 ml of citrated human blood was stained with 0.01% Rhodamine at 37°C for 15 min. As soon as the blood was infused into the chamber, 6mM CaCl_2 was included. Perfusion of 93,9 $\mu\text{l/min}$ and a high shear rate of 1000/s [112], were used since this is commonly acknowledged to simulate ex-vivo arterial-shear conditions. Images were captured by multi-fluorescence microscopy (Zeiss, Germany), every 5 sec over 3 min. Platelet aggregate and thrombus surface coverage were analyzed by macro-scripting (which is an automation of analyses by processing and analysis then recording all steps and finally applying to complete experimental series) using

ImageJ/FIJI to avoid any error or non-specificity in measuring the thrombus formation over time.

3.1.3 Plaque preparation and flow chamber

3.1.3.1 Plaque preparation from human thrombi

Frozen human thrombi sequestered from patients at LMU, were first placed on sterile Petri dishes on ice to take pictures, sizes, weights, and brief allure descriptions of each of the samples. Subsequently, plaque material was cut into small pieces and transferred to a glass potter including cold dialysis buffer (NaCl & EDTA) on ice. The tissue was minced in a homogenizer potter in the dialysis buffer for 30 min. The dissociated sample was frozen at -80°C. Before the use of plaque in the flow chamber, a newly generated plaque was tested with a multiplate analyzer (Roche) for the clotting time and AUC (area under the curve) with citrate blood and hirudin blood. The best plaque criteria were by having the clotting time of citrated blood under 5 min, and the AUC of Hirudin blood after 6 min incubation was more than 50. The five best plaques were mixed in equal volumes and stored at -80°C for future use under a flow chamber.

3.1.3.2 Flow chamber assay on plaque

Coverslips for sticky slides (Ibidi) were first soaked in 100% ethanol and left to dry before being used. A small rectangle of 5x8 mm was drawn on the backside in the center exactly the same on all slides used for this experiment. Plaque was diluted (1:200 in PBS), vortexed, and then left on ice for 30 min. 5 µl of supernatant was distributed in the small rectangle as a thin layer and left to dry overnight at 4 °C. Next day, slices with plaque were wedged to the flow chamber (sticky-Slide I^{0.2} Luer) and then perfused with PBS for 1 min at 100 µl/min flow rate. Subsequently, flow chamber was flushed by 4% BSA at the same rate. Similarly to the above-described blood preparation, 100 µl of Rhodamine was added to 2 ml of citrated whole blood as done before with collagen. Immediately before starting the syringe blood perfusion at 400 u/min, 12 µl of CaCl₂ (1mol) was added to incubated blood. Platelet aggregate and thrombus surface coverage were analyzed by macro-scripting with ImageJ/FIJI.

3.1.4 Human whole blood freezing

Lysing/fixation Buffer 10x (1:10) diluted in distilled water and added to whole citrated blood for 20 min at RT (room temperature). Following centrifugation, the pellet was suspended with

a freezing buffer consisting of 45% DMSO, 45% FBS, and 10% RPMI-1640 in cryogenic tubes stored for 24 hours in Mr. Frosty followed by long-term storage at -80 °C.

3.1.5 Sorting of neutrophils from frozen whole blood

1ml of PBS was added to the FACS tube containing whole blood. The mixture underwent centrifugation at 650g for 7 minutes. Next, the liquid above the sediment was discarded and only 100 µl of the pellet was left. Antibodies for neutrophils CD16-FITC (1:100, clone 3G8 BioLegend), and CD11b-PE (1:100, clone ICRF44 BioLegend) were incubated with the pellet for 30 minutes in a place without light at RT. PBS (500 µl) was added, then the sorting of cells was performed. These cells underwent centrifugation at 1200g for 7min and then the pellet was stored at -80°C. A minimum of 360,000 (to 1.1 million) neutrophils were sorted from 500 µl of blood for mass spectrometry-based proteome analysis.

3.1.6 FlowSOM clustering methodology and tSNE analysis

Clustering algorithms and non-linear dimensionality reduction methods such as flowSOM and tSNE analysis were implemented on high-dimensional cytometry data sets from whole blood of patient/control samples. A set of platelet antibodies at 1:100 dilution in PBS were used including CD41-PE/Cy5 (ITGA2B or gpIIb), CD29-PE, CD61-PE/Dextered, CD41/CD61-AF647, CD63-APC/Cy7, CD154-BV510 (or CD40L), CD42b-BV650 (GPIb α), CD62p-AF700 (P-selectin), and GPVI-BV421. 90 µl of the antibody dilution was added to 10 µl frozen blood and incubated for 10 min before being fixed with 1% PFA (paraformaldehyde) and processed into flow cytometry analysis. A compensation protocol for all colors was set up using beads before any measurement. The same number of platelets (10,000) was gated by down-sampling before concatenation for further analysis with tSNE and flowSOM plugins of FlowJo software.

3.1.7 Quantification and imaging of human RPs

3.1.7.1 Measurement of RPs

20 µl of human blood was fixed with 1% PFA for 10min. The sample is washed by adding PBS and centrifuged to get a pellet. RPs were labelled with CD41-PE/Cy5 (1:100) and TO of 250 ng/ml for 25 minutes exactly to be measured using flow cytometry. The same number of events was gated in both samples of individual blood with TO and without TO so that the reticulated platelet population would be determined precisely in every single human sample.

3.1.7.2 Imaging of RPs

Blood cells were incubated for 15min with CD41-PE/Cy5 (1:100, clone HIP8 BioLegend) and TO (250 ng/ml). To analyze stained reticulated platelets under flow conditions, platelet adhesion on collagen surfaces was quantified after 15 sec of arterial flow (shear rate 1000/s [112]) using a confocal microscopy equipped with a 60x oil objective lens. TO fluorescence strength of platelets was analyzed using IMARIS software.

3.2 Mice general practices and methodology

3.2.1 Mice strains and ethics

C57BL/6J mice were bought from Jackson Laboratory and Charles River. Mice such as Rosa26-Confetti (Gt(ROSA)26Sortm1(CAG-Brainbow2.1)Cle/J) [113,114], Pf4-Cre (or Cxcl4-iCre) (C57BL/6-Tg(Pf4-icre)Q3Rsko/J) [115] and Lyz2-eGFP (or LysM-eGFP/ Lyz2^{tm1.1Graf}) (B6.129P-Lyz2tm1(EGFP)1.1Graf) [116], were obtained from the Jackson laboratory. Rosa26-Confetti^{-/-} Pf4-Cre(+)-Lyz2-eGFP mice were generated by a triple knock-in, first by mating the Rosa26-Confetti with Pf4-Cre mice, then crossing with the mouse line Lyz2-eGFP. Mrp8-Cre/CXCR4^{fl/fl} transgenic mice were generated by crossing Mrp8-Cre (B6.Cg-Tg(S100A8-cre,-EGFP)1Ilw) with CXCR4^{fl/fl} mice (B6.129P2-Cxcr4tm2Yzo/J); provided by Prof. Hidalgo. vWF-eGFP mice were also used in this study; vWF is the promoter driving GFP in transgenic mice, to visualize platelets and megakaryocytes [117].

Every mouse strain underwent backcrossing and had a C57BL/6 background. Mice of the similar sex and age were matched and allocated to experimental cohorts, unless stated otherwise. Mice of both genders were 10-14 weeks old at the time of performing experiments. All murine experiments were conducted at the Walter-Brendel center and hospital of LMU. Mice experiments were approved by the local authorities and were conducted under regulations and guidelines of Bavarian regulations of the animal welfare.

3.2.2 Anesthesia

Mice were exposed to Isoflurane of around 5.0 Vol. % and Oxygen (2%) until the respiration rate of mice became very slow and all reflexes were lost. Mice were then injected intraperitoneally (i.p., 100µg/10g of body mass) with a mixture termed MMF consisting of

Medetomidine (0.05 mg/kg), Midazolam (5 mg/kg) in addition to Fentanyl (0.05 mg/kg). Upon deeply anesthetizing mice, harvesting of tissues was carried out following cardiac perfusion with PBS for flow cytometry experiments and followed with 4% PFA for staining experiments. During surgeries, heating lamps/maps were used to keep mice with a steady body temperature (BT). To mitigate the pain after myocardial infarction/ischemia-reperfusion surgeries, Buprenorphine of 0.1 mg/kg [118] was administered subcutaneously to operated mice. Following experiments, mice were immediately sacrificed by cervical dislocation.

3.2.3 Mice models

3.2.3.1 Intermittent hypoxia treatment model

IH treatment was performed on age- and sex-paired mice. Mice of the same age and type were randomly assigned into either normoxia mice or hypoxic mice undergoing IH condition with repetitive cycles (60 events/hour [119]) of apneic events decreasing O₂ concentration to 6% (20 sec), followed by a 40-sec long period of reoxygenation to 21% O₂ [120] over seven days. Briefly, the hypoxic chamber is regulated by time periods during which oxygen and nitrogen gases are released and their levels are calculated using a sensor placed in the cover of the chamber which is safely isolated from mice for security and hygienic concerns. The programmed display and on/off switch were connected to the murine chamber with the help of mechanical and electronic engineers. Directly after treatment, mice were sacrificed and sample analysis was performed. For long-term IH, mice were exposed to 21 days of IH with the same settings as mentioned above.

3.2.3.2 Myocardial infarction ischemia-reperfusion model

Male mice at 10-14 weeks old were ligated for one hour of the left anterior descending (LAD) coronary artery or operated as a sham. Mice were sedated on a heating map/pad to preserve their BT. Subsequently, the skin was removed to expose the trachea, and a tube was connected to the ventilator and positioned inside the visible trachea so the mouse had a constant rate of respiration of 150 breaths per minute. The third and fourth ribs were pulled away from each other to expose the thoracic cavity. The LAD artery was uncovered after carefully removing the pericardium. Afterward, a stitching needle of silk (8-0) was gently entered approximately 2.5 mm beneath the LAD. The occlusion of LAD and thereby ischemia was maintained for one hour followed by reperfusion [121]. For operated sham mice, the stitch was softly passed underneath the LAD, without undergoing any ligation.

LAD was cautiously liberated from the ligature after 60 min. Later, the skin layer, muscle, and chest cavity were sutured respectively with a stitch filament (5-0). Post-operation, mice were held in sterile warmed cages with Buprenorphine given every 8 hours. Blood samples and organs were harvested from mice 48 hours following the surgery for flow cytometry and imaging analysis.

3.2.3.3 Carotid artery model

After mice were anesthetized, a 2-minute application of a 1 mm² Whatman paper immersed with of 1 µL FeCl₃ (10%), injured the right carotid artery and induced thrombus formation in the murine artery [122]. Labeled platelet antibody GPIb with X488 fluorescence was injected (0.5 µg/g body mass) to visualize and record the attachment of platelets to the area of injury. The video was recorded for an hour with an intravital microscope and later analyzed using Zen software.

3.2.4 Intravital live imaging using multiphoton microscopy

The calvarium mouse model was prepared as explained in our published paper [123]. In summary, mice were sedated by repetitively injected with MMF every 40-45 min. Subsequently, the head hair was shaved and a PE-10 (polyethylene) catheter was inserted using tissue adhesive into the mouse tail vein to deliver fluid and antibodies. A custom-made metal ring was fixed on the skull using glue (Permabond 910, GJ1705) to include PBS and then ultrasound gel and avoid dehydrating the tissue throughout imaging. Using a special platform and a heated pad to preserve BT, the mouse was secured immobile. Neutrophils were visualized by intravenous injection of Ly6G-PE antibody (20 µl, clone 1A8), megakaryocytes were labeled by GPIX-AlexaFluor488 (p0p6 derivative, 15 µl, provided by Stegner Lab) and vessels were visualized with Qtracker705 (around 15 µl).

3.2.5 Whole-mount bone imaging using confocal microscopy

Tissue preparation: After mice were anesthetized, the murine chest was open and the liver was cut. Then, the blood is flushed by cardiac puncture by injecting PBS and subsequently 4% PFA. Bones, lungs, spleen, and heart were isolated from mice and incubated for 1-2 hours in 4% PFA and subsequently in sucrose (30%) refrigerated for a night. Later, tissue was inserted in Tissue-Tek[®] OCT and then stored at -80°C. Tissues were cautiously cut using a HistoCryostat

instrument. Frozen Bones were cut horizontally until bone marrow was fully exposed. Thereafter, bones were immersed in a blocking solution of a goat serum (10%) and BSA (3%) overnight at 4°C to be stained for vessels, megakaryocytes, and neutrophils as described next.

After washing the samples carefully with PBS, bones are incubated directly with 1:100 dilution of CD144 antibody for 6-8 hours at 4°C. After washing gently in PBS, the tissue was incubated with a secondary antibody Streptavidin eFluor 450 (eBioscience™ REF 48-4317-82) (1:50 dilution) overnight at 4°C. The next morning, bones were repetitively cleaned with PBS and then conjugated antibodies CD41-FITC and Ly6G-PE (1:100 dilution) were added for 6-8 hours at 4°C or RT for 2-3 hours. Nuclei were then counter stained with DAPI (2:1000) or Hoechst (1:1000) for 10-15 min and washed for 5 min 3 times in 1x PBS before being 3D imaged using confocal microscopy. Images were processed and quantified using Imaris software.

3.2.6 Neutrophil adoptive transfer

Bones were isolated to collect bone marrow from Lyz2-eGFP (LysM-eGFP) mice or Mrp8-Cre/CXCR4^{fl/fl}/LysM-eGFP mice with increased fluorescent (green) proteins in neutrophil populations. Subsequently, neutrophils were isolated using a kit. Afterward, mice (C57BL/6) received an injection of 2.5×10^6 neutrophil cells through the tail vein. 60 minutes post the adoptive transfer, the injected mice were MMF-tranquillized and underwent heart perfusion with PBS followed by 4% PFA. After fixation, bones were frozen in OCT at -80°C and then stained utilizing the whole mount staining technique as described before.

3.2.7 Lung tissue staining and confocal imaging

Mice were subjected to cardiac perfusion and then lungs were cryoprotected as defined before. Tissue was sectioned in 30 µm sections and fixed on slides using PFA (4%) for 10-15 min and rinsed in a liquid mixture that consists of 0.5% BSA, 10% PBS (10x) along with 0.1% Tween-20 in distilled water before permeabilizing with Triton (X-100, 0.5%). The blocking of samples was for a night in goat serum (10%) and Triton. The next morning, sections were stained for 8 hours using CD31 (clone: ME13.3 BD Pharmingen #550274) then washed and stained in a secondary antibody goat anti-rat AF647 (1:200 Invitrogen #A21247). After being washed thoroughly, blocking of tissue sections took place for 45-60 min in BSA (10%) at RT. Antibodies like CD41-PE or/and CD54 (ICAM-1)-FITC were added for a few hours. To make sure of the megakaryocyte population in the lung, MK was double stained with CD41 and CD42b

antibodies. Sections were counterstained with Hoechst (1:1000) or DAPI (2:1000) and pictured using a confocal microscope enhanced with Z-stack and airyscan processing. Post-image processing was performed using Imaris.

3.2.8 Bone marrow (BM) and lung cell isolation

Briefly, bones were separated from muscle and skin and cut at both ends to uncover BM which was flushed out using PBS with 2% FBS. BM was homogenized into single cells using a 20G needle, purified via the use of a strainer (70 μ m), and resuspended in RBC Lysis buffer. After a few minutes, the lysis effect was congested in PBS comprising EDTA (2 mM) and centrifuged. Trypan blue elimination was used to specify the number of viable/dead cells.

Postperfusion, lungs were harvested, and chopped into small pieces using a scalpel prior to digestion in a buffer that contains DPBS with calcium and magnesium (Sigma-Aldrich), DNase I (Sigma cat. D4527), dispase (Gibco 17105-041), and collagenase D (Roche cat. 11088882001) [124]. This lung digestion cocktail was gently agitated for 45 min at 37°C before being filtered and RBC lysed.

3.2.9 Flow cytometry and cell quantification

Post centrifugation and pellet collection, cells were then incubated with antibodies (1:100) in a buffer including PBS complemented with 2% FBS for half an hour on ice. Sytox blue was used to exclude the presence of dead cells. Murine neutrophils were detected by Ly6G-PB (Biolegend127612); T cells, and B cells were identified by CD3-FITC (BD Bioscience 555274) and CD45R-PE/Cy5 (eBioscience™ 15-045282), respectively. The monocyte population was gated by GR-1^{high}-PB (Biolegend 108430) and CD115^{high}-PE (Biolegend 135506).

3.2.10 Quantification of murine platelets and RPs

ACD (Acid citrate dextrose) buffer (1:7 dilution ACD: Blood) was used with blood withdrawal from the murine heart. For platelet staining, a few microliters (2 μ l) of murine blood were labeled with CD42d-APC (1:100 diluted in PBS). Cells were incubated in a dark place at 20-25°C for 30 min. PBS (300 μ l) was pipetted to the sample along with 1:100 counting beads just before flow cytometry analysis.

For RPs staining, 5 μ l of murine whole blood was stained in 100 μ l PBS with 1 μ l CD42d-APC and 1 μ g/ml thiazole orange (TO). Following incubation for half an hour in an obscure place and at RT, 1% PFA was added to the cells prior to flow cytometry analysis. The double positive population of CD42d and TO (FITC channel) was gated as young RPs population.

3.2.11 Measurement of platelet lifespan

To quantify the lifespan of platelets, mice were i.v. labeled with SulfoNHSBiotin (30 mg/kg of body weight) [125]. Starting with the first day following biotinylation, 20 μ l anticoagulated blood was punctured from the tail vein, at specified time points. CD42d-APC along with streptavidin-PE were then added at 1:100 dilution in PBS for half an hour in place without light. The positive population of CD42d identified the proportion of platelets attached to biotin/streptavidin. 100% of platelets were streptavidin positive at day one and later the ratio of platelet population declined gradually.

3.2.12 BM cytokine profiling in mice

Seven days after initiation of intermittent hypoxia or normoxia, mice were sacrificed and bones were sequestered. Bones were cut open at one end and then centrifugated for five minutes at 10,000 g speed in another Eppendorf tube containing 300 μ l PBS to separate the BM interstitial fluid.

A murine kit for cytokine profiling (XL) was utilized in compliance with the instructions provided by the company [126] to analyze quantitatively cytokine levels in BM. In summary, the cocktail antibody was mixed in BM fluid and left for 60 minutes to incubate. Afterward, streptavidinHRP was added to the membranes for 30 minutes. ECL substrate was included to identify the specific chemiluminescence membrane signal and image it by AMERSHAM Image Quant 800. Using ImageJ, the mean intensity of each dot in relation to the reference signal was analyzed by the densitometry of every cytokine signal.

3.2.13 LFA-1 antibody blocking experiment

A 50 μ g of CD11a antibody or its isotype (used as a control) was i.v. administered to mice (C57BL/6) at day1, day3, day5 and day7 of intermittent hypoxia treatment. Subsequently, mice were sacrificed for organ and blood collection.

3.2.14 Tail bleeding assay

After sedating mice with MMF, the terminal part of the tail was chopped at 1 cm and directly dipped in a Falcon tube including warmed water of around 37°C until bleeding stopped [127] (Fig. 4.19). The tail was placed vertically and every mouse was supervised for approximately 25 min even though bleeding concluded, to identify any recurring blood flow. A timer was used to define the time interval of bleeding. The total of all bleeding periods within 25 minutes was calculated if the on/off phases of the bloodstream happened. Following the trial, mice were terminated by cervical dislocation. The time interval between the tail cut and cessation of bleeding was assessed by visual inspection of the tubes and was described as the bleeding time.

3.3 Further experiments

3.3.1 Measurements of blood count

A heart puncture was used to collect murine blood in a tube containing ACD buffer (1:7 ratio of ACD: blood) to be analyzed by a hematology machine. Citrated blood samples from healthy donors and patients were drawn venously and quantified using an automated system (hematocytometer) at the hospital of LMU.

3.3.2 Calculation of ROS

The level of ROS was quantified in murine neutrophils of bone marrow and blood. Cells were lysed in 1x erythrolysis blood buffer for 10 min at 4°C then washed and centrifuged for pellet collection. Either PMA (phorbol 12-myristate 13-acetate, 50 nM) or SDF-1 (200 ng/ml) together with PMA (50 nM) were used for 30min to activate neutrophils. Successively, DCFDA (2',7'Dichlorodihydrofluorescein diacetate, 10 nM) along with Ly6G-PE (1:100) were added to cells for 20 min. The same neutrophil counts underwent an identical DCFDA labeling but in the absence of stimuli to be used as control.

To measure ROS in human blood, 1% PFA was used to fix around 20 µl citrate blood for 10 min. Then PBS was added and the sample was centrifuged for 700g for 5 min at RT with acceleration of 4 and no brake. The pellet was stained for 15 min with 5mM DCFDA, CD16-BV421 (1:100) for

neutrophil staining along with CD41-PE/Cy5 (1:100) for platelet staining to be analyzed using flow cytometry.

3.3.3 CXCR4 quantification

After the lysis of cells and wash, murine neutrophils were subsequently stained with Ly6G-BV421 (1:100) and CD184-PE CXCR4 antibody (1:50) or isotype (1:50) for half an hour. Then, the sample is washed before undergoing flow cytometry analysis.

Human CXCR4 quantification in neutrophils was performed similarly but with anti-human antibodies CD16-Fitc (1:100, clone 3G8 BioLegend), CD184-PE (clone12G5) and PE mouse IgG2a, k isotype control.

3.4 Statistical analysis

Data was tested for significance using Prism7 (GraphPad) and all bars presented in the figures of this project showed mean \pm SEM (unless written otherwise) with a significant statistical p-value < 0.05 . Please note that “ns” presented in the figures means non-significance of p-value and symbols used in the figures indicate single animals or individuals. Replicates or the number of animals/subjects in every group “n” of every experiment can be found in each figure legend. The normality was checked using Shapiro-Wilk (for $n \leq 4$) or Kolmogorov-Smirnov normality tests (for $n \geq 5$). For comparing the two groups, a Student’s t-test was applied. Mann-Whitney test (used for nonparametric distribution) or unpaired 2-sided t-test were used to compare a set of data of two. The paired Student’s t-test was presented in studies involving samples from the same mouse or patient; otherwise, Wilcoxon rank sum test was utilized. A test of Tukey-HSD for one-way ANOVA (analysis of variance) or a two-way ANOVA was applied to compare multiple data sets for normally distributed data. In addition, plaque and collagen surface coverage aggregation over time was calculated using computational Macro-scripting on FIJI/ImageJ.

3.5 Clinical characteristics of human samples

Table 7. Clinical descriptions of OSA patients and controls (healthy individuals) recruited in this study project.

Obesity is considered with body mass index over 30; SD: standard deviation, y: years, n: number, h: hour, %: percentage.

| Clinical Characteristics of OSA Patients and Healthy Individuals | | |
|--|----------------|---------------|
| | OSA | Healthy |
| Total number [n, female] | 50 [13] | 9 [4] |
| Age [y], ± SD | 53.69 ± 10.19 | 56.00 ± 10.43 |
| Erythrocyte (T/l), ± SD | 4.82 ± 0.42 | 5.00 ± 0.34 |
| Hemoglobin (g/dl), ± SD | 14.48 ± 1.17 | 14.91 ± 1.21 |
| Platelet (G/l), ± SD | 255.72 ± 57.68 | 241.71 ± 35.6 |
| Leukocyte (G/l), ± SD | 6.49 ± 1.74 | 6.21 ± 1.43 |
| Neutrophil (%), ± SD | 58.90 ± 8.73 | 57.50 ± 1.43 |
| Creatinine (mg/dl), ± SD | 0.96 ± 0.18 | 0.84 ± 0.14 |
| PDW (fL), ± SD | 11.86 ± 1.42 | 11.00 ± 1.58 |
| Apnea-Hypopnea Index (AHI) (n/h), ± SD | 31.85 ± 25.44 | 1.83 ± 1.15 |
| Minimal Oxygen Saturation (%), ± SD | 80.18 ± 8.20 | 86 ± 2.61 |
| Arterial Hypertension, n [%] | 26 [52] | 4 [44.4] |
| Diabetes, n [%] | 7 [14] | 2 [22.2] |
| Smoke, n [%] | 16 [32] | 1 [11.1] |
| Bronchial asthma, n [%] | 9 [4.5] | 0 [0] |
| Hypercholesterolemia, n [%] | 10 [20] | 2 [22.2] |
| Obesity, n [%] | 8 [16] | 3 [33.3] |

Table 8. Clinical characteristics of OSA patients pre- & post-therapy recruited in this study (n=9 per group).

Obesity is considered with body mass index over 30; SD: standard deviation, y: years, n: number, h: hour, %: percentage.

| Clinical Characteristics of OSA Patients PRE & POST CPAP Therapy | | |
|--|----------------|---------------|
| | PRE | POST |
| Total number [n, female] | 9 [3] | |
| Age [y] , ± SD | 57.33 ± 17.64 | |
| Erythrocyte (T/l), ± SD | 4.67 ± 0.46 | 4.58 ± 0.43 |
| Hemoglobin (g/dl), ± SD | 14.28 ± 1.23 | 13.81 ± 1.24 |
| Platelet (G/l), ± SD | 241.11 ± 48.98 | 225 ± 49.17 |
| Leukocyte (G/l), ± SD | 7.76 ± 1.84 | 7.08 ± 1.18 |
| Neutrophil (%), ± SD | 58.5 ± 11.07 | 55.57 ± 11.08 |
| Creatinine (mg/dl), ± SD | 1.2 ± 0.72 | 1 ± 0.15 |
| PDW (fl), ± SD | 13.13 ± 2.23 | 12.87 ± 1.88 |
| Apnea-Hypopnea Index (AHI) (n/h), ± SD | 43 ± 27.10 | 11.61 ± 9.88 |
| Minimal Oxygen Saturation (%), ± SD | 78 ± 5.93 | 83.14 ± 6.59 |
| Arterial Hypertension, n [%] | 8 [88.88] | |
| Diabetes, n [%] | 1 [11.11] | |
| Smoke, n [%] | 3 [33.3] | |
| Bronchial asthma, n [%] | 0 [0] | |
| Hypercholesterolemia, n [%] | 0 [0] | |
| Obesity, n [%] | 4 [44.44] | |

4. Results

4.1 Obstructive sleep apnea and intermittent hypoxia

4.1.1 PDW, MPV, and platelet immature fraction are boosted with the severity of OSA

OSA is a common sleeping disorder that can influence platelet function [128]. Since platelet function is considered a key mechanism leading to cardiovascular diseases in OSA, it was postulated that the severity of sleep apnea will predict the response of platelets regardless of identified comorbidities [128,129]. To address the clinical significance of our project and to examine the effects of OSA on platelet compartments and thrombopoiesis, OSA subjects were recruited with an AHI (OSA severity index) of more than 5 after undergoing polysomnography (Table 7) along with healthy controls. Although platelet counts of OSA patients did not display a positive correlation with disease severity (i.e. AHI); MPV along with PDW presented an increase with the severity of the disease (Fig. 4.1A). Gunbay et al. reported a similar increase in PDW and MPV levels of OSA patients [130].

Different methodologies including various dyes for RNA and diverse gating strategies were applied in research studies to identify the immature platelet fraction [131]. In our project, reticulated platelets (RPs, i.e. RNA-rich platelets) counts were measured using CD41 and TO (Thiazole orange) dye that stains residual cytosolic RNA in young immature platelets (or RPs). Likewise, a positive correlation of RP counts with AHI of OSA patients was found (Fig. 4.1B). In summary, these results indicate an augmented platelet volume and distribution width with disease severity in OSA patients, and RPs may be a new potential marker of severe OSA patients.

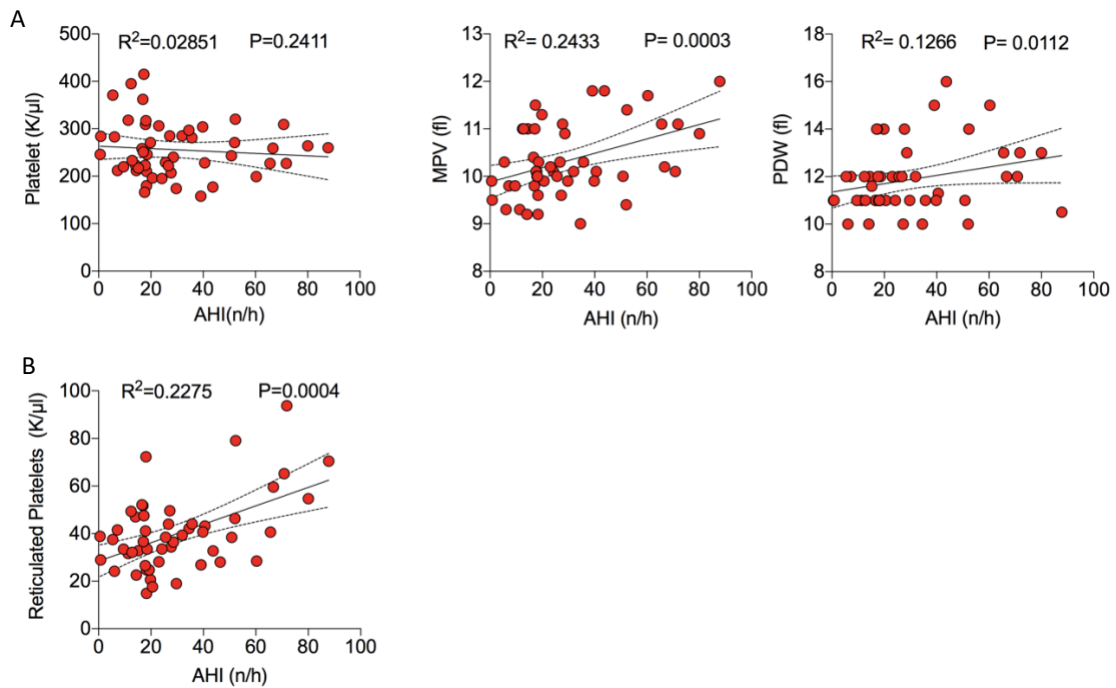


Figure 4.1. Effects of OSA on platelet compartments.

(A) Linear correlation analysis of AHI (Apnea-hypopnea index) vs. platelet, mean platelet volume (MPV), platelet distribution width (PDW), or (B) reticulated platelets of OSA patients, respectively (n=50 patients). Significance levels are shown, *<0.05, **<0.01, ***<0.001 and ns. P-values were measured with linear regression.

4.1.2 Thrombus formation is driven by RPs under arterial flow conditions

Accumulating evidence indicates the association of OSA with arterial thrombosis, atherosclerosis, and a high risk of mortality [132,133]. The formation of arterial thrombus after the rupture of plaque is induced by atherosclerotic and thrombogenic plaque components such as collagen and tissue factor (TF), triggering an avalanche of accumulating platelets and coagulation [133,134]. It was stated that von Willebrand factor (vWF) is an essential mediator in the adhesion of platelets to atherosclerotic plaques and collagen fibers resulting in platelets' aggregation at high shear flow conditions [133,135]. To define whether the increased release of RPs in OSA patients contributes to increased thrombotic risk, ex-vivo thrombus formation was examined under arterial flow conditions. Fluorescent-labeled whole blood from OSA patients showed an increased platelet aggregation and thrombus formation on collagen compared to healthy controls (Fig. 4.2A). This increased thrombus formation was due to exaggerated recruitment of RPs to collagen under OSA as shown by preferential recruitment of TO high RPs (Fig. 4.2B). Arterial thrombus formation was also investigated on human plaque

under the flow, plaque was collected from a pool of patients as described in the methods section above. Data presented an increased trend of thrombus formation of OSA blood on plaque although statistical analysis did not show significance (Fig. 4.2C); further research with a larger sample size may validate the observed pattern. These results conclude that excessive young reticulated platelets expose OSA patients to increased thrombotic risk.

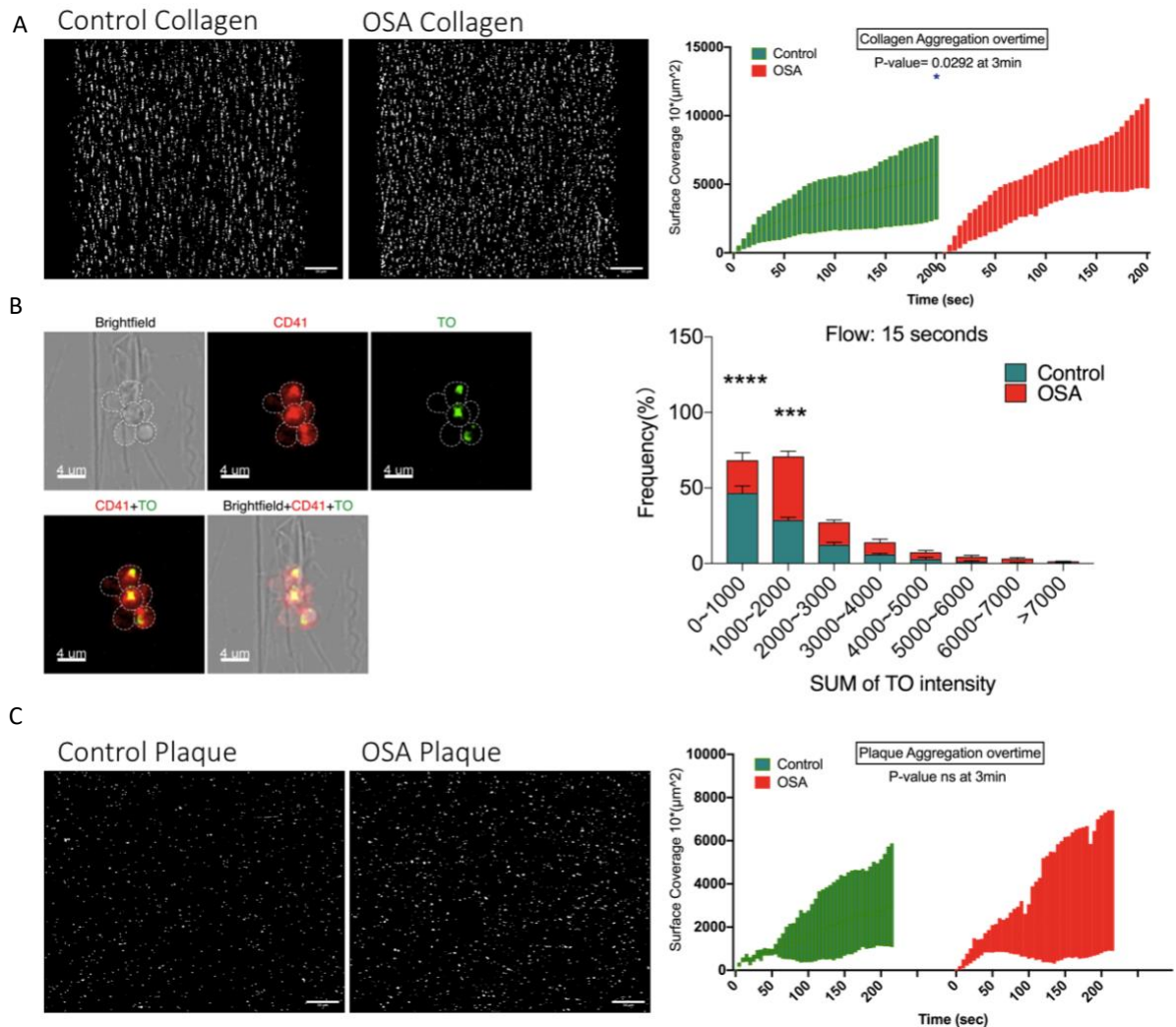


Figure 4.2. Platelet aggregation and accumulation of OSA blood.

(A) Representative images (100 μm) of adhesion and aggregate accumulation of platelet on collagen-coated flow chambers after 3 minutes of blood flow (left panel) and quantification of total surface coverage is automated and quantified by macro-scripting with ImageJ/FIJI (right panel) (n=7-8 individuals per group). (B) Representative image (4 μm) of thiazole orange (TO) staining of whole blood in OSA patients or controls after 15 sec of flow (left panel). The dashed line indicates platelet shape and red and green fluorescence represents CD41 and TO respectively. Distribution analysis of total TO fluorescence intensity in OSA patients or healthy controls; n=4 individuals per group (right panel). (C) Representative images (100 μm) of adhesion and aggregate accumulation of platelet on plaque-coated flow chambers after 3 minutes of blood flow (left panel) and quantification of total surface coverage is automated and quantified by macro-scripting with ImageJ/FIJI (right panel) (n=4-5 healthy controls or

patients per group). Significance levels are implied with * <0.05 , *** <0.001 , **** <0.0001 or ns calculated with two-way ANOVA.

4.1.3 Platelet activation markers are highly expressed in OSA patients

Platelet activation markers are crucial indicators in estimating the thrombotic risk in different diseases. The augmented hyperactive profile of platelets has been correlated with numerous inflammatory diseases [136]; yet, there is a lack of studies on platelet activation markers and thrombosis associated with sleep apnea. Therefore, the platelet activation in patients subjected to OSA was quantified along with a control group using an in-depth high-dimensional flow cytometric examination (tSNE plus flowSOM) of eight platelet populations (Pop0-Pop7) (Fig. 4.3B-D). OSA platelet showed a prothrombotic phenotype with elevated expression of activation markers of subpopulation 6 (Pop6) (Fig. 4.3C,D), which are P-selectin, PAC-1/active α IIb β III and CD63 under resting conditions (Fig. 4.3E); indicating that OSA' platelets exhibited a stronger thrombotic profile than these in controls. Moreover, concatenated OSA platelet populations and control platelet populations are expressed distinctly from each other as illustrated in Fig. 4.3G,H.

Thus, this analysis differentiates control from OSA by visually (heatmap and color-coded overlapping) and quantitatively distinguishing the difference in platelet markers expression; meaning that platelets are activated differently under OSA.

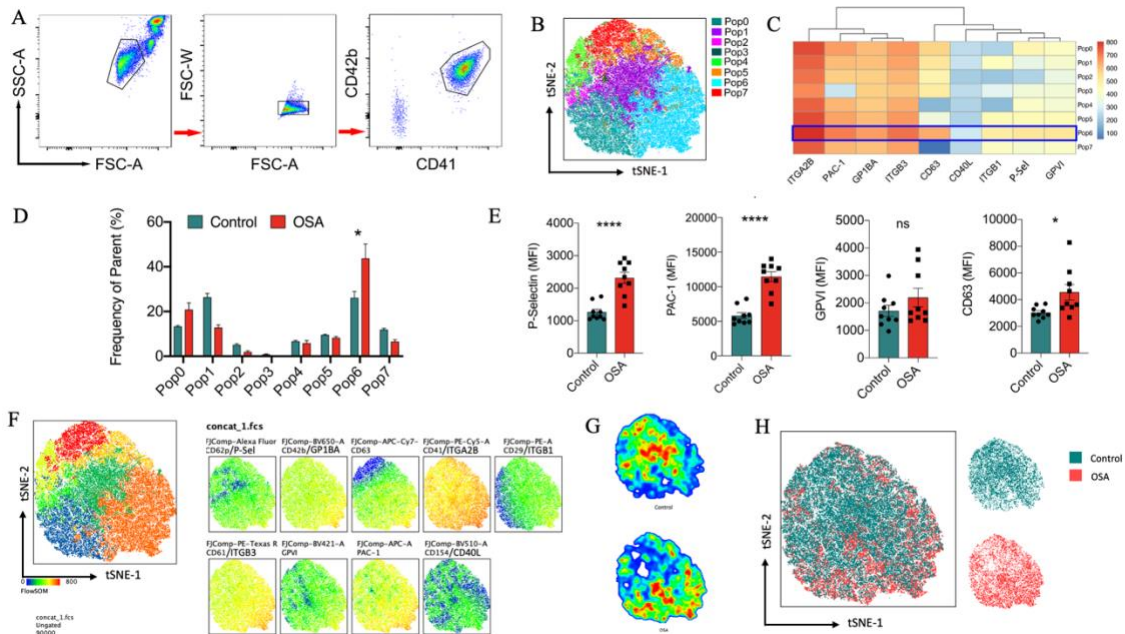


Figure 4.3. Extensive flow cytometric platelet markers evaluation.

(A) Scheme of the gating strategy of platelet population by double positive gating of CD42b and CD41. (B) Color-coded flowSOM platelet populations are illustrated. (C) A relative mean fluorescence intensity (MFI) to maximum MFI of platelet markers was presented as a heatmap for every subcluster of platelets. (D) Platelet population frequency and (E) platelet markers of sub-population 6 are presented. (F) Color-coded tSNE-flowSOM expressions of each of the platelet markers used are presented. (G) Heatmap cluster to show the difference between control and OSA. (H) Color-coded clusters overlapped for further demonstration of the two distinct populations; n=9 healthy controls or OSA patients per group. Significance levels are specified as * <0.05 , **** <0.0001 , and ns. Two-way ANOVA along with unpaired t-test were used to define p-values.

4.1.4 Activation markers are elevated on immature platelet fraction

Next, it was important to distinguish which platelet fraction is responsible for the increased platelet activation observed in OSA patients. This is why activation markers were quantified on mature platelets and RPs of resting cells. RP's population was gated by double positive TO and CD41 and then P-selectin and CD63 mean fluorescence intensity was calculated using FlowJo. As presented in Fig. 4.4C, platelet activation markers were found to be significantly elevated on immature RP fraction in healthy individuals. A noticeable upward trend of activation markers was expressed on RPs in OSA patients (Fig. 4.4D). Together, these data indicate that RPs are the major contributor to platelet hyperactivity and accordingly its clinical implications.

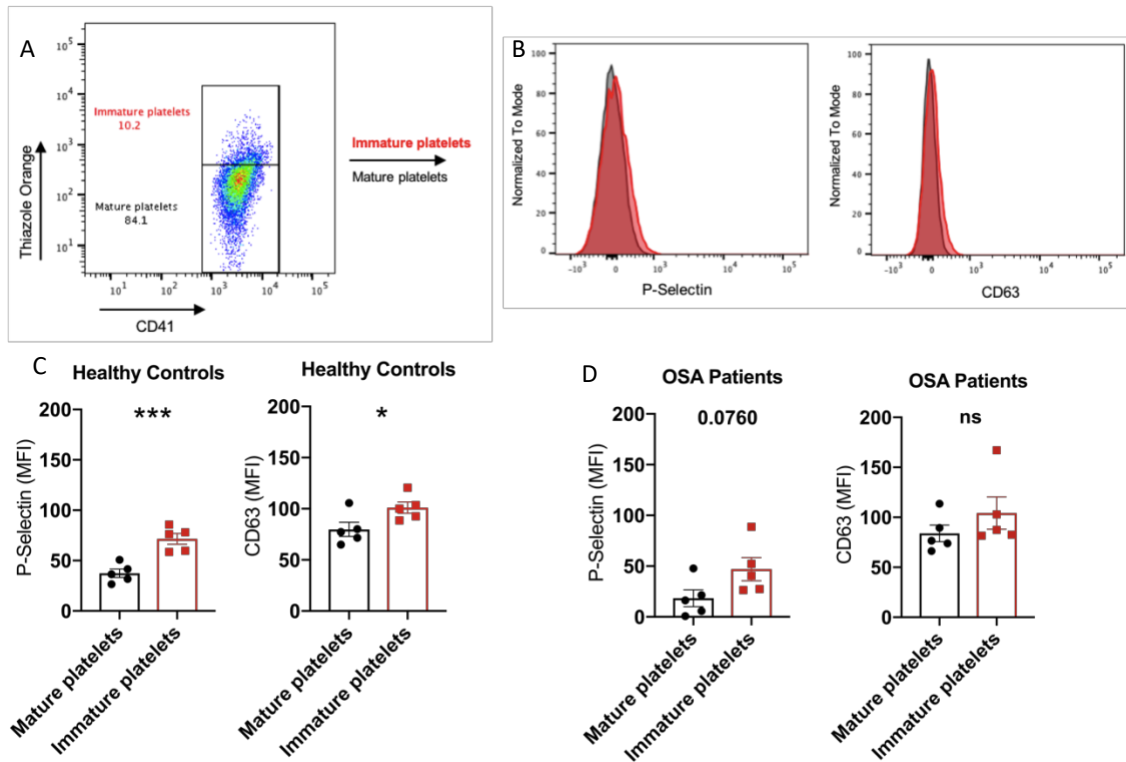


Figure 4.4. Activation markers on platelet and RP fractions.

(A) Gating scheme of mature and immature platelets using thiazole orange (TO) and CD41. (B) Histogram normalized to mode between mature platelets (black) and immature reticulated platelets (red). (C) Mean Fluorescent Intensity (MFI) of platelet markers in healthy individuals and (D) in OSA patients are represented; n=5 individuals. Significance levels are identified with * <0.05 , *** <0.001 , and ns. An unpaired t-test was used to indicate p-values.

4.1.5 Augmented neutrophil counts are associated with increased platelet number

Neutrophils may play a crucial role in enhancing thrombopoiesis under inflammatory conditions. It was thought that there is a connection between platelets and neutrophils driving thromboinflammation which is considered a key interest topic in cardiovascular diseases [137]. To understand the relation of neutrophils with the enhanced platelet counts of OSA, the correlation between platelets and neutrophil numbers was examined. Accordingly, data showed that OSA patients have elevated platelet and neutrophil counts (Fig. 4.5). This positive correlation may consequently result in the amplified generation of oxidative stress (i.e. ROS) resulting in an increased risk of thrombotic events.

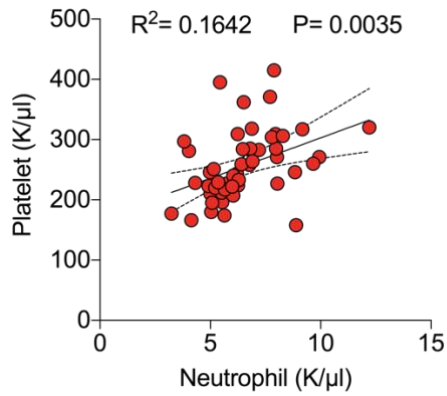


Figure 4.5. Correlation of neutrophil and platelet counts in OSA patients.

Linear correlation analysis of platelets vs. circulating neutrophils of OSA patients; (n=50 patients). P-values were determined with linear regression.

4.1.6 ROS level is boosted in circulating neutrophils under OSA

It was found that peripheral blood neutrophils in OSA patients have an increased ROS production which was attributed to the more severe OSA [138]. In addition, it was also reported that in blood platelets, ROS are generated in various signaling pathways; resulting in platelet activation [139]. To examine the exact source of ROS production in OSA, ROS expressed in platelets (CD41-PE/Cy5) and ROS expressed in neutrophils (CD16-BV421) were both quantified in the circulation of control and OSA patients; using DCFDA (5mM) (Fig. 4.6).

ROS expression in platelets showed no difference between control and OSA; however, ROS expressed on circulating neutrophils was significantly increased in OSA patients compared to control healthy individuals. Therefore, ROS production is augmented in the circulation of OSA patients and this increase in ROS level is neutrophil-derived.

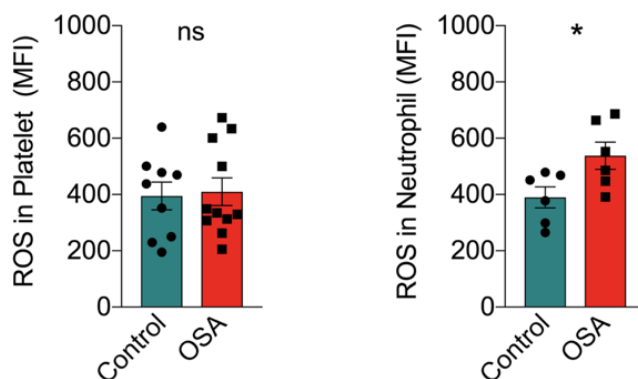


Figure 4.6. Circulating neutrophils increase ROS levels under OSA.

Flow cytometer analysis of the mean fluorescent intensity (MFI) of ROS level in platelet (n=9 control subjects and n=11 OSA patients) and ROS in neutrophils in the blood of control individuals vs. OSA patients presented as histograms (n=6 individuals per group). Significance levels are indicated, * <0.05 , and ns. An unpaired t-test was used to identify the p-values.

4.1.7 CXCR4 expression on neutrophils is enhanced in OSA

Chemokines are considered crucial mediators in the migration and release of neutrophils in homeostasis and disease [32]. CXCR4 was identified as a major chemokine regulator of neutrophil mobilization and stimulation from bone marrow under inflammatory conditions [32]. CXCR4 was demonstrated to modulate neutrophil reactions in patients with lung injury [140], atherosclerosis [141], allergic asthma [142], and other diseases. However, to date, the effect of this chemokine on neutrophils has not been studied in patients with OSA disease. Therefore, CXCR4 expression was measured on peripheral neutrophils in OSA patients vs. healthy controls (Fig. 4.7A). Neutrophils in OSA patients displayed a higher CXCR4 expression (Fig. 4.7A) and this expression is closely linked to severe OSA (Fig. 4.7B). Thus, enhanced CXCR4 expression is found on circulating neutrophils in patients with severe OSA.

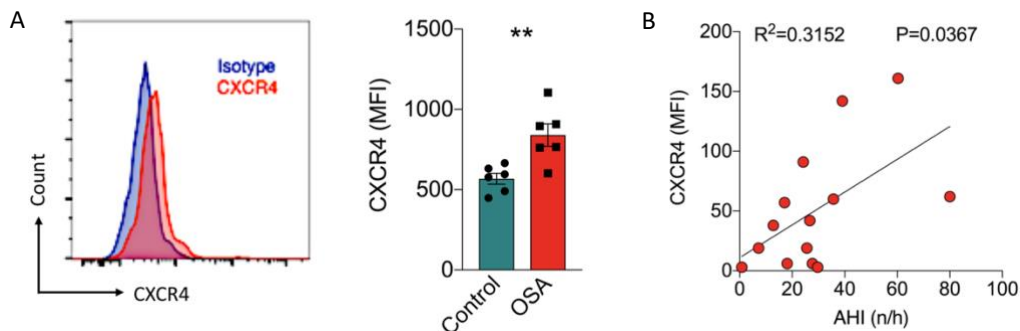


Figure 4.7. CXCR4 expression is significantly higher in severe OSA patients.

(A) Flow cytometer analysis of CXCR4 expression on neutrophils of OSA patients vs. healthy controls. An expression histogram was shown (n=6 individuals per group). (B) Linear correlation analysis of AHJ values and CXCR4 expression (subtracted from CXCR4 isotype control) in OSA patients (n=14 OSA patients). Significance levels are indicated, ** <0.01 . The presented P-values were assessed with a t-test (unpaired) or linear regression.

4.1.8 Characterization of intermittent hypoxic murine chamber

Given the vital healthcare burden presented by OSA and the ethical complications of conducting accurate mechanistic research causing OSA in patients, substantial work has been concentrating on animal models mimicking IH found in OSA patients [90,143,144]. To simulate the effects of OSA, rodents were treated with IH to simulate the oxygen profile experienced by OSA patients [145]. The use of animal models of OSA has fostered our understanding of OSA pathogenesis and its significance [90]. Animal models are being studied to explore the pathways downstream the hypoxic exposure and particularly its effect on cardiovascular disorders [146]. Normoxic mice had continuous exposure to room air [146]. Generally, numerous studies examined the effects of IH in murine models for 60 events/hour by lowering the ambient cage oxygen levels with de-oxygenation and re-oxygenation events ranging from 5% to 21% respectively; causing a change in murine arterial oxygen saturation [90,147,147].

To gain a comprehensive understanding of the molecular sequelae leading to thrombosis in more detail and to further describe the function of neutrophil-driven thrombopoiesis in OSA, an intermittent hypoxic murine model was established in our Lab mimicking the hypoxic condition in human sleep apnea patients. Mice were placed in a chamber that exposed them to repetitive cycles of low oxygen levels (6% O₂) by inducing a flow of nitrogen gas for 20 seconds, followed by 40 seconds of normal oxygen levels (21% O₂) every minute for a total of 6 hours per day, simulating the physiological relevance and pathogenesis of OSA patients. Deoxygenation and reoxygenation cycles were taking place every minute for 60 events per hour (Fig. 4.8A). The appearance of oscillating cycles and the duration of the exposure were illustrated in the display attached to the chamber as shown in Fig. 4.8B.

First, intermittent hypoxia was characterized at diverse time points; after 1 day, 3 days, and 7 days of IH exposure for 6 hours/day in comparison to normoxic mice exposed to normal air. Interestingly, IH mice sacrificed directly after hypoxic exposure showed no difference in cell count. However, a meaningful increase in PDW values was shown and most importantly in circulating platelet count after one week of IH compared to normoxic mice (Fig. 4.8C-E); reflecting the analogous results shown before in OSA patients (Fig. 4.1A). Similar to other studies, this project will further elaborate on IH directly after consecutive seven days of hypoxic exposure.

Intermittent Hypoxia 6h/day

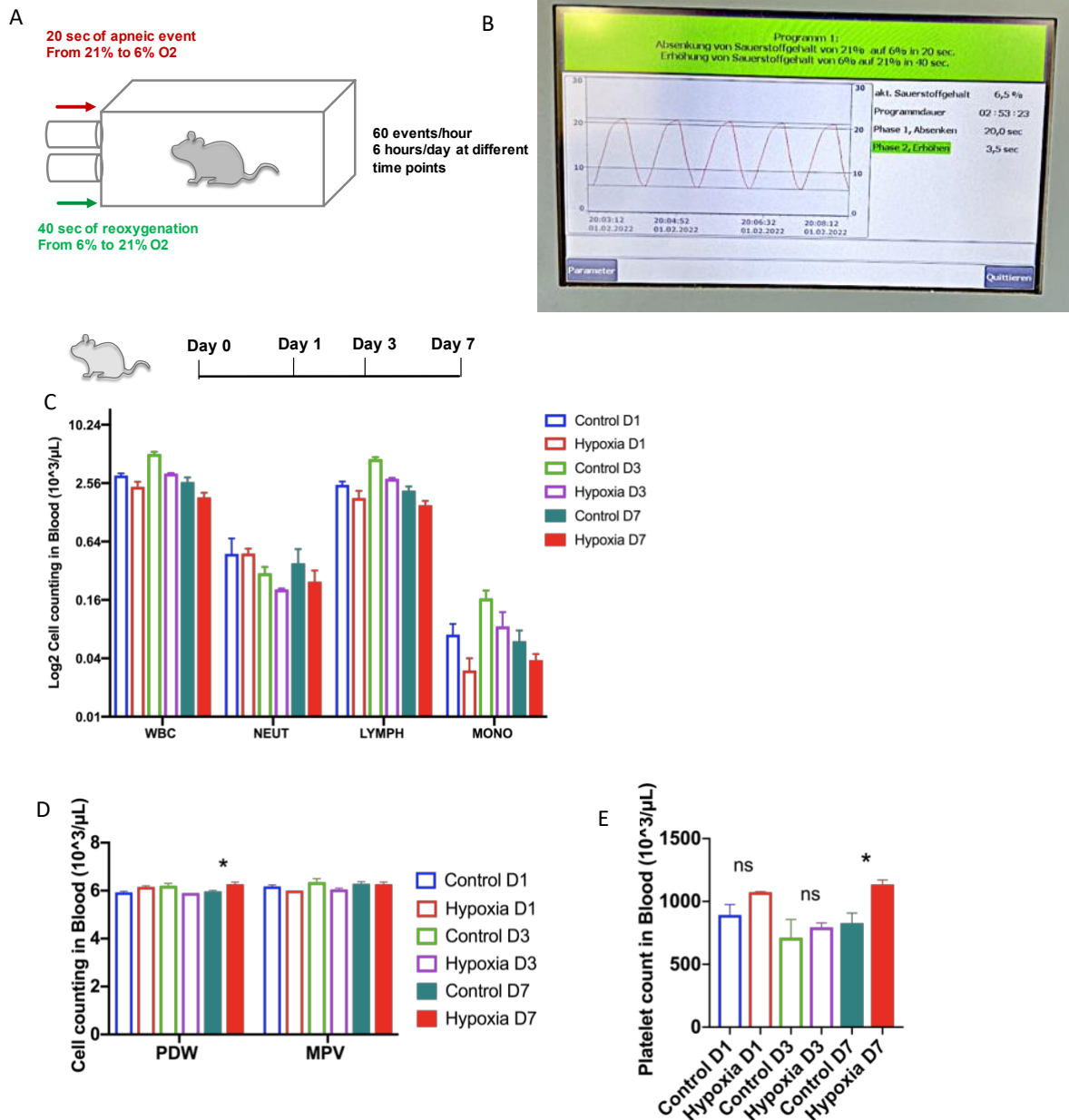


Figure 4.8. Establishing and characterization of IH at different time points.

(A) Experiments took place before IH exposure after 1 day, 3 days, and 7 days of IH exposure for 20 sec apneic events and 40 sec of reoxygenation. (B) The screen of hypoxia chamber established in our Lab presents the oscillating curve of intermittent hypoxia for 6 hours every day (the illustrative scheme is generated using PowerPoint). (C) Cell counts of WBC: white blood cell, NEUT: neutrophils, LYMPH: lymphocytes, and MONO: monocytes, (D) PDW along with MPV, (E) in addition to platelet count in blood at Day1 (D1), Day3 (D3) and Day7 (D7) were presented; n= 4-5 C57BL/6 animals per group. Significance levels are indicated with * <0.05 or ns, and determined using two-way ANOVA.

4.1.9 Thrombopoiesis is increased in mice exposed to IH

To further investigate this murine IH model and the processes leading to enhanced thrombopoiesis, flow cytometry analysis was performed on mice after seven days of IH treatment. Not only platelet but also reticulated platelet counts were amplified in IH mice (Fig. 4.9A); consistent with the results generated in OSA patients and presented in Fig. 4.1.

To question whether elevated platelet counts arise from an altered clearance, platelet lifespan was determined in the blood and was unaltered in normoxia mice vs. IH mice (Fig. 4.9B). Comparably to OSA patients, IH mice also revealed an increase in PDW values after seven days of exposure to IH (Fig. 4.9C). This increase was not seen in MPV values in IH mice (Fig. 4.9C). Cell numbers remained unaltered in blood and BM; yet, B cells presented a decrease in number in the vasculature after IH exposure for 7 days (Fig. 4.9D). Further experiments are needed to investigate the exact role of B cells under intermittent hypoxia. In summary, amplified thrombopoiesis is detected using flow cytometry in mice under IH.

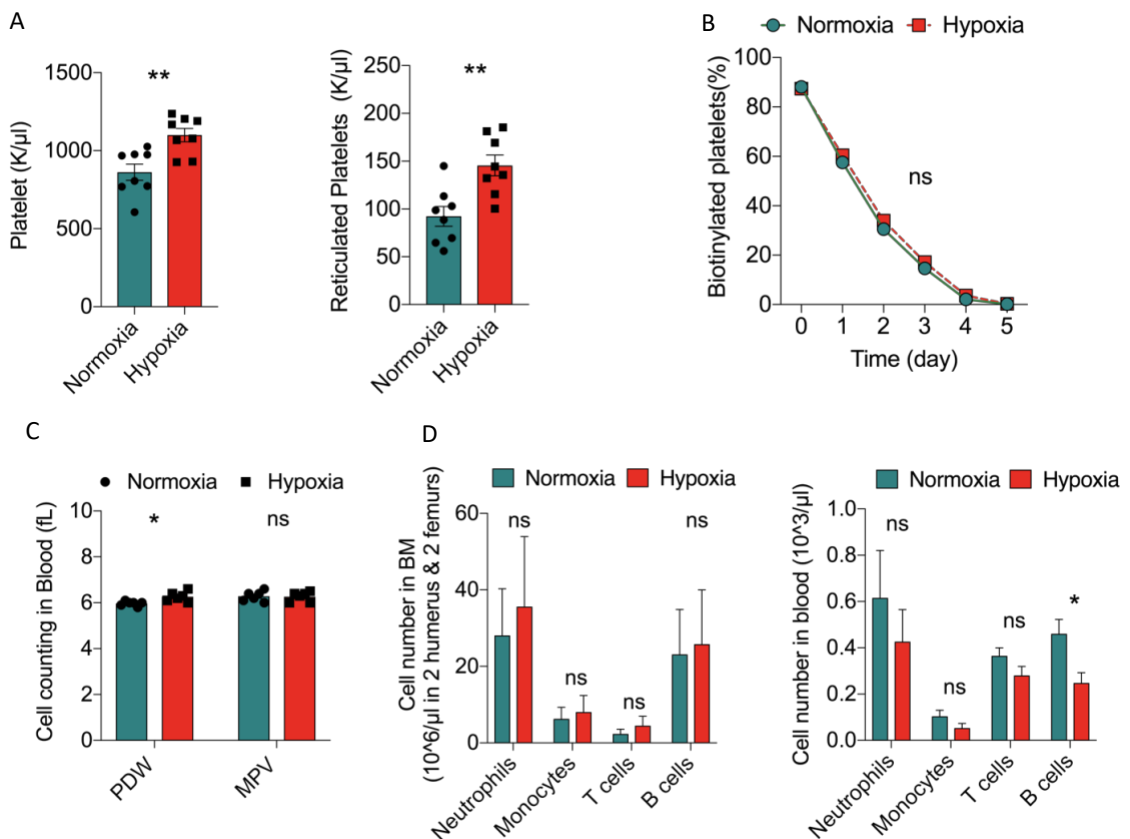


Figure 4.9. Flow cytometry measurements of mice under normoxia and hypoxia.

(A) Platelet and reticulated platelet of C57BL/6 mice (n=8 animals per group) and (B) Platelet life span in blood (n=4) were quantified under normoxic as well as 7 days of IH conditions. (C) PDW along with MPV in blood in addition to (D) leukocytes within the blood and BM of C57BL/6 mice were quantified under IH conditions; n=6. Significance levels are specified using unpaired t-test and two-way ANOVA with *<0.05, **<0.01, and ns.

4.1.10 Confocal imaging of BM shows larger megakaryocytes in IH mice

Bone marrow is the primary site of thrombopoiesis where megakaryocytes (MKs) release platelets into the vasculature and where neutrophils develop from myeloid progenitors [1,29]. Using 3D imaging, MK size, number, and ploidy were investigated and quantified in the BM of normoxia mice and mice treated for one week under intermittent hypoxia (Fig. 4.10A). Consistent with published results, Fig. 4.10A illustrated the random distribution and dispersion of MKs in BM [148].

MKs in hypoxic mice were more prominent in size compared to normoxia mice as presented in Fig 4.10B. Yet, MK numbers were unaltered in both conditions (Fig. 4.10C (left)). During the maturation of MKs, DNA replication proceeds without cytokinesis developing mature MKs of increasing ploidy to a size up to 65 μm [148,149]. MK ploidy analysis showed that MK maturation was unaffected following IH exposure (Fig. 4.10C (right)). Although Levine and his colleagues (1982) stated that the large size of MKs is correlated to greater MK ploidy [149], the findings of this study showed that the larger diameter of murine MKs was not related to greater DNA content. The neutrophil number was quantified in confocal images and showed no difference in both normoxia and hypoxic mice (Fig. 4.10D). Thus, larger MKs are visualized in BM of IH mice but no difference in the number of MKs or neutrophils is found compared to normoxic mice.

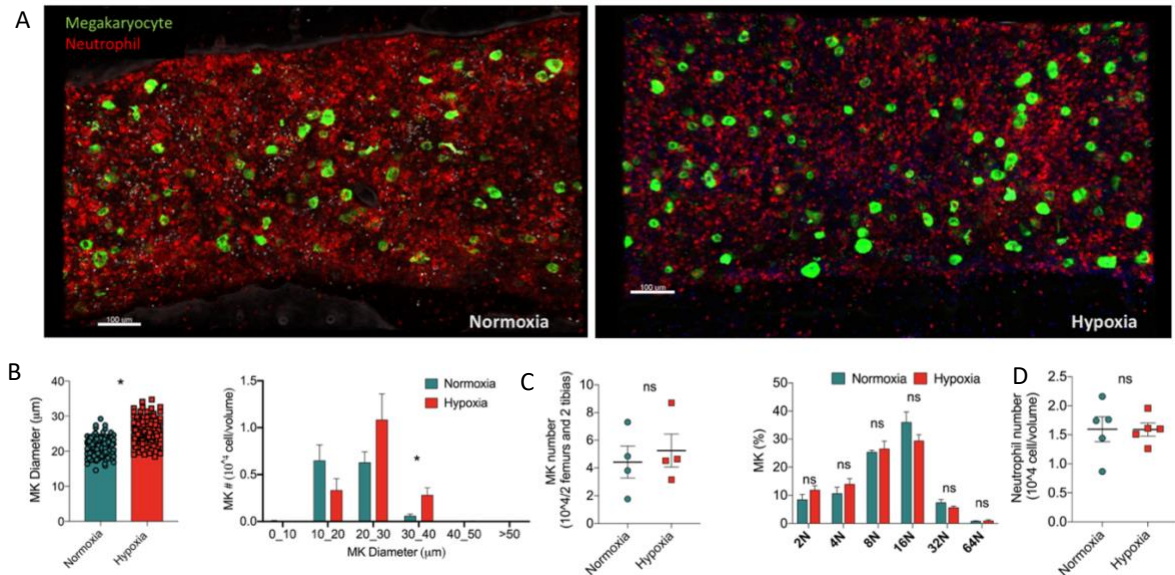


Figure 4.10. MKs in hypoxia mice have greater diameters under hypoxia.

(A) Representative 3D whole mount confocal images of bone marrow (BM) in normoxia and hypoxia mice. CD41-FITC (MK in green) and Ly6G-PE (neutrophil in red); scale bar, 100µm. (B) The diameter of megakaryocyte (MK) in µm of confocal imaging of whole bone staining and the mean number of MK (total number of MK per volume) in relation to the MK diameter (µm) were calculated (n=5 C57BL/6 animals per group). (C) MK number and ploidy (n=4 C57BL/6 animals per group) were represented. (D) Neutrophils were counted in BM and compared in normoxia and hypoxia mice (n=5 C57BL/6 mice per condition). Significance levels are indicated using unpaired t-test and two-way ANOVA with *<0.05, and ns.

4.1.11 MK comparison in BM and lung

Megakaryocytes are the progenitors of circulating platelets and until lately MKs were generally considered merely resident in BM; yet, the lung has been discovered to host MKs producing platelets [150]. Moreover, the lung is the first organ to sense oxygen level change. Thus, the megakaryocyte compartments residing within the BM and lung were reconnoitered in this project. First, a significant distinction in the MK form and sphericity was detected between BM and lung (Fig. 4.11A). Then, the MK frequency was observed in both organs; MKs were rare in the lung compared to bone marrow (Fig. 4.11B). Likewise, MK frequency and number were investigated in other studies showing that MKs in the lung are much less than MKs majorly found in BM [151–153]. MK numbers remained the same in normoxia vs. hypoxia mice in lung and BM (Fig. 4.11B). To sum up, BM MKs have higher sphericity than lung MKs and are found abundantly in BM but rarely in the lung. Besides, the number of MKs in both BM and lung

showed no difference after exposing mice to IH; meaning that the number of MK cells is not involved with increased thrombopoiesis identified under IH.

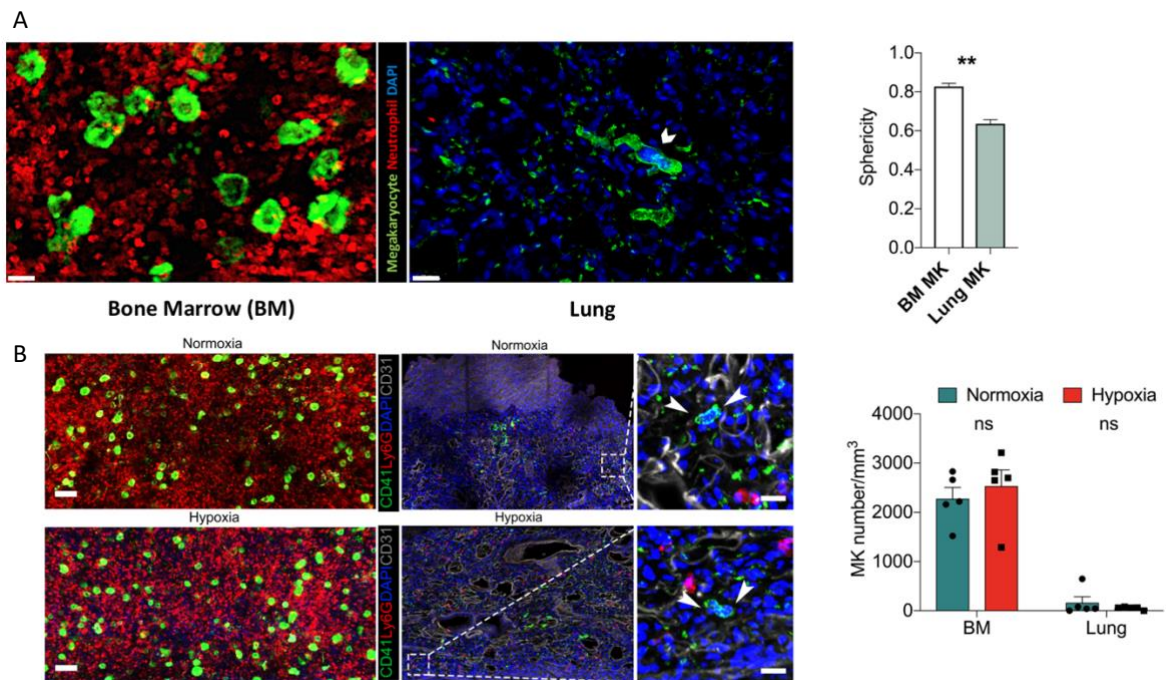


Figure 4.11. Murine BM and lung confocal imaging of MKs under normoxia and hypoxia. (A) Zoomed Representative confocal images of MKs within BM and lung, and sphericity of MK in both compartments are characterized (scale bar 20 μ m, n=4 mice). (B) Illustrative 3D images of MKs and quantification of MK frequency within BM and lung (right panel) under normoxia and hypoxia conditions; CD41-FITC (MK in green) and Ly6G-PE (neutrophil in red); scale bar in BM 50 μ m, scale bar in lung 15 μ m (n=5 animals). Significance levels are quantified by unpaired t-test and illustrated as **< 0.01 and ns.

4.1.12 ICAM-1 expression on lung arterial endothelium is higher in IH mice

ICAM-1 was found to be expressed on the endothelial wall and essential for the adhesion of neutrophils and their trans-endothelial migration [154]. Endothelial dysfunction in the vasculature was detected in OSA patients in comparison with controls [155]. Furthermore, ICAM-1 is increased in the circulation of OSA which may result in cardiovascular complications [156]. In addition, expression of ICAM-1 was found to be enhanced in the lung tissue of mice subjected to hypoxia compared with normoxic control mice [157]. Therefore, ICAM-1 was studied in this project in the lung arterial endothelium in mice to check vascular endothelial dysfunction following intermittent hypoxia in comparison to normoxic mice. ICAM-1 expression was quantified in their pulmonary endothelium and was found to be increased in

lung vessels of IH mice (Fig. 4.12). Consequently, ICAM-1 is differentially expressed in the lung endothelium and is found to be upregulated on the pulmonary epithelium of intermittent hypoxia mice; affecting neutrophil migration under IH.

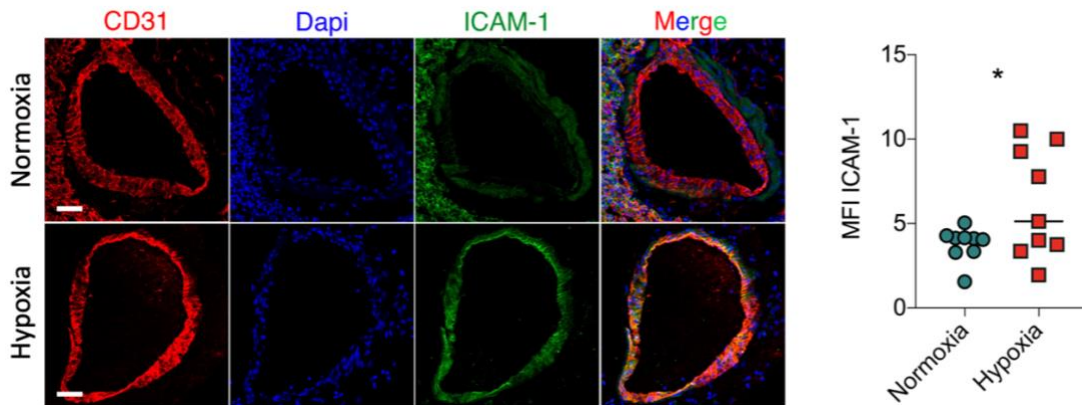


Figure 4.12. ICAM-1 is significantly expressed in the lung endothelium of IH mice
 Representative 3D images of ICAM-1 expressed on the vasculature (CD31) within the lung of normoxia and hypoxia mice and measurement of mean fluorescent intensity of ICAM-1 expression using IMARIS software, n=5 animals in every condition. The significance level is indicated as * < 0.05 and assessed using unpaired t-test.

4.1.13 MKs and neutrophils closely cooperate to increase thrombopoiesis under IH

To elucidate whether thrombopoiesis was affected under intermittent hypoxia and to identify if there is an interaction between MKs and neutrophils inside the BM, multi-photon microscopy was used to visualize the thrombopoiesis in the calvarial bone of C57BL/6 mice at normoxia vs. IH conditions (Fig. 4.13A). MKs (in green) were labeled with GPIX antibody whereas neutrophils (in red) were characterized with Ly6G antibody. It was observed that proplatelet (PPL) release speed was faster and release time was shorter in IH mice; while PPL length was similar in both groups (Fig. 4.13B). Recent studies stated that neutrophils home back to BM along with hematopoietic cells (MKs) [158] stimulating platelet production; therefore, neutrophil-MK interactions were quantified at different compartments in the bone marrow. More neutrophil-MK interactions were located in the perisinusoidal niche close to the proplatelet budding sites ($< 20\mu\text{m}$) in IH mice (Fig. 4.13C). Together, neutrophils are found to be in close engagement with MKs at the perisinusoidal PPL-budding set in the BM of IH mice promoting thrombopoiesis.

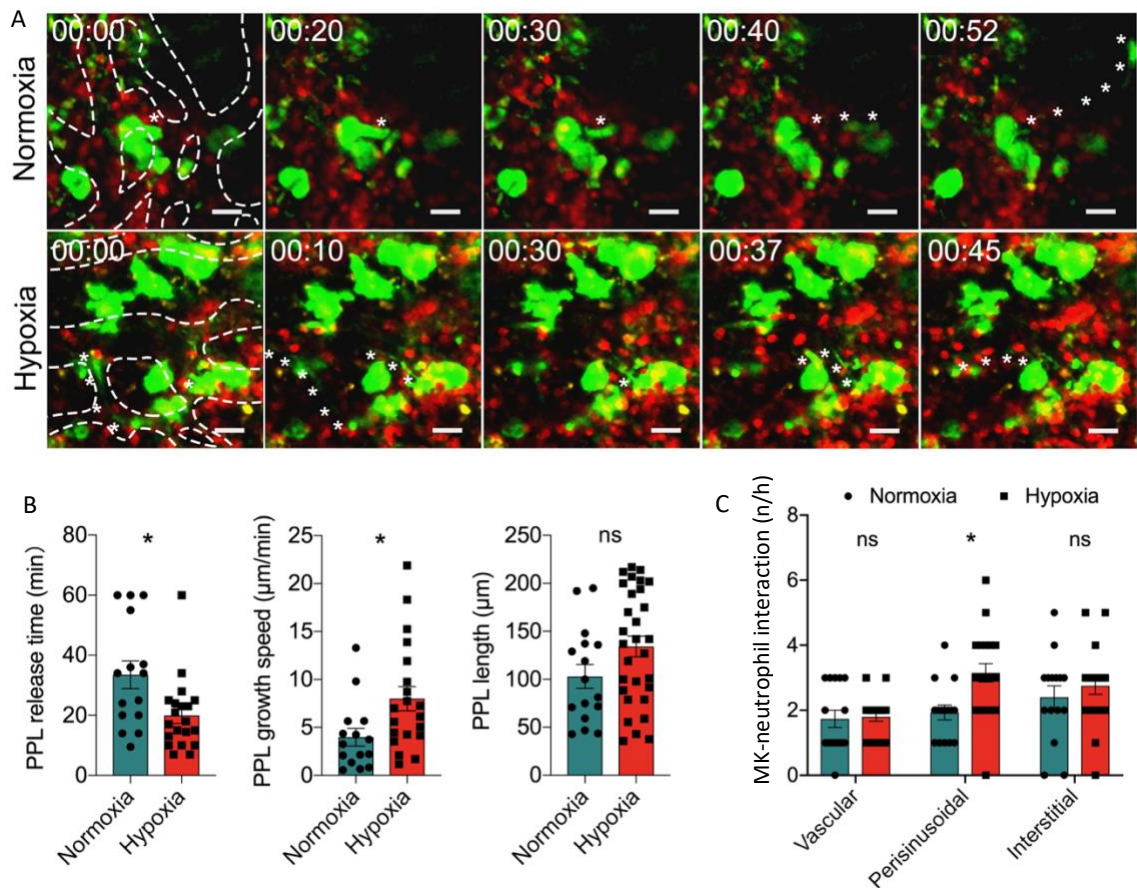


Figure 4.13. The interaction between MKs and neutrophils is visualized using two-photon imaging in normoxia and hypoxia mice.

(A) Representative image series of thrombopoiesis (green color characterizes megakaryocytes; red color represents neutrophils, an asterisk specifies proplatelet length and dash line displays the vessel border) and (B) video analysis of proplatelet growth speed, release time, and length. (C) Video analysis of MK-neutrophil interactions. 8 movies from control mice and 9 movies from IH mice were analyzed with IMARIS software, $n=3$ C57BL/6 animals per condition. Significance levels are indicated, $* < 0.05$, and ns and determined with paired t-test along with two-way ANOVA.

4.1.14 Cytokine profiling in BM is characterized under IH condition

To further ascertain whether cytokine changes within the BM interstitial, are accountable for the disparities in platelet generation in IH mice, the levels of marrow cytokines were measured (Fig. 4.14A). Key cytokines that are known to be related to MK maturation (TPO, IL6, IL11, CSF) and thrombopoiesis including IL-1 α , RANTE (CCL5), remained unaltered in both conditions (Fig. 4.14B). Some cytokines showed significance in BM of normoxia and hypoxic mice such as CCL6/C10, Endostatin, IL-33, MMP-9, RAGE, and others presented in Fig. 4.14C. Hence, the

characterization of cytokine profile in the interstitial fluid of bone marrow indicates that megakaryopoiesis/thrombopoiesis remains unaltered following IH.

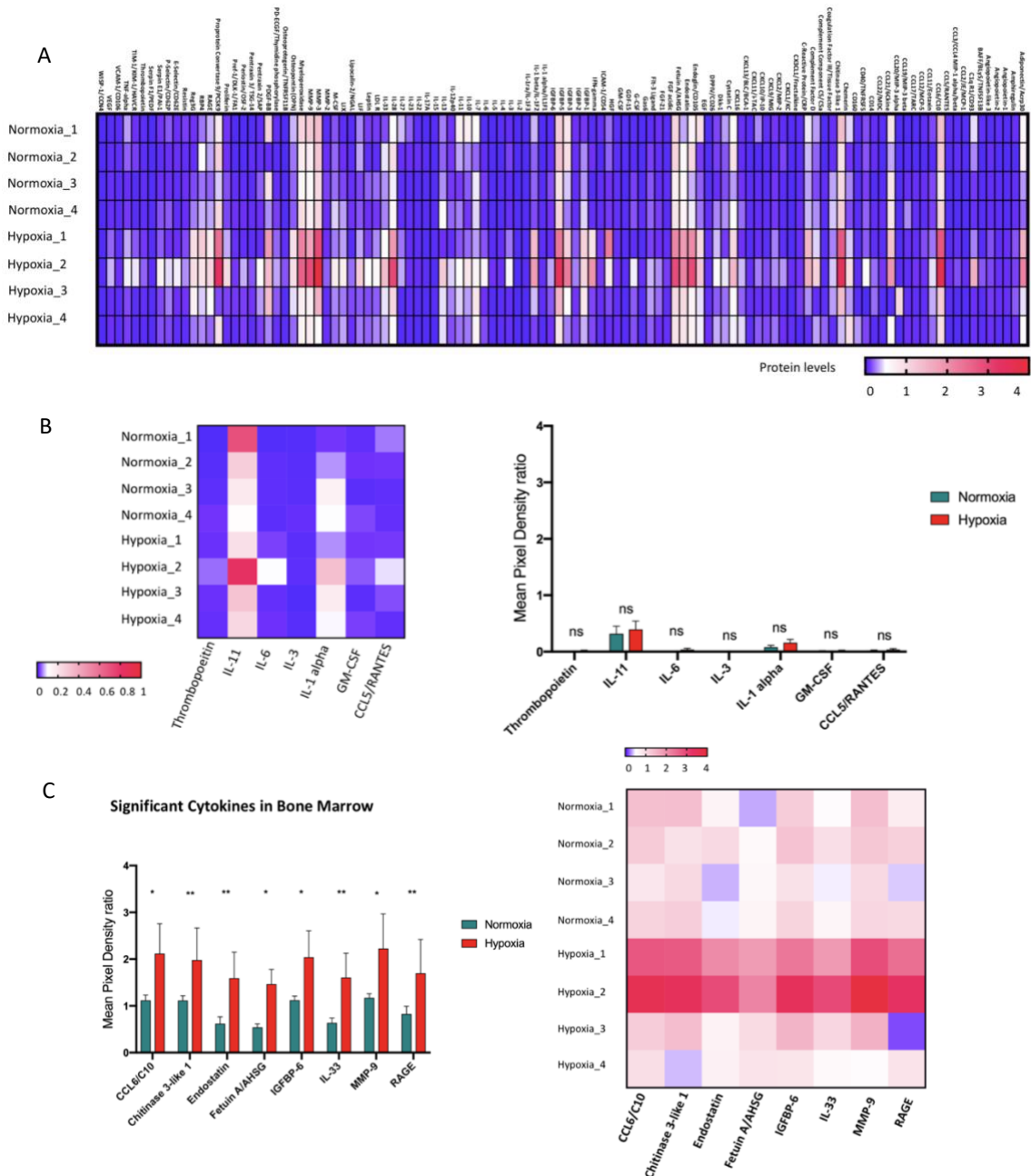


Figure 4.14. BM cytokine is quantified in normoxia and hypoxia mice.

(A) Cytokine level within the interstitial of bone marrow (BM) was quantified using a proteome profiler mouse XL cytokine kit in control normoxia mice and hypoxic (IH) mice. (B) The protein level of megakaryopoiesis/thrombopoiesis-related cytokines was quantified within BM interstitial and was examined by heat map and histogram analysis. (C) The significantly distinct cytokines levels in BM were also presented in histogram analysis by calculating the mean pixel density using FIJI/ImageJ and generating heat maps by Prism; n=4 animals per condition. Significance levels are designated (*<0.05, **<0.01, and ns) using unpaired t-test and two-way ANOVA.

4.1.15 Neutrophil-derived ROS level and CXCR4 expression in murine blood are amplified under IH

CXCR4 was identified as a major regulator of neutrophil mobilization and stimulation from bone marrow under inflammatory conditions [32]. CXCR4 expression was quantified in the blood and BM of intermittent hypoxic mice. CXCR4 expression on neutrophils was not significantly increased in BM (Fig. 4.15B). Yet, aged neutrophils which are known to upregulate CXCR4 and downregulate L-selectin [159], were studied within the bone marrow and data showed increased CXCR4^{high} neutrophils in murine bone marrow under IH (Fig.4.15C).

CXCR4/CXCL12 axis accelerates MK-neutrophil interaction to enhance proplatelet formation by direct influence and stimulation of the ROS-related mechano-signaling [123]. ROS level in blood neutrophils was found to be higher in IH mice compared to normoxia mice (Fig. 4.15D). ROS levels in BM were unaltered under hypoxic conditions (Fig. 4.15D). To sum up, CXCR4 expression and ROS level are increased in circulating neutrophils under IH, and aged neutrophils are found to be enhanced in BM of IH mice.

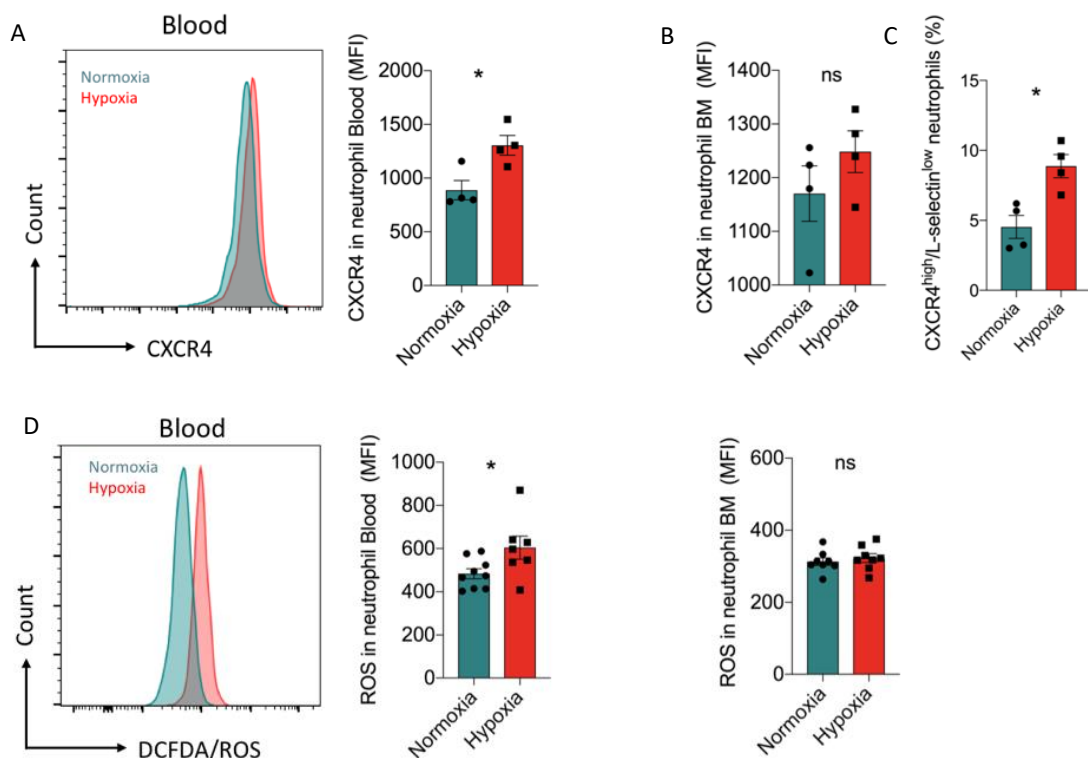


Figure 4.15. IH increases the level of neutrophil-derived ROS and CXCR4 expression.

(A) A representative histogram plot of the surface expression of CXCR4 on circulating neutrophils was presented. CXCR4 expression was quantified in blood and (B) in BM. (C) Flow

cytometer analysis of CXCR4 expression and L-selectin on BM neutrophils of normoxic versus hypoxic BL6 mice; n=4 mice per condition. (D) A histogram plot of neutrophil-derived ROS and its level was quantified in blood and BM neutrophils; n=7-9 mice per condition. Significance levels are indicated, * <0.05 or ns, and defined using unpaired t-test.

4.1.16 Neutrophil CXCR4 are critical mediators of increased platelet production

To address whether CXCR4-dependent neutrophil in close proximity to MK contributes to platelet production, the genetic ablation of CXCR4 was investigated in mice. Ablation of CXCR4 decreased platelet and RP numbers under intermittent hypoxia conditions (Fig. 4.16A), while MK number and ploidy remained unaltered (Fig. 4.16B). Unquestionably, neutrophil numbers changed rigorously in murine blood and BM (Fig. 4.16C). Thus, the CXCR4/CXCL12 signaling pathway intervenes in the interaction between MK and neutrophils leading to enhanced production of platelets and RPs.

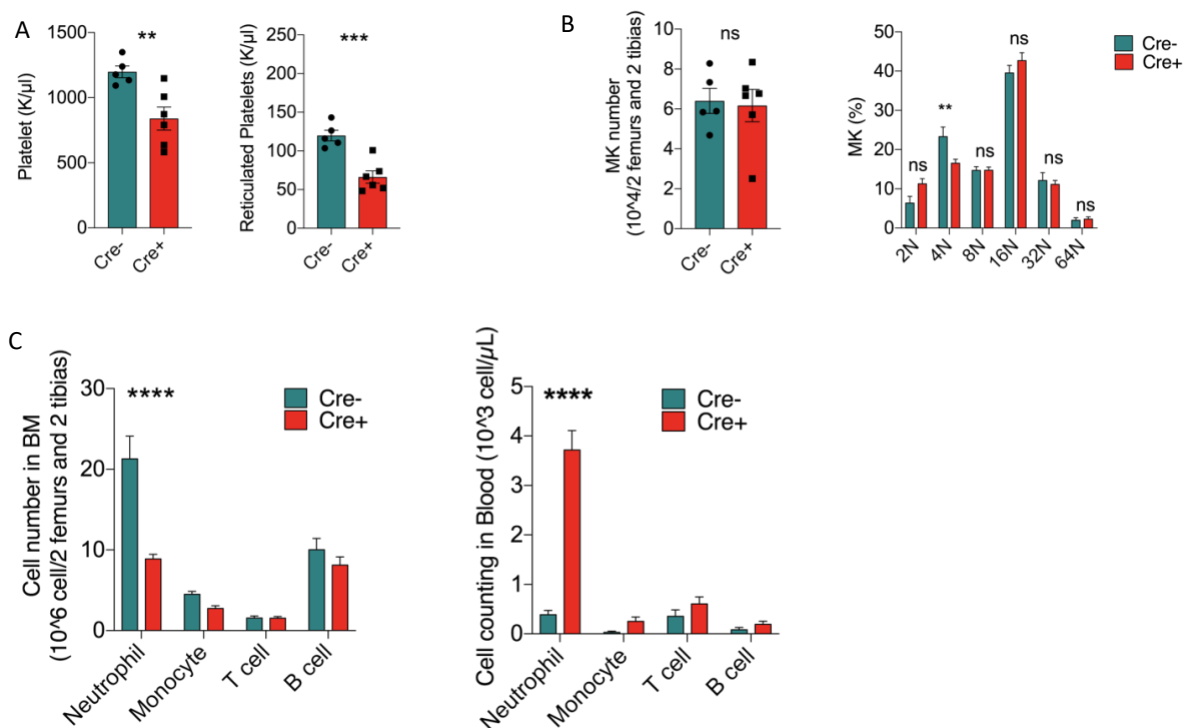


Figure 4.16. Measurements of *Mrp8-Cre/CXCR4^{fl/fl}* mice under normoxia and hypoxia.

(A) Platelets and RPs in addition to (B) MK numbers and ploidy were measured in *Mrp8-Cre/CXCR4^{fl/fl}* mice under IH conditions. (C) Leukocytes of blood and BM were determined; (n=5 *Mrp8-Cre(-)/CXCR4^{fl/fl}*; n=6 *Mrp8-Cre(+)/CXCR4^{Δ/Δ}*). Significance levels are presented, ** <0.01 , *** <0.001 , **** <0.0001 and ns. Unpaired Student's t-test or two-way ANOVA was used to identify p-values.

4.1.17 LFA-1 neutrophil mobilization to places of inflammation increases platelet production under IH

LFA-1 is a heterodimeric-integrin comprising two subunits (α L and β 2), found on the surface of all neutrophils and leukocytes; besides, it is considered indispensable for recruiting neutrophils to inflamed sites [160]. Blockage of LFA-1 by antibody injection was used in this project to examine the outcomes of inhibiting neutrophils' recruitment under IH. Data showed a substantial decrease in platelet and RP production in IH conditions after LFA-1 blockage (Fig. 4.17C); while platelet lifespan, MK number, and ploidy along with cell count in BM and blood remained unaltered (Fig. 4.17D,E). Henceforth, when the neutrophil recruitment is reduced via CD11a antibody blockage, thrombopoiesis is considerably suppressed in mice exposed to IH. Thus, neutrophil recruitment is essential in triggering platelet production under intermittent hypoxia.

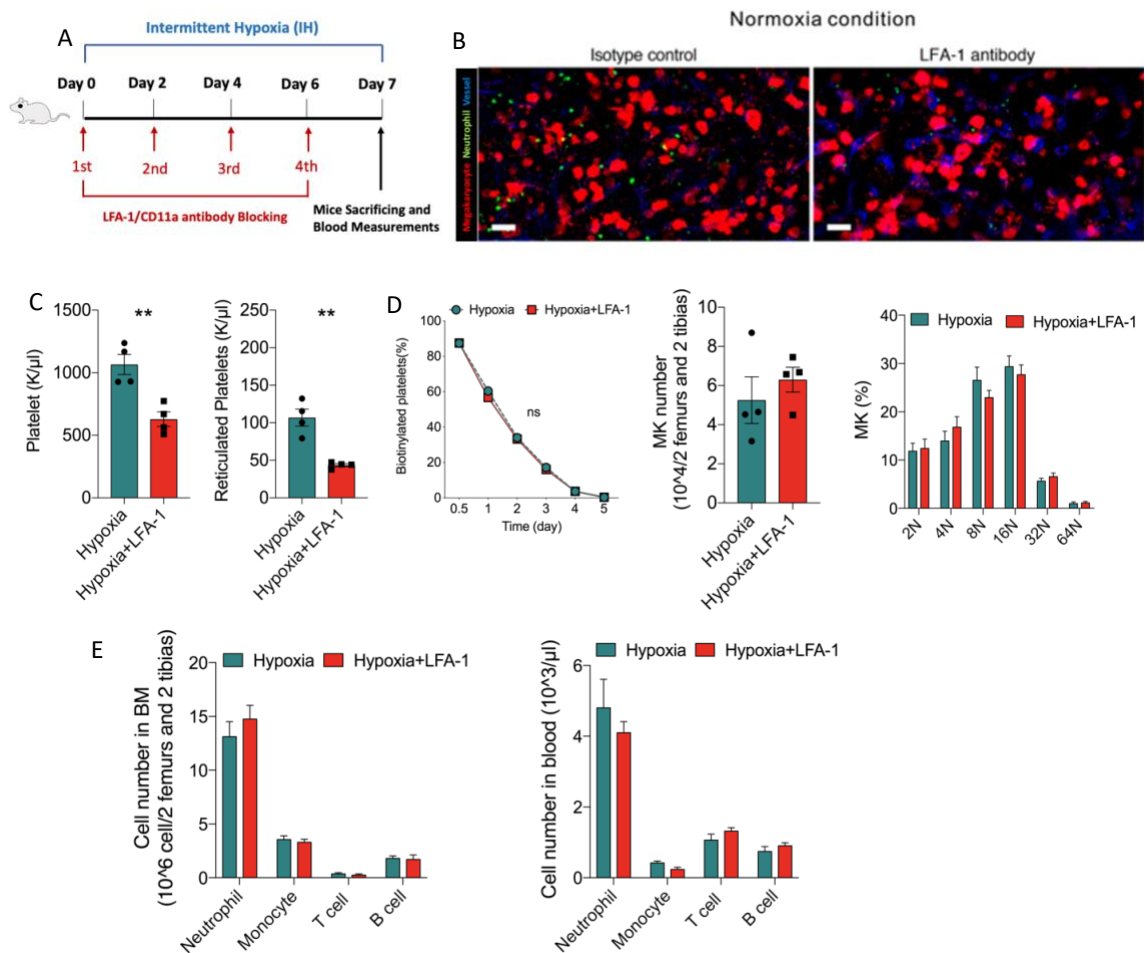


Figure 4.17. LFA-1 blockage lowers platelet and RP production in hypoxic mice.

(A) An illustrative scheme of LFA-1/CD11a antibody blocking in IH mice. (B) Representative figures of LFA-1 isotope control and LFA-1 in the bone marrow of normoxia mice. (C) Platelet and reticulated platelet, (D) lifespan of biotin-labeled platelets in blood, MK numbers, and ploidy, and (E) leukocytes of BM and blood were quantified in LFA-1 blocking antibody injected mice under IH conditions; (n=4 C57BL/6 mice in every condition). Significance levels are indicated with **<0.01, and ns, if not indicated then it is considered as not significant. Unpaired t-test or two-way ANOVA were used to assess the p-values.

4.1.18 Genetic ablation of neutrophil CXCR4 attenuates thrombus formation in IH mice

It was reported that intermittent hypoxia accelerates the formation of arterial thrombosis [161], and OSA is highly associated with markers of atherosclerosis mainly in the carotid bed [162]. Accordingly, a mouse model of carotid arterial thrombosis was visualized in-vivo to study the effects of the augmented number of circulating prothrombotic RPs in mice exposed to IH. Thrombus was induced following Fe-III-chloride-induced injury of the carotid artery (Fig. 4.18A). The frequency of occlusions and the size of the thrombus were increased following IH compared to normoxic C57BL/6 mice (Fig. 4.18B).

To check whether CXCR4 neutrophil-driven thrombopoiesis is the main driver of exaggerated thrombus formation, the carotid arterial thrombosis was imaged in genetically ablated neutrophil CXCR4 mice (Mrp8-Cre/CXCR4^{fl/fl}) exposed to IH conditions. Mrp8-Cre(+)/CXCR4^{Δ/Δ} mice showed attenuated thrombus formation and reduced embolism (Fig. 4.18C) compared to their littermate controls. In summary, neutrophil CXCR4 enhances the recruitment of immature RPs, resulting in the increase of thrombus burden under IH.

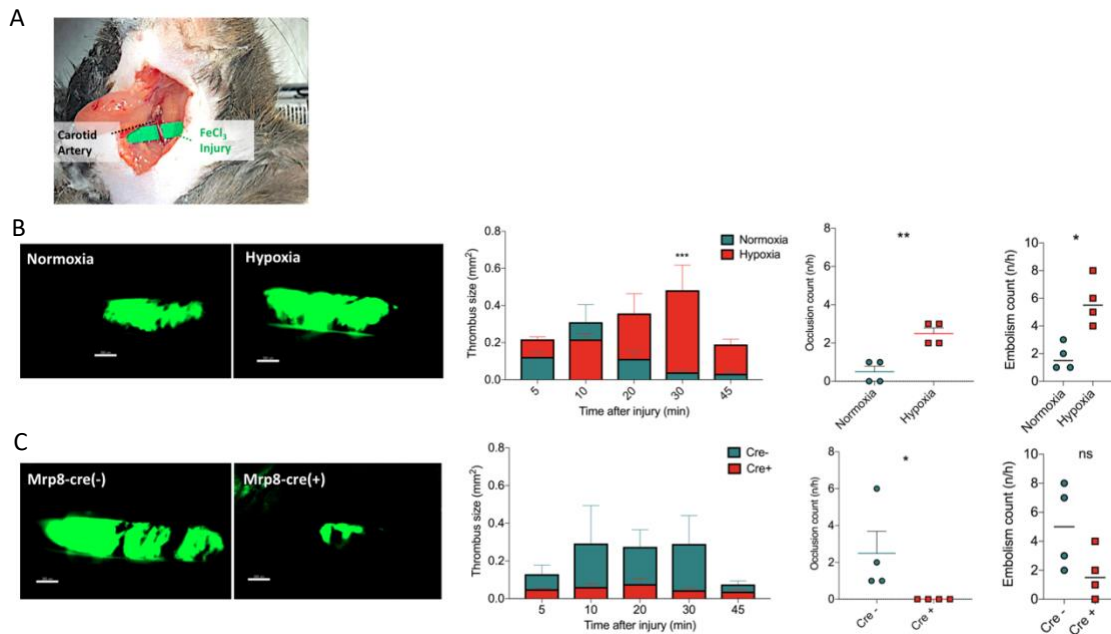


Figure 4.18. Abrogation of neutrophil CXCR4 reduces the thrombotic risk in IH mice. (A) Picture of a mouse under carotid artery injury using FeCl₃. (B) Representative fluorescent images of the thrombus in both normoxia and hypoxia conditions followed by carotid surgery (left lane; thrombus in green and scale bar, 300µm) and then quantification of thrombus size over time in addition to calculation of the occlusion and embolism of every C57BL/6 mouse. (C) Representative fluorescent images of the thrombus formation in Mrp8-Cre(-)/CXCR4^{fl/fl} along with Mrp8-Cre(+)/CXCR4^{Δ/Δ} mice after 7 days of intermittent hypoxia followed by carotid injury (left lane; thrombus in green and scale bar, 300µm) and then quantification their thrombus size over the time in addition to calculation of the occlusion and embolism of every mouse; n=4 and significance levels are suggested, *<0.05, **<0.01, or ns. Unpaired t-test or two-way ANOVA was used to show p-values.

4.1.19 Tail bleeding assay reflects impaired hemostasis in hypoxic mice

Hemostasis is described as the body's natural response to injury to cease bleeding and repair the damage. Platelets are responsible for the hemostatic plug formation as they rapidly form aggregates on the exposed subendothelium [163]. Subsequently, tail cut assay was used as a method to investigate hemostasis in mice under IH by measuring the time taken for platelet generation and vasculature constriction to happen. Data showed that IH has shortened tail-cut bleeding time (Fig. 4.19); consequently, prompt platelet hemostatic plug is accumulated in the surrounding tissue after vessel wall injury in mice exposed to intermittent hypoxia.

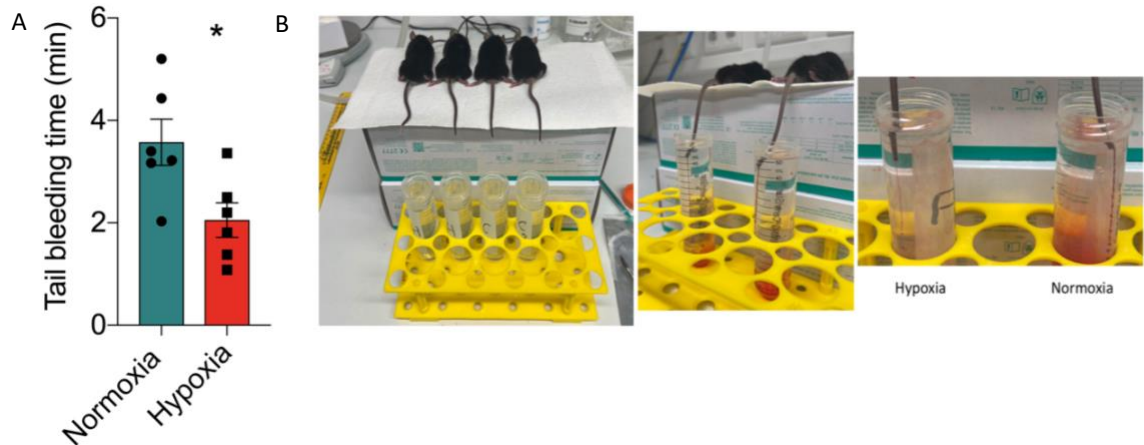


Figure 4.19. Tail bleeding assay shows reduced bleeding time in hypoxic mice.

(A) Bleeding time (minutes) measurement of rapid immersion of the amputated tail tip in a warm water of around 37°C. (B) Pictures presenting the method and the alteration in the bleeding stream in C57BL/6 mice treated with IH (left Hypoxia) or untreated (right Normoxia) (n=6 per condition). The significance level is designated by * <0.05 using unpaired t-test.

4.1.20 Intermittent hypoxia after 21 days exposure

OSA is a chronic inflammatory disorder that exerts a long-term impact on the pathogenesis of cardiovascular events challenged by OSA patients. To better simulate these long-term effects and to validate the effectiveness of our installed IH model, mice were exposed to IH for an extended duration (21 days), allowing for a thorough analysis of the resulting alterations in the long term. Platelet and RP numbers were notably higher under IH as presented in Fig. 4.20A. Interestingly, MK ploidy showed the same trend as in seven days of IH treatment; yet with very significant differences at 8N and 16N nuclei DNA content developed when MKs undergo endomitosis. Despite the increased trend in blood, ROS level and CXCR4 expression did not indicate a significant change between normoxia and IH mice in the long term.

In addition, cell counting showed no alteration except for T cell (CD3⁺) and B cell (CD45R⁺ (B220)) which decreased in blood drastically after 21 days of IH exposure. These findings are in line with results generated by Domagala-Kulawik et al. (2015) who detected a significant decrease (p value <0.05) in B cell lymphocyte subset (CD19⁺) in OSA peripheral blood; yet, T cells (CD3⁺) showed no significance when comparing OSA with healthy subjects [164]. It was reported that B cells secrete different cytokines and cofactors such as PD1-L2 (programmed death 1 ligand 2) and IL-10 which correlate with the stimulation of T cells apoptosis [165,166]; meaning that a notable decrease in B cells may also affect T cells by decreasing their number.

Nevertheless, it was stated by Xie et al. (2019) that CD19⁺ B cells augmented in moderate to severe OSA patients but CD3⁺ T cells showed no significant difference between OSA and the control group. This incongruity in results was justified by the fact that the recruited patients of Xie and his colleagues were not subjects of severe comorbidities; however, OSA patients from the study of Domagala-Kulawik had several comorbidities like metabolic syndrome (56%), diabetic disease (17%) in addition to lung diseases like COPD (chronic obstructive pulmonary disease, 8%) which may have affected the differentiation and expression of immune cells like B cells [164,167]. Of note, a mouse model of IH was used in this study and the positive population of CD45R(B220) marker detected B cells. It is argued that the CD19 antibody (used by Xie et al. and Domagala-Kulawik et al. to determine B cells in OSA patients) is more specific, as in humans than CD45R(B220) to determine murine B cell lineage [168]. In all cases, further experiments should take place to explore these lymphocytes (B cells and T cells) that can be involved in the systemic immune response in patients with OSA predisposing them to probable future complications.

PDW and MPV values were not modified when comparing normoxia and IH 21-day mice. Together, data showed that after three weeks of IH exposure, lymphocytes B and T cells may be involved in the systemic immune response to IH, thrombopoiesis continued to be increased, and MK ploidy was drastically altered in hypoxic mice (21 days of IH). These results demonstrate that 7 days of exposure to IH studied in this project did not exhibit acute response; IH is indeed a chronic condition with lasting effects.

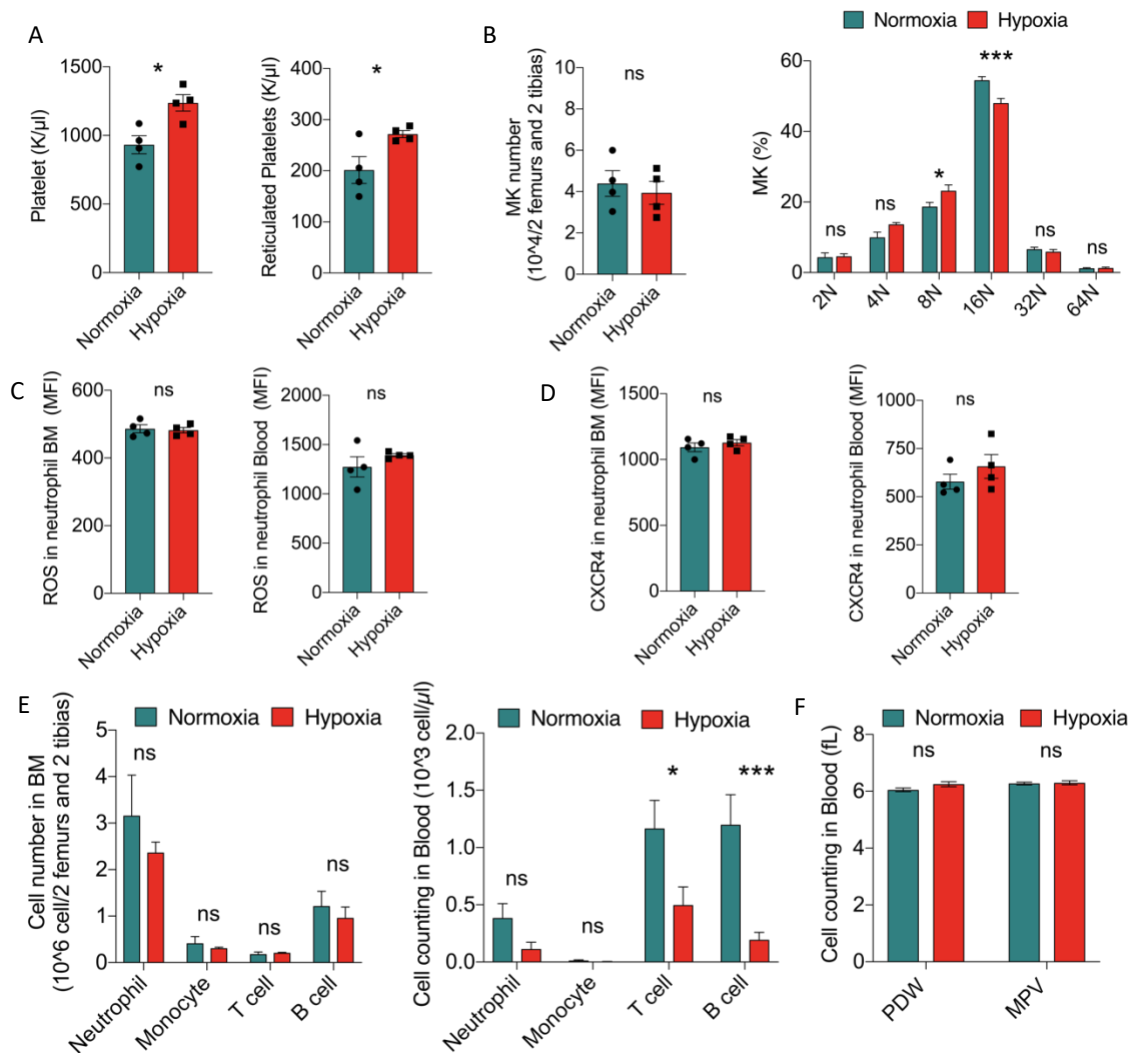


Figure 4.20. Measurements in mice after three weeks of IH exposure.

(A) Platelet and reticulated platelet of C57BL/6 mice, (B) MK number and ploidy were quantified under normoxic and 7-day IH conditions. (C) ROS level, (D) CXCR4 expression, (E) Cell count within BM and blood in addition to (F) PDW in addition to MPV were quantified under IH; (n=4 animals per condition). Significance levels are shown as * <0.05 , *** <0.001 , ns, and assessed using unpaired t-test and two-way ANOVA.

4.1.21 CPAP therapy reduces RPs related to thrombogenicity in OSA patients

CPAP is the fundamental standard therapy for OSA [169,170], and studying its effect on OSA-related mechanisms may open intriguing avenues for development in the realm of medicine. Accordingly, patients were investigated before and twelve weeks after the commencement of CPAP treatment. Upon initiation of CPAP, the severity of OSA (i.e. AHI) decreased radically indicating patient responsiveness to the therapy (Fig. 4.21A); accompanied by a significant

diminution in both total platelet counts and RP counts (Fig. 4.21B). Moreover, CPAP markedly downregulated CXCR4 expression on circulating neutrophils (Fig. 4.21C). These findings indicate the importance of CPAP treatment that may attenuate the effects of recurrent deoxygenation/reoxygenation cycles on OSA patients undergoing the right treatment.

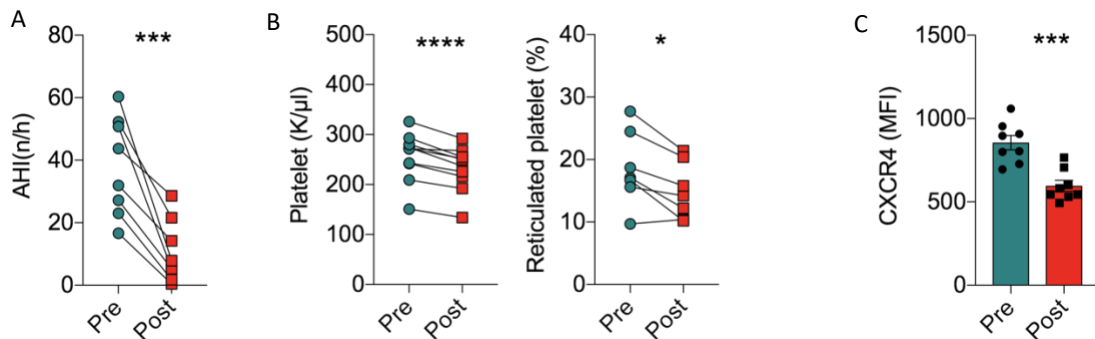


Figure 4.21. Flow cytometry measurements of OSA patients pre and post-CPAP therapy. (A) AHI values of OSA patients along with (B) measuring of platelets and RPs before and after three months of CPAP therapy were presented. (C) CXCR4 expression on circulating neutrophils before and after CPAP treatment; n=7-8 individual patients. Significance levels are presented as * <0.05 , *** <0.001 , and **** <0.0001 and evaluated using paired t-test.

4.1.22 CPAP therapy decreases the thrombotic risk in OSA patients

CPAP therapy is pronounced to prevent the subsequent occurrence of major cardiovascular events in moderate to severe OSA patients and concomitant CAD [13]. To examine whether CPAP therapy alleviates the effects of the increased activation and aggregation of prothrombotic immature platelets in OSA patients, ex-vivo thrombus formation was assessed through arterial flow-coated chambers. Following CPAP therapy, data showed an enormous decrease in the accumulation of platelets in the blood of post-therapy patients in both collagen and plaque-coated surface flow chambers (Fig. 4.22A,B). Thus, CPAP treatment may diminish the risk of cardiovascular events by reducing the thrombus burden affecting OSA patients.

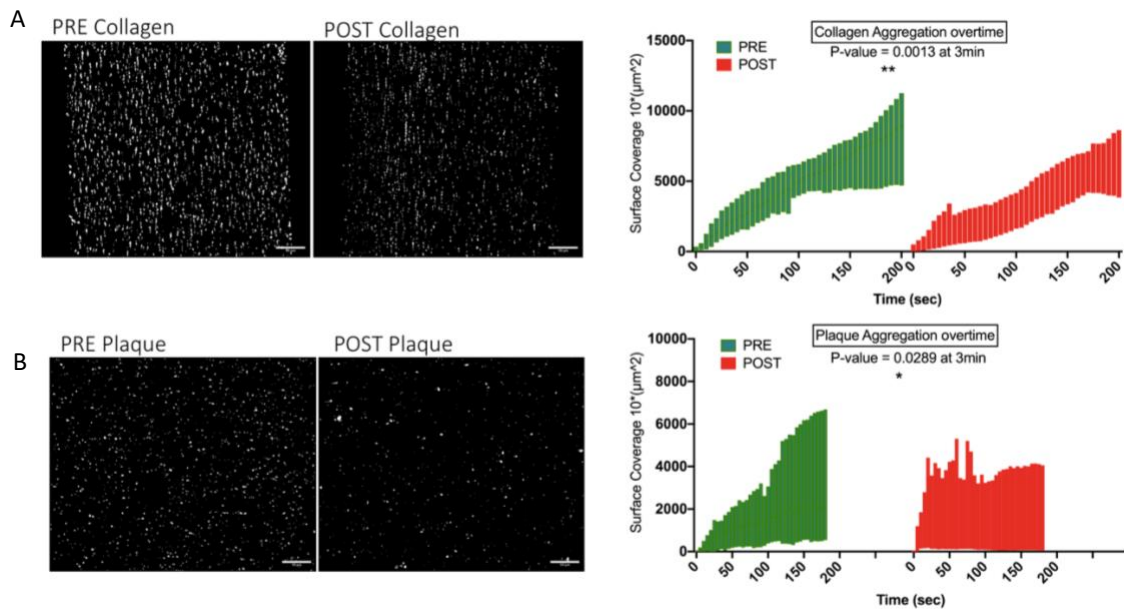


Figure 4.22. CPAP therapy minimizes platelet adhesion and aggregate generation in OSA.

(A) Representative pictures (100 μm) of platelet adherence and accumulation on collagen-coated flow chambers after 3 minutes of blood flow (left panel) and quantification of total surface coverage was automated and quantified by macro-scripting with ImageJ/FIJI (n=6 patients per group). (B) Representative pictures (100 μm) of platelet aggregation on plaque-coated flow chambers (left panel) and quantification of total surface coverage were automated and quantified by macro-scripting with ImageJ/FIJI (n=6 patients per group). Significance levels are measured using two-way ANOVA and presented with * <0.05 and ** <0.01 .

4.1.23 CPAP therapy decreases platelet reactivity in OSA

To investigate how CPAP treatment affects platelet activation markers and subsequently, the thrombus burden that OSA patients may encounter, frozen whole blood from OSA patients pre and post-therapy was analyzed on resting cells. Pop1 was the population greatly expressing platelets' markers (Fig. 4.23C) with the highest frequency of parent (Fig. 4.23D). CPAP therapy showed a reduction in the prothrombotic activation markers in the platelet population (Pop1) (Fig. 4.23D) and decreased enormously the manifestation of its activation indicators (e.g., P-selectin along with PAC-1) in patients after therapy (Fig. 4.23E). Moreover, the collagen receptor GPVI displayed a reduction in post-therapy patients as well (Fig. 4.23E). The population of pre-therapy patients was represented differently by heatmap and color-coded profiling than that of post-CPAP therapy patients as illustrated in Fig. 4.23G,H. Hence, CPAP therapy decreases the activation markers of platelets and consequently the thrombotic risk in OSA patients.

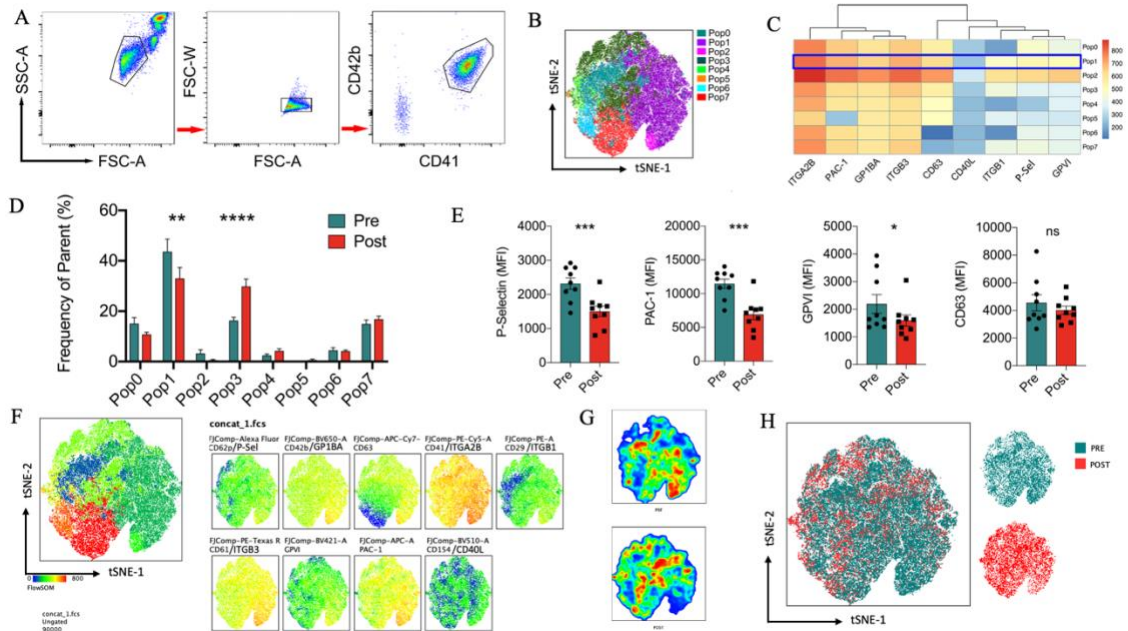


Figure 4.23. tSNE and flowSOM measurements of platelet markers pre and post-therapy. (A) Scheme of the gating strategy of platelet population by double positive gating of CD42b and CD41. (B) Color-coded flowSOM platelet populations and (C) a heatmap showing the MFI of all platelet subclusters in relation to the parent MFI value of the surface platelet marker are illustrated. (D) The rate of platelet populations and (E) platelet markers of sub-population 1 are presented. (F) Color-coded tSNE-flowSOM expressions of each of the markers are presented. (G) Heatmap clusters to show the difference in the expression of platelet markers. (H) Color-coded clusters overlapped for further demonstration of the distinct populations; n=9 pre and post-CPAP therapy patients per group. Significance levels are shown as * < 0.05, ** < 0.01, *** < 0.001, **** < 0.0001 or ns and calculated using paired t-test or two-way ANOVA.

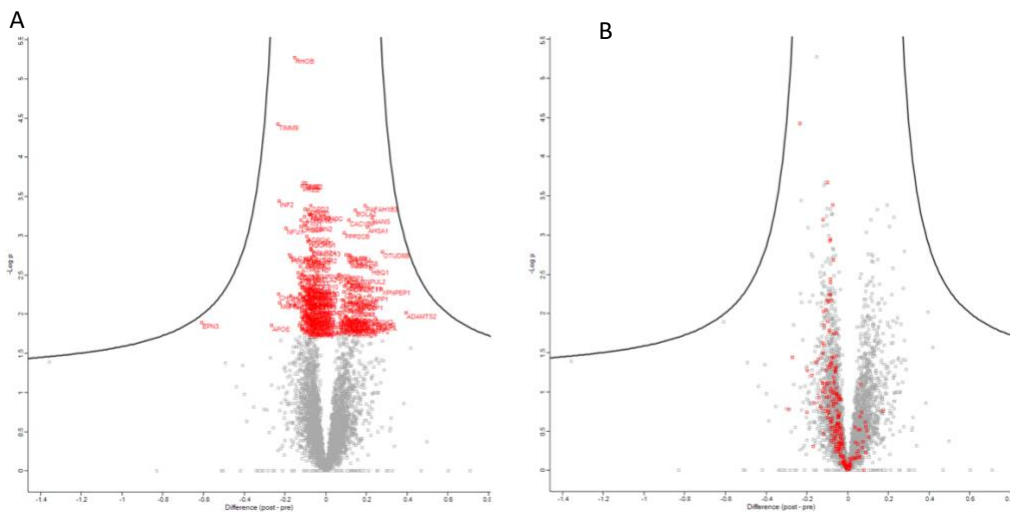
4.1.24 Neutrophils from untreated OSA patients are characterized by upregulation of mitochondrial proteins

High-resolution examinations on neutrophil biology are still needed, in particular at the proteomic level to further decipher their biomolecular interactions and alterations in the blood of patients. The aim was to better understand the underlying potential biomarkers of neutrophils in OSA using MS-based proteomics.

Consequently, neutrophils were sorted from frozen whole blood (citrate blood) of eight pre and post-CPAP therapy patients and were set out to measure different protein trajectories. Enrichment analysis of neutrophils was performed for biological gene interpretation of sorted neutrophils from OSA patients and was tested with keywords and GOBP (gene ontology biological process), cellular component (GOCC), and molecular function (GOMF) using

student's T-test. Data showed that there were no drastic protein changes in OSA patients before and after CPAP therapy (Fig. 4.24A); nevertheless, the keyword "mitochondria" had a high number of annotations in untreated OSA patients (Pre) reflecting the excessive ROS production in OSA (Fig. 4.24B-D). Indeed, mitochondria are pronounced as the main source of endogenous ROS production in response to hypoxia along with cellular membranes and other subcellular compartments [171,172]. Studies have explored the role of neutrophils possessing mitochondrial networks that maintain the potential of mitochondrial membrane to generate enhanced ROS levels in hypoxic conditions [173].

In summary, there is upregulation of mitochondrial activity in OSA patients consistent with the increased neutrophil ROS production examined in this study; suggesting that CPAP treatment plays an important role at the proteomic level.



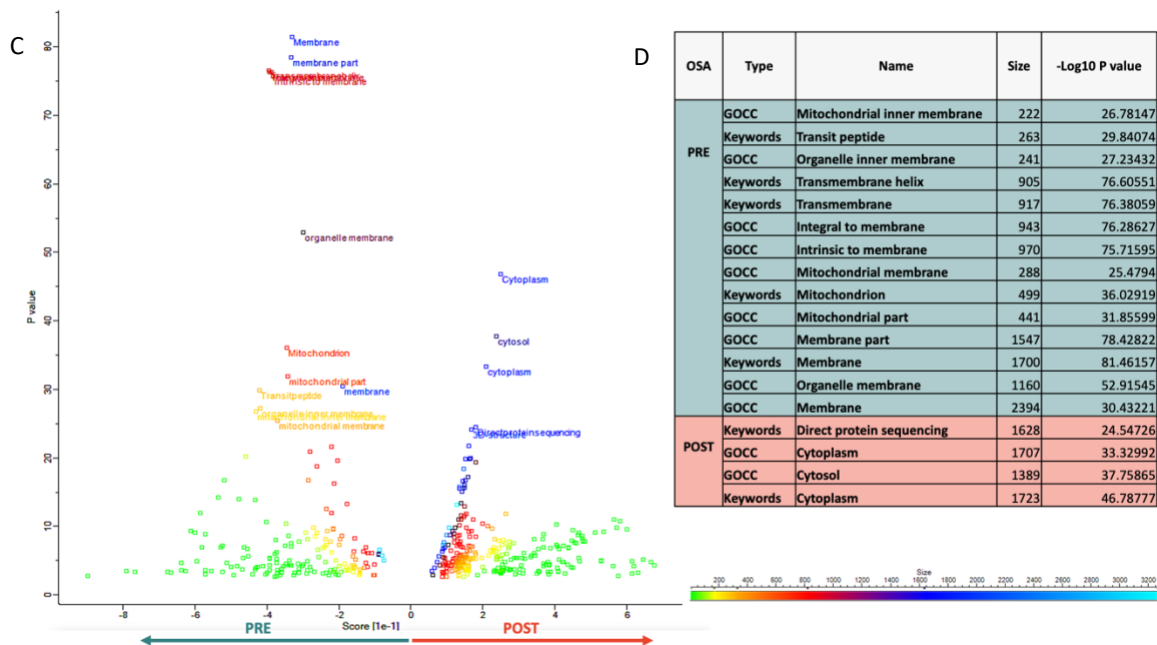


Figure 4.24. Functional enrichment analysis of sorted neutrophils in OSA pre- and post-therapy. After freezing blood of pre- and post-CPAP therapy from OSA patients (n=8 per group) and performing the sorting of neutrophils, (A) neutrophil proteomics were analyzed in volcano plots. (B) Enriched plotting analysis in pre-patients. Annotated in red are proteins related to the mitochondrion and mitochondrial inner membrane; protein values (and therefore differences) are in log10. (C) Volcano plots of functional enrichment analysis presenting pre-therapy OSA patients (left side) and post-therapy OSA patients (right side); t-test was used and p-values are in -log10. Main keywords and GOCC (gene ontology cellular component) were presented as single dots, group size was annotated with color coding. (D) Table of the most significant keywords and GOCC of neutrophils. Sorted neutrophil samples were handed to Johannes Müller (Max Plank Institute of Biochemistry) who did the proteomics analysis.

4.2 Myocardial infarction/ischemia-reperfusion (MI/IR) murine model and STEMI patients

Obstructive sleep apnea and intermittent hypoxia studied above are known to trigger cardiovascular disorders [174]. IH is described by cycles of deoxygenation followed by reoxygenation which may contribute to an increased risk of ischemic reperfusion injury [107]. Consequently, this project will focus on examining the same underlying processes investigated under IH but in myocardial infarction induced by ligation and followed by I/R injury. The main pathways that will be further explored in MI/IR are inflammatory immune activation, increased ROS formation and CXCR4 expression, in addition to platelet aggregation and thrombus formation. This project is aimed at elucidating the pathways contributing to the progression of cardiovascular conditions.

4.2.1 MI/IR murine model is established to translate the responses in patients

To decipher the wide range of effects evolving from I/R injury, a mouse model of MI/IR closely imitating the clinical condition in MI patients, was established to identify key aspects of I/R on thrombopoiesis and to understand the responses provoked by the disease. This mouse model was initiated by 1-hour transient left anterior descending (LAD) ligation followed by ischemia-reperfusion (I/R) where blood flow is restored. The sham model was experiencing the same effects of the chest opening and cardiac injury but without enduring the 1-hour of reduced blood supply and reperfusion. To understand the progressive sequel of ischemic reperfusion damage specifically on bone marrow, this project investigated the initial response of I/R injury at 6-8 hours, then the continued cellular damage at 24 hours, and finally the outcome of the injury and tissue repair after 48hours (Fig. 4.25).

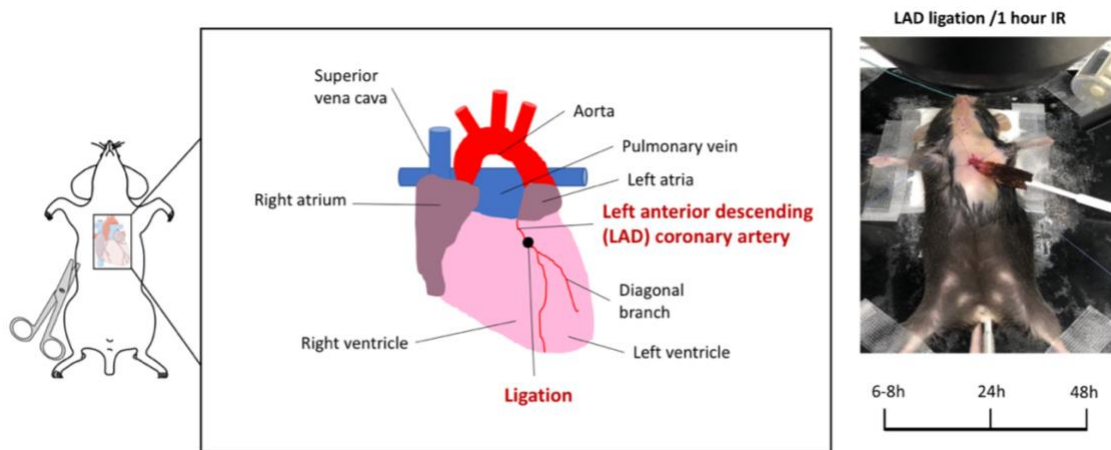


Figure 4.25. Establishing of MI after 1-hour ischemia-reperfusion and characterization. Labeled heart structure of LAD (left anterior descending coronary artery) and ligation injury including 1 hour of ischemia-reperfusion (I/R) at time-specific points. The illustrative scheme is generated using PowerPoint.

4.2.2 Studying MI/IR model at different time points highlights the temporal dynamics of the injury on megakaryocytes

To characterize the MI/IR model developed in this project closely, various time points (6-8 hours, 24 hours, and 48 hours) were studied to elucidate the progressive development of the cardiac damage on the platelet progenitors (MKs) in BM. Whole-mount staining of BM was investigated by calculating the number and the diameter of MKs along with the volume and area of the imaged bone section using Imaris 3D software tools of the MI/IR model in comparison to the sham murine model. It was observed that MKs were larger in size in MI/IR mice and mainly in 48-hour MI/IR mice that showed 40-50 μm and more than 50 μm MK diameter bigger than other time-points BM samples (Fig. 4.26B). The results in Fig. 4.26C showed that MK sizes are greater at 6-8 hours MI/IR when reperfusion is initially generating stress and damage and the largest MK size was after 48 hours of I/R injury. Based on these results, all experiments in this study were performed two days following I/R injury and sham conditions.

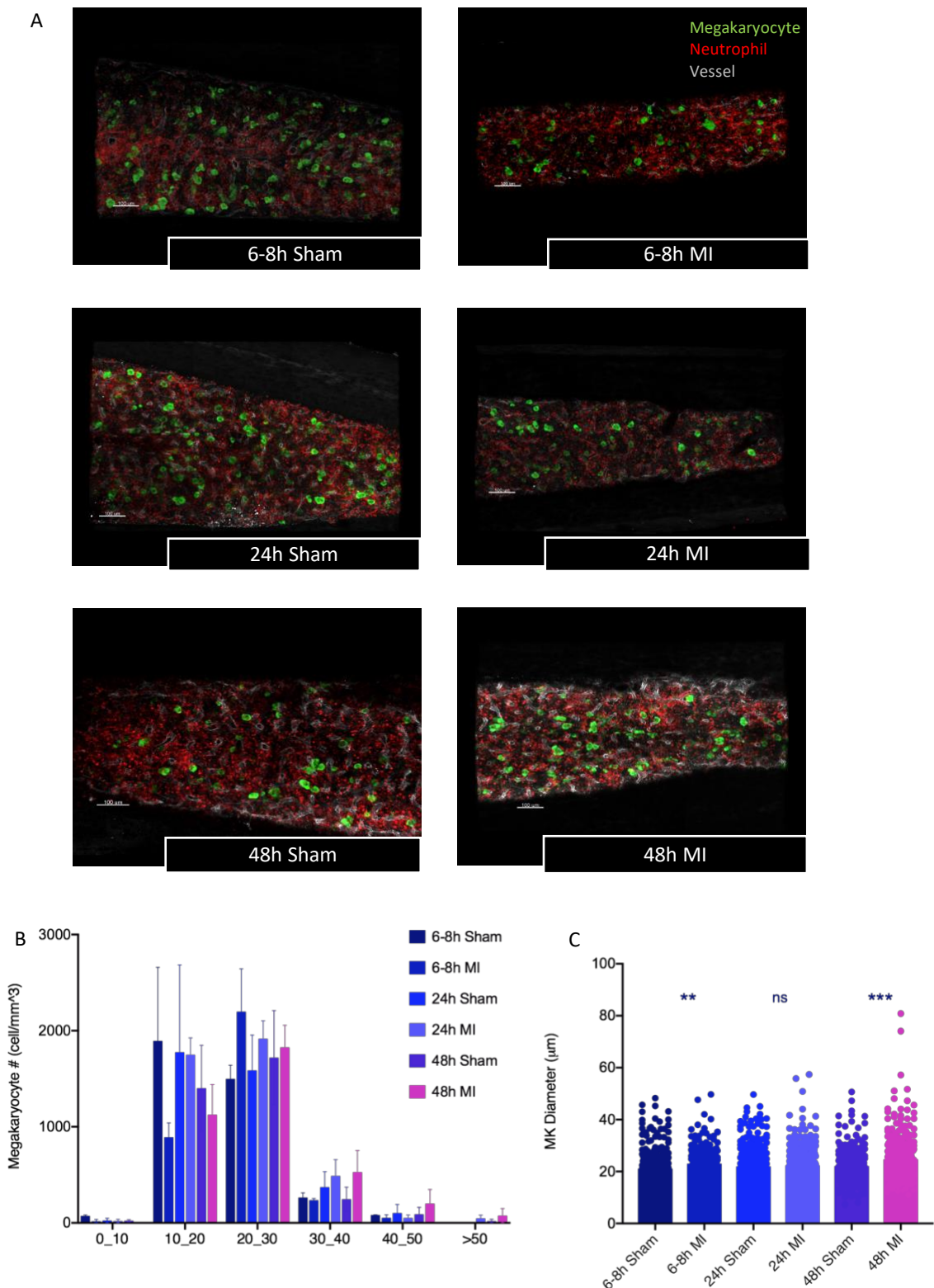


Figure 4.26. Characterizing the established MI/IR model at different time points.

(A) Representative 3D whole-mount images of BM in sham and I/R mice. CD144 VE-cadherin and Streptavidin 450 (vessels in grey), CD41-FITC (megakaryocytes in green) and Ly6G-PE (neutrophils in red); scale bar, 100 μm . (B) The mean number of megakaryocytes (MK) (total number of MK per volume) in relation to MK diameter in μm . (C) MK diameter of sham vs MI using confocal imaging of whole bone staining at different time points 6-8h, 24h, and 48h;

(h=hour) n=3 mice per group. Significance levels are specified as **<0.01, ***<0.001 or ns, and calculated using unpaired t-test or two-way ANOVA.

4.2.3 Thrombopoiesis is increased in ischemia-reperfusion myocardial infarction

Platelets have been considered a key contributing aspect in understanding the onset of injury following ischemia-reperfusion [175]. Consequently, platelets in their mature and immature forms were quantified after I/R in mice. The data below showed that RPs and platelet counts were increased in the circulation of MI/IR mice; whereas PDW and MPV were unchanged (Fig. 4.27A). MK number and maturity remained unaltered in both sham and MI/IR (Fig. 4.27B). Cell quantification was also investigated in blood and BM. Although white blood cells showed an increasing trend in MI; however, it was not significant (Fig. 4.27C). Neutrophils and T cell counts were significantly enhanced in the circulation of MI mice but cell counts were not affected in BM (Fig. 4.27C). These findings showed that elevated platelet production is associated with I/R injury contributing to cardiac damage.

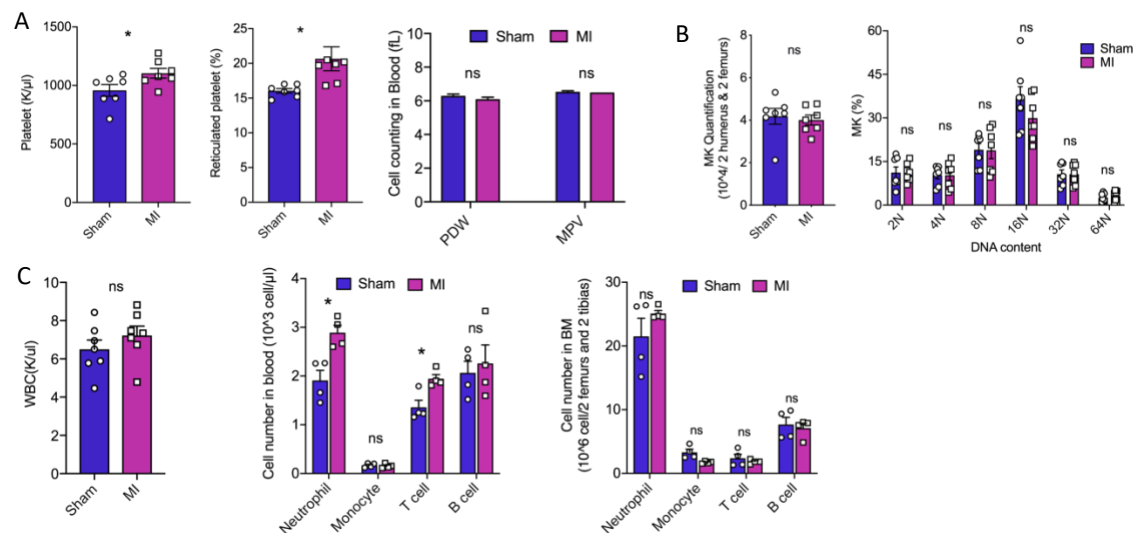
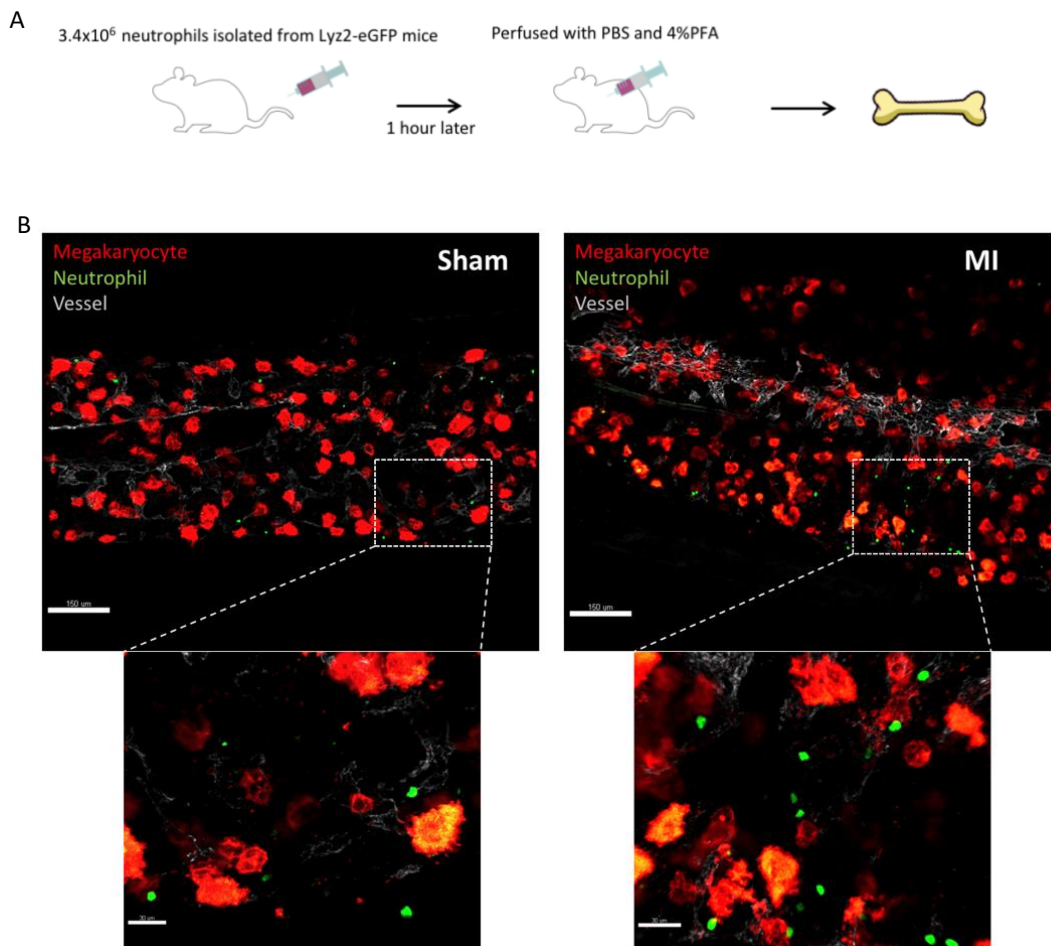


Figure 4.27. Platelet and RP counts are amplified in MI/IR murine models.

(A) Analysis of platelet and reticulated platelet counts in addition to PDW and MPV of 48h sham or MI. (B) Megakaryocyte number and ploidy are calculated in BM; n=7 mice in every group. (C) Quantification of white blood cells (WBC) (n=7 mice per group) and immune cells in blood and BM (n=4 mice per group). Significance levels are implied as *<0.05 and ns, and assessed using an unpaired t-test or a two-way ANOVA test.

4.2.4 Transferred neutrophils preferentially localize around BM MKs of MI

To test the effect of neutrophil-driven thrombopoiesis following I/R injury, an adoptive neutrophil transfer experiment was performed using GFP expressing neutrophils harvested from Lyz2-eGFP mice as illustrated in Fig. 28A. The localization of homing neutrophils was studied under MI and sham conditions at 48h (Fig. 28B). The minimal distance between MK and neutrophil (edge-to-edge), total number of neutrophils in volume, and mean MK diameter were analyzed (Fig. 4.28C) by assessing the existing 2D sections to the complete 3D image as presented in Fig. 4.28D. Primarily, data revealed the interaction of neutrophil-MK by detecting close distances between MK and neutrophils of less than 5 μm in the I/R model compared to the MK-neutrophil distances in sham models (Fig. 4.28B,C). To sum up, a favored localization of transferred neutrophils was found closely adjacent to MKs residing in BM in MI mice compared to sham.



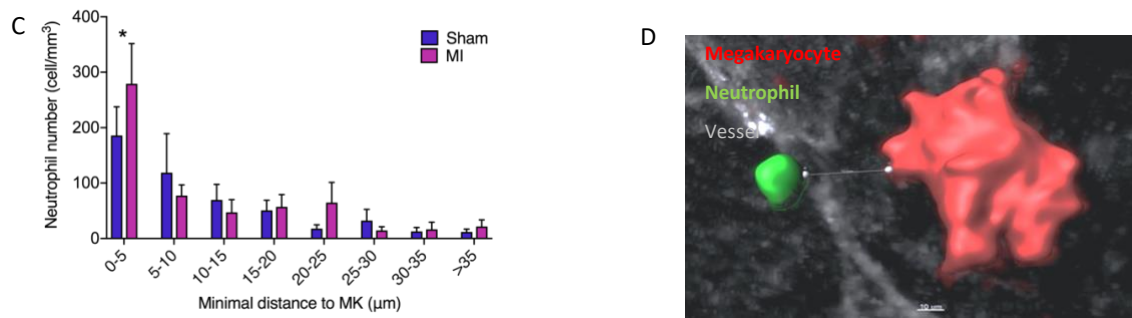


Figure 4.28. Close MK-neutrophil interaction following adoptive neutrophil transfer. (A) Representative scheme of neutrophils transfer from Lyz2-eGFP (LysM-eGFP) mice to C57BL/6 operated mice. (B) Whole mount confocal images of GFP positive neutrophils inside the BM following 60 minutes of transfer. Anti-CD144 VE-cadherin (vessels in grey), anti-CD41 PE (megakaryocyte in red), green anti-GFP (neutrophil); scale bar, 150 µm, and 30 µm for the zoomed imaged as indicated. (C) Localization of 3.4×10^6 transferred neutrophils (48h sham and 48h MI I/R) relatively to megakaryocytes was quantified; n=5 animals per group. (D) Representative 3D picture of megakaryocyte (in red), eGFP neutrophil (in green), and vessels in grey was reconstructed using IMARIS software (24 layers, 2 µm depth); 10 µm scale bar, as indicated in the image. The descriptive mouse scheme is generated using PowerPoint. The significance level is shown as * < 0.05 and examined using two-way ANOVA.

4.2.5 Direct engagement of neutrophils at PPL budding sites drives thrombopoiesis in MI

To investigate in-vivo the neutrophil colocalization with PPL-forming MKs in the BM of MI model, the calvarian model was used to visualize cell-to-cell interaction (Fig. 4.29A,B). Accordingly, faster proplatelets release was observed in MI model in comparison to sham controls (Fig. 4.29C). The live imaging revealed the very close gathering of neutrophils to PPL budding sites of MKs within the perisinusoidal niche (Fig. 4.29B,D). These in-vivo findings may lead us to hypothesize that neutrophils play an active part in platelet production by direct interaction with PPL budding sites on MKs in BM.

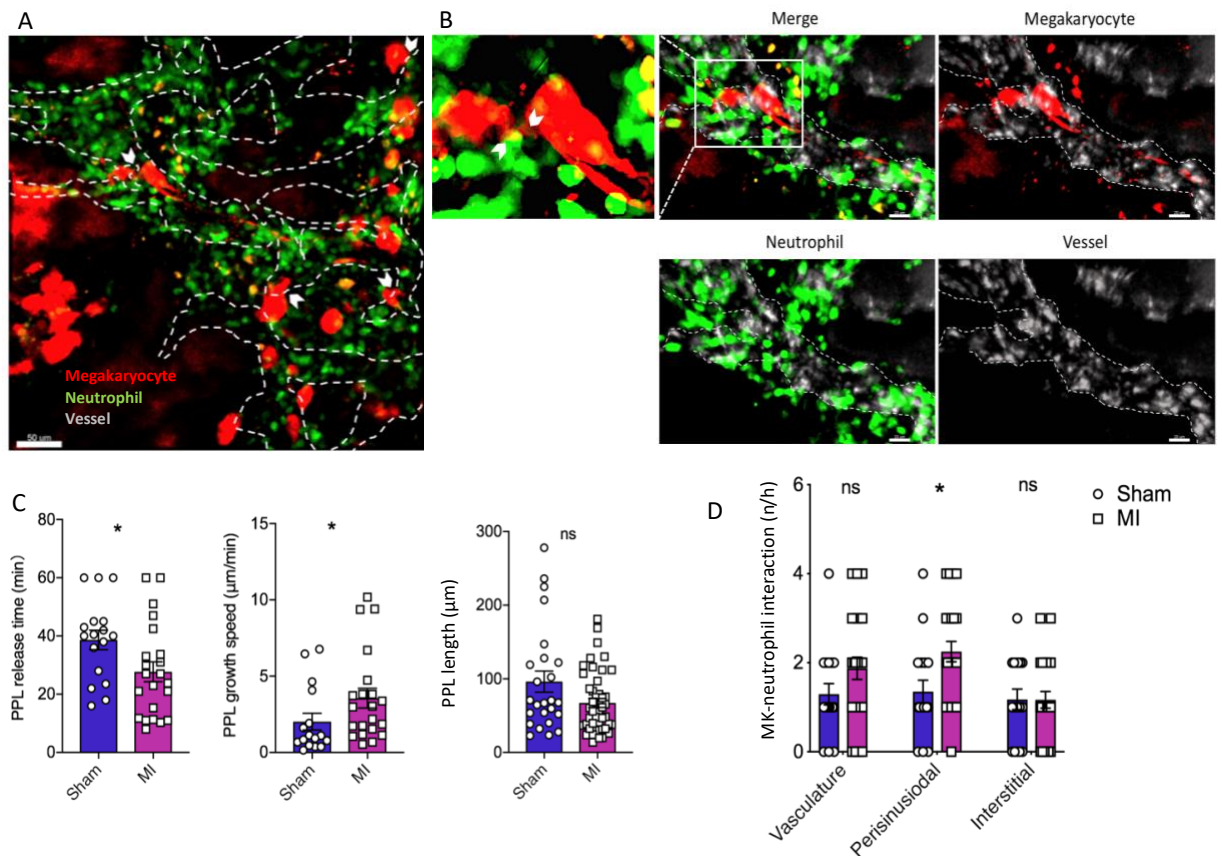


Figure 4.29. Augmented thrombopoiesis and MK-neutrophil interaction are visualized under MI. (A) White arrows show the platelet release from MK into the vasculature (50 µm scale bar). (B) Representative figures of MK-neutrophil interaction (20 µm scale bar indicated in the image). Dotted lines present the linings of the vessels (in grey), MKs/platelets are in red, and neutrophils are in green. (C) Examination of PPL release time, speed of growth in addition to length (each symbol indicates individual PPL). (D) The interaction between MK and neutrophil is measured in diverse compartments (n=3 C57BL/6 mice in every group). Significance levels are presented with * <0.05 or ns, and calculated by the use of unpaired t-test or two-way ANOVA.

4.2.6 Myocardial ischemia-reperfusion amplifies ROS production and CXCR4 on neutrophils

CXCL12-CXCR4 signaling is disordered following MI permitting the mobilization of neutrophils to the peripheral blood [176,177]. CXCR4 was studied after MI/IR in mice to explore its role in our model. The expression of CXCR4 on neutrophils is enhanced in the bloodstream of MI although it showed no significance in BM (Fig. 4.30A). In addition, dysregulated increase in ROS production has been implicated in a host of cardiac diseases including myocardial I/R injury [178]. Following the induction of MI and I/R, ROS showed a significant increase in MI blood and

BM compared to sham mice (Fig. 4.30B). Thus, both ROS production and CXCR4 expression on neutrophils are boosted after MI/IR.

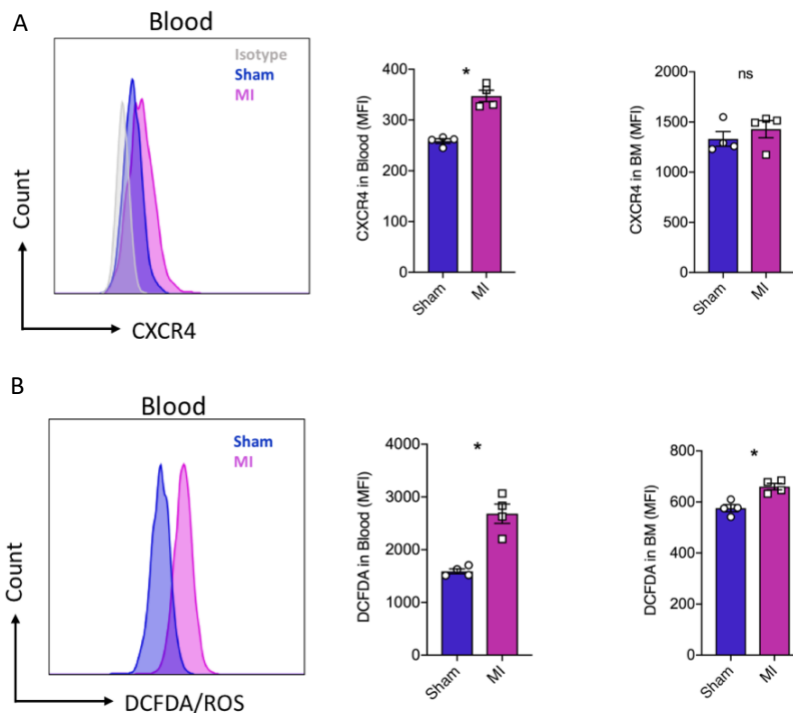


Figure 4.30. Neutrophil-derived ROS and CXCR4 expression augment in MI/IR.

(A) A representative histogram plot of CXCR4 expressed on circulating neutrophils was shown along with CXCR4 isotype in MI/IR or sham 48h operated C57BL/6 mice by flow cytometry. CXCR4 expression on blood and bone marrow neutrophils. (B) A representative histogram of the level of ROS in peripheral neutrophils; in addition, ROS level was quantified in blood and bone marrow neutrophils; n=4 animals per condition. Significance levels are designated with * <0.05 or ns and measured by unpaired t-test.

4.2.7 Genetic ablation of neutrophil CXCR4 decreases platelet production after MI/IR injury

Next, this project focused on the neutrophil CXCR4 role after MI/IR and studied if these ablated CXCR4 can affect the neutrophil involvement in producing platelets. Ablation of CXCR4 diminished platelet and RP numbers notably following MI, while MK number and ploidy remained unaltered (Fig. 4.31A). White blood cell number in addition to cell count in blood showed no difference; yet, neutrophil number in BM decreased significantly in Cre+ mice (Fig. 4.31B). Hence, neutrophil CXCR4 is a crucial mediator of platelet formation under inflammatory conditions.

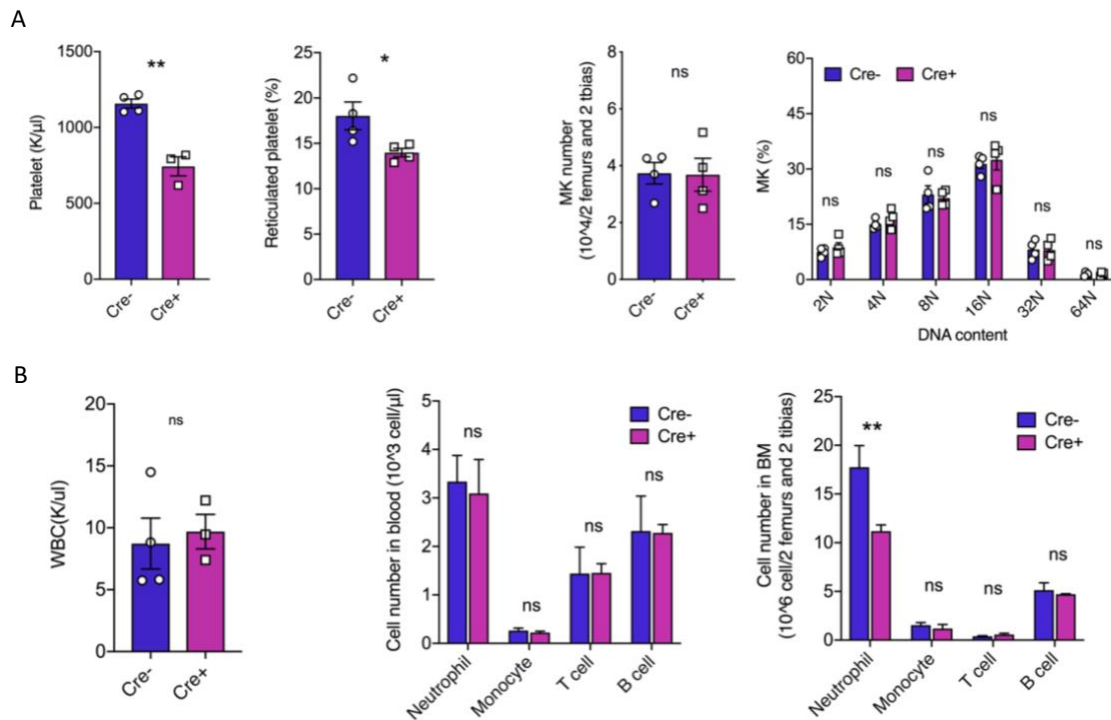


Figure 4.31. Ablation of neutrophil CXCR4 affects platelet production after MI/IR injury. (A) Measuring of platelets along with RPs, MK numbers and ploidy, and (B) white blood cells (WBC) along with cell count in blood and BM isolated from MI/IR or sham 48h operated mice; (n=4 animals Mrp8-Cre(-)/CXCR4^{fl/fl} and n=3 animals Mrp8-Cre(+)/CXCR4^{Δ/Δ}). Significance levels are defined p-values as * <0.05 , ** <0.01 , and ns using unpaired t-test and two-way ANOVA.

4.2.8 CXCR4 neutrophil-driven thrombopoiesis drives exaggerated arterial thrombus formation in MI

To study arterial thrombosis in MI and to address the effects of augmented counts of prothrombotic platelets in circulation, MI/IR was provoked in mice. Subsequently, mice were visualized in-vivo for thrombus formation following arterial carotid injury. The frequency of the occluded vessels and the size of the formed thrombus were amplified after MI in comparison to sham mice (Fig. 4.32A).

To ask whether CXCR4 neutrophil-driven thrombopoiesis is the main driver of amplified thrombosis burden, the thrombus formation as a result of carotid injury was visualized in Mrp8-Cre/CXCR4^{fl/fl} mice who underwent MI/IR surgery. Mrp8-Cre(+)/CXCR4^{Δ/Δ} mice showed attenuated thrombus formation and reduced embolism (Fig. 4.32B) compared to their

littermate controls. Targeting neutrophil CXCR4 signaling may correct the enhanced platelet production and can recover the thrombus burden under MI.

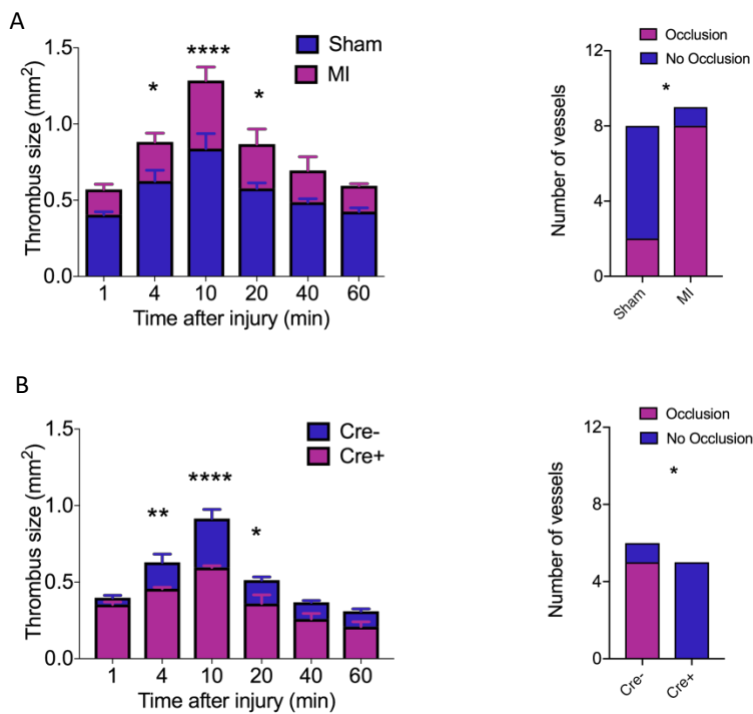


Figure 4.32. Arterial thrombosis burden is corrected by abrogated neutrophil CXCR4 in MI/IR mice.

(A) Quantification of thrombus size over the time following 48h after myocardial infarction surgery and FeCl₃ carotid artery injury was performed on sham and MI/IR mice in addition to calculation of the occlusion of every mouse (vessel=mouse; n=8,9 C57BL/6 mice per group). (B) Quantification of thrombus size over the time following 48h after myocardial infarction surgery and FeCl₃ carotid artery injury was performed on both Mrp8-Cre(-)/CXCR4^{fl/fl} along with Mrp8-Cre(+)/CXCR4^{Δ/Δ} animals in addition to the calculation of the occlusion of every mouse (n=5,6 Mrp8-Cre/CXCR4^{fl/fl} mice per group). Significance levels are shown as *<0.05, **<0.01 or ****< 0.0001, and measured using two-way ANOVA or unpaired t-test.

4.2.9 RPs counts and neutrophil CXCR4 expression increase in ST-elevation myocardial infarction patients

To clinically examine the effects of MI/IR on patients and to validate the findings found in animal models, STEMI patients enduring a percutaneous coronary intervention were examined in this study. Data showed a transient proliferation in RP amounts (i.e. RPs +50.7%), which were normalized to the RP counts detected in control subjects having stable CAD (at day 5) post-STEMI (Fig. 4.33A). It was stated that CXCL12-CXCR4 signaling is disturbed following MI,

resulting in the mobilization of neutrophils to the peripheral circulation which causes neutrophilia [177,179]. Accordingly, CXCR4 was investigated in this project and was found to be increasingly expressed on neutrophils of peripheral blood in STEMI patients (Fig. 4.33B). Consequently, these findings were correlated with murine results showing an increase in both RPs and neutrophil-derived CXCR4 in MI circulation. Therefore, these observations postulate a therapeutic approach targeting the underlying molecular mechanisms and the immune continuum to mitigate the disease progression.

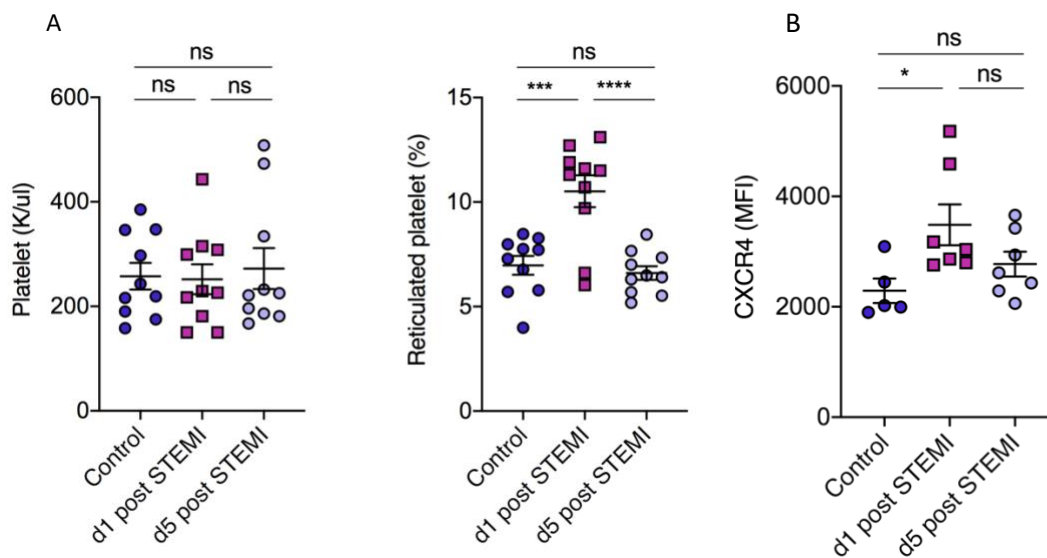


Figure 4.33. Measurements of platelets, RPs, and CXCR4 in STEMI patients.

(A) STEMI patients were recruited having less than 12 h symptom onset and undertaking revascularization or control subjects as described above. Counts of platelets and RPs (n=10 STEMI or control patients) in addition to (B) CXCR4 expression on neutrophils was analyzed using flow cytometry with n=5 control patients and n=7 STEMI. Significance levels are presented as * < 0.05, *** < 0.001, **** < 0.0001 or ns, and measured using one-way ANOVA. STEMI data were generated by Amin Polzin (Düsseldorf) and retrieved from [123].

5. Discussion

5.1 Intermittent hypoxia and myocardial infarction enhance the production of mature and immature platelets

Inflammatory disorders are identified to influence thrombopoiesis; nevertheless, the precise processes by which IH or MI affects bone marrow remain unclear. Hence, this project studied OSA patients and intermittent hypoxic mice to elaborate on the mechanism of intermittent hypoxia in bone marrow. Besides, we studied STEMI patients and myocardial infarction/ischemic reperfusion mice to investigate further the mechanisms of thrombopoiesis and if MI effects are similar to IH outcomes in individuals and mice. OSA patients and IH-exposed mice display a prothrombotic phenotype that originated from increased reticulated platelet counts due to exaggerated neutrophil-driven thrombopoiesis. Higher numbers of reticulated platelets in the bloodstream have been demonstrated to be related to increased platelet reactivity, higher rates of cardiovascular (CV) outcomes in addition to increased mortality within the patient population suffering from CAD [180,181]. In addition, this study demonstrated that immature platelet formation is boosted in STEMI patients and mice that have been operated on after 48 hours following MI/IR; therefore increasing the threat of arterial thrombosis along with the recurring ischemic incidents after myocardial infarction. These findings along with previously published data insinuate the critical involvement of immature reticulated platelets on the enhanced threat of repeated ischemia in patients with MI [25] who possibly had sleep apneic events.

5.2 Plucking neutrophils on proplatelet-forming megakaryocytes triggers thrombopoiesis and boosts thrombotic risk

This research study elucidated the role of neutrophils and their association with inflammation, platelet production, and thrombotic risk. We demonstrated that neutrophils are responsible for thrombopoiesis by accelerating the growth and release of platelets and reticulated platelets into the vasculature. Indeed, neutrophils under hypoxic conditions and CV ischemic

reperfusion can influence platelet progenitors, megakaryocytes, at the perisinusoidal niche via CXCR4-CXCL12, leading to a substantial proliferation in platelet formation within the BM by direct physical interaction. This project showed that under IH or MI/IR, neutrophils interacted with PPLs at the perisinusoidal niche in a manner resembling the active plucking of neutrophils on PPLs until PPL parts were extricated into the vasculature. Plucking neutrophils to MKs in BM is a regulator of platelet homeostasis conserving platelet reckons under a steady state; nonetheless, it enhances the production of RPs during thromboinflammation causing increased thrombotic risk following OSA and MI/IR. The stimulation of mechano-signaling in MKs by neutrophils is commanded by the development of more platelets through NOX2-dependent ROS [123]. Neutrophils enhance the release of immature platelets by positioning close to PPL budding sites at MKs; consequently, augmenting the thrombus burden under hypoxic conditions as well as enhancing the rate of recurring ischemic occurrences after MI.

5.3 Characterization of the BM cytokine profile following intermittent hypoxia

Hypoxia, as well as ischemic injury (in which interruption of blood supply leads to tissue hypoxia), may drive inflammatory mechanisms manifested by increased cytokine levels in the body. Indeed, IH is directly correlated to an oxidative imbalance in ROS production and stimulation of an inflammatory cascade [66] by enhancing the pro-inflammatory cytokines, like IL-6 and IL-1. However, it remains unclear how IH influences the expression of cytokines in BM. No alteration was detected in IL-6 and IL-1 concentrations in BM of intermittent hypoxic mice investigated in this study. Characterization of cytokine profile in the interstitial fluid of bone marrow indicated that the most recognized regulators of megakaryopoiesis and thrombopoiesis including thrombopoietin and IL-1 α were unaltered under intermittent hypoxia.

It was shown that the multi-ligand receptor for the advanced glycation of end-products termed RAGE is downregulated within the lungs but relatively increased in the circulation of chronic hypoxia [182]. Interestingly in this project, RAGE was significantly increased in the BM of intermittent hypoxic mice. Indeed, RAGE was found to be the promoter region in which HIF1- α , which is the principal molecular effector of hypoxia signaling, binds to its binding site and

activates the genetic transcription [183]. It is important to note that chronic sustained hypoxia increases HIF1- α by enabling it to relocate into the nucleus forming HIF transcription complex; yet, HIF1- α activation and regulation under IH from OSA is still ambiguous [184]. It was mentioned that the induction of IH of the synthesis and stability of HIF1- α is due to augmented ROS generated by NADPH oxidases, mainly NOX2; suggesting that NOX2 is critical for the activation of HIF1 by IH [185]. Besides, it was described that RAGE expression is boosted in the ischemic heart of rats after IR injury in the myocardium [186]. Together, RAGE may have a key role in hypoxic/ischemic conditions which need further investigation to develop interventions decreasing the tremendous effects of hypoxia followed by reperfusion in OSA and MI.

The largest and most complex member of gelatinaseB identified as the matrix of metalloproteinase-9 (MMP-9) [187], was also found to be significantly increased in BM of IH mice in this project. MMP-9 is recognized to trigger the vascular endothelial growth factor-A (VEGF-A) [188] by inducing the recruitment of BM-derived myeloid cells (CD45⁺) [189]. Emerging evidence is detected in the contribution of HIF1- α and its downstream axis as SDF-1 α /CXCL12 along with VEGF-A in the mobilization and retainment of leukocytes in settings of angiogenesis [189–191]. Together, these findings may suggest that MMP-9 may be an effector protein in neutrophil recruitment and homing in BM under hypoxic/ischemic conditions.

5.4 Reticulated platelets are better prognostic markers than controversial platelet indices (PDW and MPV) in OSA and MI

OSA patients showed an alteration within the platelet compartment, given that elevated MPV [192], as well as PDW, were reported [193]. In this study, platelet count was not correlated with AHI (severity of OSA disease); however, MPV and PDW were significantly correlated with AHI suggesting increased platelet production in OSA patients. It was reported that MPV and PDW values in OSA patients were higher than those of control individuals [192–194]. Yet, other studies showed that MPV and PDW are not sensitive platelet indices and PDW only shows high values in severe OSA patients [195]. Although MPV was found to be elevated in acute MI and is associated with a higher chance of reoccurring infarction [196], MPV and PDW values were not elevated in MI mice operated in this study. Moreover, MPV and PDW are easily affected by genetic polymorphisms, sex, or lifestyles [197]; thus, deciding whether the patient has a

normal or slight increase in MPV is challenging [198]. Despite the multiple investigations on MPV, it was stated that MPV is increased in patients with thrombotic profiles due to the augmented counts of RPs and platelet activation markers [198,199]. Accordingly, measuring RPs and platelet activation markers may represent a more adequate and direct approach than the modest standard method of measuring MPV which cannot define diagnosis and prognosis in any disease [198]. Reticulated platelets in this project showed a strong correlation with AHI values in a limited number of patients and exhibited significant changes before and after therapy. In addition, MI/IR-operated mice along with STEMI patients indicated an eminent increase in RPs counts; therefore, RPs might be a useful marker for predicting thrombotic risk in patients with sleep apnea or myocardial infarction.

5.5 Hyperactive reticulated platelets act as prothrombogenic drivers in IH and MI

Immature platelets showed a hyperactive phenotype, accelerating thrombogenicity and platelet aggregation in patients with CV diseases such as acute MI [15]. Parallely, OSA patients showed an increased level of platelet activation indicators (e.g. CD63 and CD62P) [200]. This study detected a higher expression trend of P-selectin and CD63 in immature platelets (TO stained) compared with mature platelets in OSA patients and healthy donors; meaning that RPs are the platelet fractions majorly contributing to platelet hyperactivity. In addition, adopting high dimensional flow cytometry analysis on concatenated resting platelet populations distinguished and quantitated the distinct platelet subsets in OSA and controls by color-coded tSNE-flowSOM and heatmap clusters; importantly, these platelet populations expressed an upsurge of platelet activation markers (P-selectin, PAC-1, and CD63) in OSA. Thus, it can be hypothesized that platelets were activated differently and exhibited a higher activation profile under inflammatory conditions encountered by OSA patients. In conclusion, increased number and activity of reticulated immature platelets may be helpful to be a new prognosis biomarker to highlight patients at elevated risk of CV events.

OSA and STEMI patients displayed prothrombotic platelet characteristics linked to increased reticulated platelet counts. In this project, flow chamber studies of the blood of OSA patients on collagen showed a significant increase in thrombus formation than in healthy individuals.

Originally, Wright and his colleague (1942) detected that platelet adhesiveness varied by differences in the concentration of anticoagulants in the circulation of postoperative and postpartum samples. It was proposed that the intensification of platelet stickiness is due to the increased rapid proliferation of young platelets into the circulation; hence, immature young platelets may be more adhesive than mature old platelets [201]. Afterward, evidence was provided indicating that reticulated platelets had a higher adhesiveness to collagen than the older platelet compartments by in-vivo and ex-vivo studying of rabbits [202]. Indeed, altered molecular and intrinsic properties are found in hyperactivated immature platelets [203] and upregulation of various prothrombotic transcripts in reticulated platelets including the collagen receptor GPVI, thromboxane receptor A2, thrombin, and ATP receptors postulating a first biological clarification for the hyperactivity of immature platelets [204]. Indeed, amplified recruitment of RNA-rich RPs of OSA patients to collagen was identified in this project. Hence, RPs elucidated a higher activated profile accelerating platelet aggregation and inducing coagulation at injury sites.

It was hypothesized that immature prothrombotic platelets comprise more RNA and increased arterial thrombotic activity in comparison to older counterparts [205,206]. Primarily, this research project explained that RPs were excessively driven to regions of vascular impairment leading to arterial thrombus formation following intermittent hypoxia or myocardial ischemic reperfusion. The results of this project are consistently aligned with other investigations hypothesizing that immature platelets have a boosted tendency to be involved in arterial thrombus formation compared to older mature platelets [206]. Still, immature RPs are shown to be less responsive to available dual antiplatelet treatments with aspirin and clopidogrel [181]. Hence, focusing on platelet production stimulated by neutrophils to diminish the development of thrombogenic RPs may foster an antithrombotic methodology to constrain recurring ischemic events in the first stages of MI and other conditions of thromboinflammation that can also be experienced under intermittent hypoxia. In summary, neutrophil-driven thrombopoiesis is identified in this study as an indicator of thrombotic CV events, accentuating its future implication as an innovative antithrombotic target.

5.6 Excessive production of neutrophil-derived ROS may lead to severe cardiovascular outcomes

This project uncovered the evidence validating the concept of recurrent apnea related to hypoxic/reoxygenation events in OSA, similar to ischemia-reperfusion in MI, enhancing oxidative stress (ROS). Reperfusion injury implies damage happening as an outcome of restoring the flow of blood to the hypoxic (ischemic) tissue. While numerous processes impose this impairment, it is mostly ascribed to ROS formation throughout the cycles of reperfusion/reoxygenation [94,207–209]. OSA is accompanied by apneic/hypoxic events followed by intermittent rapid reoxygenation of the blood which may be similar to the repeated reperfusion injury due to ROS production [210]. ROS formation is investigated especially where a duration of hypoxia exposure is followed by reperfusion, and studied during a stroke that is clinically elucidating the myocardial infarcts' consequences. ROS was identified directly when the ischemic heart's blood circulation was repaired [207,211,212]. Reperfusion injury has been associated with OSA during which transient episodes of hypoxia (airway obstruction) are followed by reoxygenation cycles [94]. This project showed that neutrophils exposed to intermittent hypoxia in OSA and ischemic reperfusion in MI indicated an increased production of ROS that has been extensively associated with inflammatory CV responses and thrombosis [213]. CPAP treatment guided neutrophils to a fast and extended reduction of oxidative stress in OSA [214]. Similarly, ROS production decreased drastically in this study after CPAP therapy of sleep apnea patients. Hence, oxidative stress (ROS) is a crucial player in the hypoxia/reoxygenation processes that may lead to increased CV morbidity in OSA and MI.

5.7 Targeting neutrophil-driven thrombopoiesis diminishes platelet overproduction and thrombus burden

Targeting neutrophil-driven thrombopoiesis attenuates platelet and young platelet activation which may have the potential to limit thrombus formation under hypoxia/reoxygenation conditions in OSA and MI. CXCR4 is a chemokine receptor that has been indicated to be important in controlling neutrophil migration as well as its function [15]. Neutrophils developing increased expression of CXCR4 are implicated in various diseases, including lung

inflammation and infectious diseases [140]. This project now illustrates that inhibition of neutrophil-driven thrombopoiesis by LFA-1 blockade or genetic ablation of CXCR4 in neutrophils efficiently reduced RP fraction in the OSA mouse model. Besides, the abrogation of neutrophil CXCR4 also decreased the augmented formation of platelets and RPs in murine models of MI/IR.

CXCR4-deficient neutrophils of Mrp8-Cre(+)/CXCR4^{Δ/Δ} mice failed to increase thrombopoiesis by considerably lowering platelets and reticulated platelets production after IH 7-days exposure of mice and following 48h MI/IR murine injury in comparison to normoxic mice and sham mice, respectively. Inhibitors and modulators of CXCR4 signaling are tested as co-medication and modulators in cancer therapy and inflammatory diseases [215]. In this project, data showed that CXCR4 was highly expressed in the circulating neutrophils of IH and MI/IR, and interestingly CXCR4^{high} neutrophils under hypoxic conditions were increasingly observed within the bone marrow of IH mice. This finding was in line with a study reporting that neutrophils do not die at the place of damage; instead, they return into the blood flow then they traffic in the lung to subsequently travel to bone marrow via CXCR4 [216]. The findings of our study highlighted the complex interactions between neutrophils, their microenvironment, and the chemokine receptor CXCR4 that regulate their function and homing back to BM under inflammatory conditions (IH and MI).

Increasing evidence was uncovered that OSA patients, who may manifest CV disease burden, are indeed experiencing endothelial malfunction [64]. ICAM-1 expression was seen to be increased in the pulmonary tissue of mice exposed to hypoxia compared to normoxic mice [157]. In this project, increased ICAM-1 expression was likewise observed in the pulmonary endothelium of IH mice. It was found that a disturbance in endothelial vasculature is manifested in OSA patients compared to controls [155]. OSA patients were described to have moderated resistance-endothelial dilation to acetylcholine that boosts the release of NO in the endothelium leading to vasodilation, in comparison with control subjects [217]; consequently, predispose OSA patients to heart failure.

Hence, dysfunction of vascular endothelium, increased CXCR4 expression on circulating neutrophils as well as enhanced RP formation may exacerbate sequelae of CV events in OSA patients.

5.8 CPAP therapy alleviates the thrombotic risk of intermittent hypoxia

This project demonstrated that CPAP, which is the standard intervention for severe OSA, can attenuate excessive platelet production. Despite its humble long-term adherence as well as its variable efficacy [218,219], CPAP therapy has already been reported to reduce platelet reactivity and aggregability in patients with OSA [194,220,221] and can also attenuate the oxidative stress in OSA patients [222]. In this study, CPAP therapy enormously reduced the activation of platelet markers (P-selectin and PAC-1); in addition, the GPVI collagen receptor was also reduced in the platelet population of patients post-therapy. Stimulated platelet population markers after treatment with CPAP were downregulated and were illustrated with a normal profile comparable to healthy controls. The findings of this project emphasized the importance of CPAP therapy that decreased CXCR4 expression on circulating neutrophils; relieving OSA patients from the consequences of recurrent deoxygenation/reoxygenation cycles which they have encountered before using this therapy.

Moreover, to better understand the biomolecular interactions and changes in circulating neutrophils of OSA patients before and after CPAP therapy, a functional proteomic analysis was performed in this study on sorted neutrophil cells. Upregulated mitochondrial regulations were mainly reported in untreated OSA patients, which may advocate the important role of neutrophil-derived ROS production in OSA. Based on former studies, it is postulated that mitochondrial dysfunction may reflect the excessive ROS production under IH and OSA [223,224]. Hence, CPAP therapy may intervene in the regulation of cellular neutrophil components by diminishing neutrophil-related mitochondrial activity in sleep apnea patients.

In addition, it was also investigated that this CPAP intervention in OSA diminished the possibility of CV morbidity leading to myocardial infarction, stroke, and acute coronary disease [104,225]. Many favorable outcomes have been attributed to CPAP therapy in the literature, which is considered a “stent” for the airway [226]. It was demonstrated that CPAP decreases arterial stiffness and blood pressure in patients with existing CV diseases and concomitant OSA [227]. This beneficial effect was detected after the first night and increased robustly after 6 months of CPAP treatment [227]. Moreover, CPAP therapy was associated with a repairing capacity on endothelial function attributable to decreased inflammation and oxidative stress, along with enhanced NO availability [228]. Nevertheless, recent studies suggested that these

effects might not result in a reduction of CV risk. Particularly, trials in SAVE (sleep apnea CV endpoints) [229] and RICCADSA (CPAP Randomized Intervention in CAD and OSA) [230] revealed the disappointment of CPAP therapy in diminishing the future CV events in OSA patients. This failure may be due to the experimental limitations which are worth mentioning. One of these limitations was the absence of a real sham CPAP consisting of a mask and its tube without applying pressure which might disturb patients during sleep and negatively affect the patients (in the RICCADSA study). An additional limitation was the adherence criterion of CPAP duration (mainly in the SAVE study) which is described as not less than 4 hours of CPAP usage every night and not all patients met this norm. Accordingly, it is difficult to draw assumptions that may misjudge the advantages of CPAP in OSA patients.

Importantly, the findings of this project demonstrated that CPAP therapy decreases the thrombotic risk by reducing reticulated platelet production in OSA patients. Patients post-CPAP treatment showed a significant decrease in platelet adhesion and aggregate formation ex-vivo underflow on both collagen and plaque. Taken together, this project identified RPs as a prothrombotic diagnostic tool in monitoring the response of patients with sleep apnea to CPAP therapy.

It is necessary to mention that research endeavors may face challenges from patients with CV diseases who may have asymptomatic OSA [231]. It has been reported that treating patients with OSA without daytime symptoms using CPAP therapy does not improve their subjective well-being [232]. Continued research in this field is essential, as investigation of possible targets for novel therapies to complement CPAP may alleviate the injurious effects of CV events. The data provided in this project can pave the way for investigators to improve health outcomes in patients with or prone to CV disease by identifying potential therapeutic targets and addressing sleep-related breathing disorders.

5.9 Limitations of this study

Several important caveats apply to this research investigation. Most importantly, bone marrow of OSA and STEMI patients samples was not examined in this study; only murine bone marrow was investigated. Yet, similar results from circulating platelets and neutrophils were observed in both mice and human samples. Lungs are the primary sites to sense the fluctuations of oxygen levels and hypoxia. The in-vivo pulmonary investigation was not done in this study due to technical difficulties attributed to the respiratory rate of the pulmonary area and the palpitation cardiac rhythm.

IH murine chamber has limitations as a model of OSA, lacking features of thoracic pressure variation, airway closure, complete synchrony with sleep, and hypercapnia. The model used in this study mimics only the intermittent hypoxic episodes occurring in OSA patients but fails to reproduce transient hypercapnia determined by airway occlusion observed in OSA; nonetheless, permitting us to separate the mechanical effect of obstruction from the consequences of IH itself. In addition, this project lacks the development of a sophisticated animal model that may mimic the CPAP therapy to explore a wide range of biological activation of the pivotal signaling pathways and to make a development in treating sleep apnea and consequently myocardial infarction risk. The study is constrained by difficulties in matching controls to patients with the same age, gender, and BMI. Furthermore, not all controls underwent polysomnography since most of the controls were recruited by advertisement.

6. Conclusion and Future Work

The close cellular interaction between neutrophils and megakaryocytes at the proplatelet budding niches in bone marrow increases the production of both mature and immature platelets; and consequently, elevates the thrombotic risk under cardiovascular diseases and intermittent hypoxic conditions.

To summarize, exaggerated neutrophil-driven thrombopoiesis not only enhances the CV risks in an acute inflammatory condition such as myocardial infarction, but it also displays a prothrombotic phenotype that originated from excessive reticulated platelet recruitment in conditions of intermittent hypoxia. Immature reticulated platelets are hyperactive and abundant at the site of injury resulting in arterial thrombus formation following intermittent hypoxia or ischemia-reperfusion myocardial infarction. Despite the controversial results regarding the validation of reticulated platelets as a prognostic marker, this study showed that reticulated platelets can be used as a promising diagnostic biomarker for evaluating the risk of CV occurrences in individuals having OSA and MI. Quantifying the level of reticulated platelets in the circulation, along with targeted pharmacological interventions to inhibit the overflow of these cells, may serve as a method for shaping personalized antithrombotic treatments in OSA and MI patients; aiming to minimize adverse CV events. CPAP therapy alleviated the detrimental outcomes of IH in OSA by decreasing the augmented reticulated platelet production and reducing the thrombus burden. Since immature platelets revealed their insensitivity to current antiplatelet therapy, targeting neutrophil-derived thrombopoiesis may open prodigious avenues in diminishing the formation of prothrombotic immature reticulated platelets and inhibit recurrent CV outcomes in OSA and correspondingly MI.

OSA is repeatedly undertreated and underestimated in cardiovascular practice. Limited published data have elucidated the processes by which sleep apnea can accelerate thrombotic risk or precipitate myocardial infarction. The findings achieved in this study may provide a key understanding of the cellular mechanisms for additional investigations to prevent myocardial infarction risk and attenuate recurrent hypoxic/ischemic events.

This study can be further developed by investigating the direct physical forces induced between neutrophils and MKs. Additional translational studies are required to dissect novel therapeutic strategies to decrease the thrombotic risk in both MI and OSA conditions. More research is needed to explore the possible clinical benefits of targeting immunothrombopoiesis of the various immune cells, not only neutrophils; but also monocytes, lymphocytes B and T cells may be also further investigated with platelet production under IH and myocardial ischemia-reperfusion. In-depth future explorations into the biology of RPs, especially at the proteomic level, are essential to gain a deeper understanding of the cellular processes driving their heightened reactivity. Oxygen levels in tissues were not investigated and might be subsequently examined to further clarify the exact role of intermittent hypoxia in tissues.

The results of this project might deepen our understanding of the cardiovascular burden on OSA patients. Nevertheless, studying the relationship between MI and OSA is limited; therefore, additional experiments are required to completely elucidate the putative involvement of OSA with increased cardiovascular risk in MI.

Bibliography

1. Machlus, K.R.; Italiano, J.E. The Incredible Journey: From Megakaryocyte Development to Platelet Formation. *J. Cell Biol.* **2013**, *201*, 785–796, doi:10.1083/jcb.201304054.
2. Cardier, J.E.; Foster, D.C.; Lok, S.; Jacobsen, S.E.W.; Murphy, M.J.; Cardiel, J.' E.; Fostecb, D.C.; Jacobsen, ? S E W; Murphy, M.J."; Cardier, J.E. Megakaryocytopoiesis In Vitro: From the Stem Cells' Perspective. *Stem Cells* **1996**, *14*, 163–172.
3. Kaushansky, K.; Lok, S.; Holly, R.D.; Broudy, V.C.; Lin, N.; Bailey, M.C.; Forstrom, J.W.; Buddle, M.M.; Oort, P.J.; Hagen, F.S.; et al. Promotion of Megakaryocyte Progenitor Expansion and Differentiation by the C-Mpl Ligand Thrombopoietin. *Nat.* **1994**, *369*, 568–571, doi:10.1038/369568a0.
4. Tijssen, M.R.; Ghevaert, C. Transcription Factors in Late Megakaryopoiesis and Related Platelet Disorders. *J. Thromb. Haemost.* **2013**, *11*, 593–604, doi:10.1111/jth.12131.
5. Kaushansky, K. The Molecular Mechanisms That Control Thrombopoiesis. *J. Clin. Invest.* **2005**, *115*, 3339–3347, doi:10.1172/JCI26674.
6. Broudy, V.C.; Lin, N.L.; Kaushansky, K. Thrombopoietin (c-Mpl Ligand) Acts Synergistically with Erythropoietin, Stem Cell Factor, and Interleukin-11 to Enhance Murine Megakaryocyte Colony Growth and Increases Megakaryocyte Ploidy in Vitro. *Blood* **1995**, *85*, 1719–1726.
7. Metcalf, D.; Di Rago, L.; Mifsud, S. Synergistic and Inhibitory Interactions in the In Vitro Control of Murine Megakaryocyte Colony Formation. *STEM CELLS* **2002**, *20*, 552–560, doi:10.1002/stem.200552.
8. Yagi, M.; Roth, G.J. Megakaryocyte Polyploidization Is Associated with Decreased Expression of Polo-like Kinase (PLK). *J. Thromb. Haemost. JTH* **2006**, *4*, 2028–2034, doi:10.1111/J.1538-7836.2006.02092.X.
9. Zimmet, J.; Ravid, K. Polyploidy: Occurrence in Nature, Mechanisms, and Significance for the Megakaryocyte-Platelet System. *Exp. Hematol.* **2000**, *28*, 3–16, doi:10.1016/S0301-472X(99)00124-1.
10. Machlus, K.R.; Thon, J.N.; Italiano, J.E. Interpreting the Developmental Dance of the Megakaryocyte: A Review of the Cellular and Molecular Processes Mediating Platelet Formation. *Br. J. Haematol.* **2014**, doi:10.1111/bjh.12758.
11. Machlus, K.R.; Johnson, K.E.; Kulenthirarajan, R.; Forward, J.A.; Tippy, M.D.; Soussou, T.S.; El-Husayni, S.H.; Wu, S.K.; Wang, S.; Watnick, R.S.; et al. CCL5 Derived from Platelets Increases Megakaryocyte Proplatelet Formation. *Blood* **2016**, *127*, 921–926, doi:10.1182/blood-2015-05-644583.
12. Nishimura, S.; Nagasaki, M.; Kunishima, S.; Sawaguchi, A.; Sakata, A.; Sakaguchi, H.; Ohmori, T.; Manabe, I.; Italiano, J.E.; Ryu, T.; et al. IL-1 α Induces Thrombopoiesis through Megakaryocyte Rupture in Response to Acute Platelet Needs. *J. Cell Biol.* **2015**, *209*, 453–466, doi:10.1083/jcb.201410052.
13. Yang, S.; Wang, L.; Wu, Y.; Wu, A.; Huang, F.; Tang, X.; Kantawong, F.; Anuchapreeda, S.; Qin, D.; Mei, Q.; et al. Apoptosis in Megakaryocytes: Safeguard and Threat for Thrombopoiesis. *Front. Immunol.* **2023**, *13*, 1025945, doi:10.3389/fimmu.2022.1025945.
14. WRIGHT, J.H. The Origin and Nature of the Blood Plates. <http://dx.doi.org/10.1056/NEJM190606071542301> **1906**, *154*, 643–645, doi:10.1056/NEJM190606071542301.
15. Bongiovanni, D.; Han, J.; Klug, M.; Kirmes, K.; Viggiani, G.; Von Scheidt, M.; Schreiner, N.; Condorelli, G.; Laugwitz, K.L.; Bernlochner, I. Role of Reticulated Platelets in

- Cardiovascular Disease. *Arterioscler. Thromb. Vasc. Biol.* **2022**, *42*, 527–539, doi:10.1161/ATVBAHA.121.316244.
16. Leeksa, C.H.W.; Cohen, J.A. DETERMINATION OF THE LIFE SPAN OF HUMAN BLOOD PLATELETS USING LABELLED DIISOPROPYLFLUOROPHOSPHONATE. **1956**.
 17. Odell, T.T.; McDonald, T.P. Life Span of Mouse Blood Platelets. *Httpsdoiorg10318100379727-106-26252* **1961**, *106*, 107–108, doi:10.3181/00379727-106-26252.
 18. Quach, M.E.; Chen, W.; Li, R. Mechanisms of Platelet Clearance and Translation to Improve Platelet Storage. **2018**.
 19. van der Meijden, P.E.J.; Heemskerk, J.W.M. Platelet Biology and Functions: New Concepts and Clinical Perspectives. *Nat. Rev. Cardiol.* **2019**, *16*, 166–179, doi:10.1038/s41569-018-0110-0.
 20. Bongiovanni, D.; Han, J.; Klug, M.; Kirmes, K.; Viggiani, G.; Von Scheidt, M.; Schreiner, N.; Condorelli, G.; Laugwitz, K.-L.; Bernlochner, I. Arteriosclerosis, Thrombosis, and Vascular Biology ATVB IN FOCUS: The Science of ATVB Early Career Committee Role of Reticulated Platelets in Cardiovascular Disease. **2022**, doi:10.1161/ATVBAHA.121.316244.
 21. Leslie, M. Beyond Clotting: The Powers of Platelets. *Science* **2010**, *328*, 562–564, doi:10.1126/SCIENCE.328.5978.562.
 22. Clancy, L.; Beaulieu, L.M.; Tanriverdi, K.; Freedman, J.E. The Role of RNA Uptake in Platelet Heterogeneity. *Thromb. Haemost.* **2017**, *117*, 948–961, doi:10.1160/TH16-11-0873.
 23. Gaertner, F.; Massberg, S. Patrolling the Vascular Borders: Platelets in Immunity to Infection and Cancer. *Nat. Rev. Immunol.* **2019**, *19*, 747–760, doi:10.1038/s41577-019-0202-z.
 24. Lee, L.G.; Chen, C. -H; Chiu, L.A. Thiazole Orange: A New Dye for Reticulocyte Analysis. *Cytometry* **1986**, *7*, 508–517, doi:10.1002/CYTO.990070603.
 25. Lakkis, N.; Dokainish, H.; Abuzahra, M.; Tsyboulev, V.; Jorgensen, J.; Ponce De Leon, A.; Saleem, A. Reticulated Platelets in Acute Coronary Syndrome: A Marker of Platelet Activity. *J. Am. Coll. Cardiol.* **2004**, *44*, 2091–2093, doi:10.1016/J.JACC.2004.05.033.
 26. Corpataux, N.; Franke, K.; Kille, A.; Valina, C.M.; Neumann, F.J.; Nührenberg, T.; Hochholzer, W. Reticulated Platelets in Medicine: Current Evidence and Further Perspectives. *J. Clin. Med.* **2020**, *9*, 1–12, doi:10.3390/jcm9113737.
 27. Kennedy, A.D.; Deleo, F.R. Neutrophil Apoptosis and the Resolution of Infection. *Immunol. Res.* **2009**, *43*, 25–61, doi:10.1007/S12026-008-8049-6/METRICS.
 28. Lawrence, S.M.; Corriden, R.; Nizet, V. The Ontogeny of a Neutrophil: Mechanisms of Granulopoiesis and Homeostasis. *Microbiol. Mol. Biol. Rev. MMBR* **2018**, *82*, doi:10.1128/MMBR.00057-17.
 29. Raskov, H.; Orhan, A.; Gaggar, S.; Gögenur, I. Neutrophils and Polymorphonuclear Myeloid-Derived Suppressor Cells: An Emerging Battleground in Cancer Therapy. *Oncog. 2022 111* **2022**, *11*, 1–16, doi:10.1038/s41389-022-00398-3.
 30. Link, D.C. Neutrophil Homeostasis: A New Role for Stromal Cell-Derived Factor-1. *Immunol. Res.* **2005**, *32*, 169–178, doi:10.1385/IR:32:1-3:169/METRICS.
 31. Vietinghoff, S. von; Ley, K. Homeostatic Regulation of Blood Neutrophil Counts. *J. Immunol. Baltim. Md 1950* **2008**, *181*, 5183, doi:10.4049/JIMMUNOL.181.8.5183.
 32. Katia De Filippo, S.M.R. CXCR4, the Master Regulator of Neutrophil Trafficking in Homeostasis and Disease. *Eur. J. Clin. Invest.* **2018**, doi:10.1111/eci.12949.
 33. Lerman, Y.V.; Kim, M. Neutrophil Migration under Normal and Sepsis Conditions. *Cardiovasc. Hematol. Disord. Drug Targets.* **2015**, *15*, 19, doi:10.2174/1871529X15666150108113236.

34. McCracken, J.M.; Allen, L.-A.H. Regulation of Human Neutrophil Apoptosis and Lifespan in Health and Disease. *J. Cell Death* **2014**, *7*, JCD.S11038, doi:10.4137/JCD.S11038.
35. Shi, J.; Gilbert, G.E.; Kokubo, Y.; Ohashi, T. Role of the Liver in Regulating Numbers of Circulating Neutrophils. *Blood* **2001**, *98*, 1226–1230, doi:10.1182/BLOOD.V98.4.1226.
36. Nauseef, W.M. How Human Neutrophils Kill and Degrade Microbes: An Integrated View. *Immunol. Rev.* **2007**, *219*, 88–102, doi:10.1111/j.1600-065X.2007.00550.x.
37. Kojda, G.; Harrison, D. Interactions between NO and Reactive Oxygen Species: Pathophysiological Importance in Atherosclerosis, Hypertension, Diabetes and Heart Failure. *Cardiovasc. Res.* **1999**, *43*, 562–571, doi:10.1016/S0008-6363(99)00169-8/2/43-3-652-FIG5.GIF.
38. Misra, M.K.; Sarwat, M.; Bhakuni, P.; Tuteja, R.; Tuteja, N. Oxidative Stress and Ischemic Myocardial Syndromes. *Med. Sci. Monit. Int. Med. J. Exp. Clin. Res.* **2009**, *15*, RA209-219.
39. Dyugovskaya, L.; Polyakov, A.; Cohen-Kaplan, V.; Lavie, P.; Lavie, L. Bax/Mcl-1 Balance Affects Neutrophil Survival in Intermittent Hypoxia and Obstructive Sleep Apnea: Effects of p38MAPK and ERK1/2 Signaling. *J. Transl. Med.* **2012**, *10*, 211, doi:10.1186/1479-5876-10-211.
40. Townsend, K.J.; Zhou, P.; Qian, L.; Bieszczad, C.K.; Lowrey, C.H.; Yen, A.; Craig, R.W. Regulation of MCL1 through a Serum Response Factor/Elk-1-Mediated Mechanism Links Expression of a Viability-Promoting Member of the BCL2 Family to the Induction of Hematopoietic Cell Differentiation. *J. Biol. Chem.* **1999**, *274*, 1801–1813, doi:10.1074/jbc.274.3.1801.
41. Bogoyevitch, M.A.; Gillespie-Brown, J.; Ketterman, A.J.; Fuller, S.J.; Ben-Levy, R.; Ashworth, A.; Marshall, C.J.; Sugden, P.H. Stimulation of the Stress-Activated Mitogen-Activated Protein Kinase Subfamilies in Perfused Heart: P38/RK Mitogen-Activated Protein Kinases and c-Jun N-Terminal Kinases Are Activated by Ischemia/Reperfusion. *Circ. Res.* **1996**, *79*, 162–173, doi:10.1161/01.RES.79.2.162.
42. Jiang, M.; Wang, L.; Jiang, H.-H. [Role of spinal MAPK-ERK signal pathway in myocardial ischemia-reperfusion injury]. *Zhongguo Dang Dai Er Ke Za Zhi Chin. J. Contemp. Pediatr.* **2013**, *15*, 387–391.
43. Itkin, T.; Gur-Cohen, S.; Spencer, J.A.; Schajnovitz, A.; Ramasamy, S.K.; Kusumbe, A.P.; Ledergor, G.; Jung, Y.; Milo, I.; Poulos, M.G.; et al. Distinct Bone Marrow Blood Vessels Differentially Regulate Haematopoiesis. *Nature* **2016**, *532*, 323–328, doi:10.1038/nature17624.
44. Boisset, J.-C.; Vivié, J.; Grün, D.; Muraro, M.J.; Lyubimova, A.; Van Oudenaarden, A. Mapping the Physical Network of Cellular Interactions. *Nat. Methods* **2018**, *15*, 547–553, doi:10.1038/s41592-018-0009-z.
45. Centurione, L.; Di Baldassarre, A.; Zingariello, M.; Bosco, D.; Gatta, V.; Rana, R.A.; Langella, V.; Di Virgilio, A.; Vannucchi, A.M.; Migliaccio, A.R. Increased and Pathologic Emperipoiesis of Neutrophils within Megakaryocytes Associated with Marrow Fibrosis in GATA-1low Mice. *Blood* **2004**, *104*, 3573–3580, doi:10.1182/blood-2004-01-0193.
46. Cunin, P.; Bouslama, R.; Machlus, K.R.; Martínez-Bonet, M.; Lee, P.Y.; Wactor, A.; Nelson-Maney, N.; Morris, A.; Guo, L.; Weyrich, A.; et al. Megakaryocyte Emperipoiesis Mediates Membrane Transfer from Intracytoplasmic Neutrophils to Platelets. *Elife* **2019**, *8*, doi:10.7554/elife.44031.
47. Sharma, S.; Tyagi, T.; Antoniak, S. Platelet in Thrombo-Inflammation: Unraveling New Therapeutic Targets. *Front. Immunol.* **2022**, *13*, 1039843, doi:10.3389/fimmu.2022.1039843.
48. Jackson, S.P.; Darbousset, R.; Schoenwaelder, S.M. Thromboinflammation: Challenges of Therapeutically Targeting Coagulation and Other Host Defense Mechanisms. *Blood* **2019**, *133*, 906–918, doi:10.1182/blood-2018-11-882993.

49. Gabryelska, A.; Łukasik, Z.M.; Makowska, J.S.; Białasiewicz, P. Obstructive Sleep Apnea: From Intermittent Hypoxia to Cardiovascular Complications via Blood Platelets. *Front. Neurol.* **2018**, *9*, 635, doi:10.3389/fneur.2018.00635.
50. Chaudhary, P.K.; Kim, S.; Kim, S. An Insight into Recent Advances on Platelet Function in Health and Disease. *Int. J. Mol. Sci.* **2022**, *23*, 6022, doi:10.3390/ijms23116022.
51. Cognasse, F.; Laradi, S.; Berthelot, P.; Bourlet, T.; Marotte, H.; Mismetti, P.; Garraud, O.; Hamzeh-Cognasse, H. Platelet Inflammatory Response to Stress. *Front. Immunol.* **2019**, *10*, 1478, doi:10.3389/fimmu.2019.01478.
52. Jenne, C.N.; Urrutia, R.; Kubes, P. Platelets: Bridging Hemostasis, Inflammation, and Immunity. *Int. J. Lab. Hematol.* **2013**, *35*, 254–261, doi:10.1111/ijlh.12084.
53. Diacovo, T.; Roth, S.; Buccola, J.; Bainton, D.; Springer, T. Neutrophil Rolling, Arrest, and Transmigration across Activated, Surface-Adherent Platelets via Sequential Action of P-Selectin and the Beta 2-Integrin CD11b/CD18. *Blood* **1996**, *88*, 146–157, doi:10.1182/blood.V88.1.146.146.
54. Bennett, J.S.; Berger, B.W.; Billings, P.C. The Structure and Function of Platelet Integrins. *J. Thromb. Haemost.* **2009**, *7*, 200–205, doi:10.1111/j.1538-7836.2009.03378.x.
55. Von Hundelshausen, P.; Weber, C. Platelets as Immune Cells: Bridging Inflammation and Cardiovascular Disease. *Circ. Res.* **2007**, *100*, 27–40, doi:10.1161/01.RES.0000252802.25497.b7.
56. Mause, S.F.; Von Hundelshausen, P.; Zerneck, A.; Koenen, R.R.; Weber, C. Platelet Microparticles: A Transcellular Delivery System for RANTES Promoting Monocyte Recruitment on Endothelium. *Arterioscler. Thromb. Vasc. Biol.* **2005**, *25*, 1512–1518, doi:10.1161/01.ATV.0000170133.43608.37.
57. Arnaud, C.; Beguin, P.C.; Lantuejoul, S.; Pepin, J.-L.; Guillermet, C.; Pelli, G.; Burger, F.; Buatois, V.; Ribuot, C.; Baguet, J.-P.; et al. The Inflammatory Preatherosclerotic Remodeling Induced by Intermittent Hypoxia Is Attenuated by RANTES/CCL5 Inhibition. *Am. J. Respir. Crit. Care Med.* **2011**, *184*, 724–731, doi:10.1164/rccm.201012-2033OC.
58. Nanduri, J.; Nanduri, R.P. Cellular Mechanisms Associated with Intermittent Hypoxia. *Essays Biochem.* **2007**, *43*, 91–104, doi:10.1042/bse0430091.
59. Ramirez, T.A.; Jourdan-Le Saux, C.; Joy, A.; Zhang, J.; Dai, Q.; Mifflin, S.; Lindsey, M.L. Chronic and Intermittent Hypoxia Differentially Regulate Left Ventricular Inflammatory and Extracellular Matrix Responses. *Hypertens. Res.* **2012**, *35*, 811–818, doi:10.1038/hr.2012.32.
60. Savransky, V.; Nanayakkara, A.; Li, J.; Bevans, S.; Smith, P.L.; Rodriguez, A.; Polotsky, V.Y. Chronic Intermittent Hypoxia Induces Atherosclerosis. *Am. J. Respir. Crit. Care Med.* **2007**, *175*, 1290–1297, doi:10.1164/rccm.200612-1771OC.
61. Kendzerska, T.; Leung, R.S.; Aaron, S.D.; Ayas, N.; Sandoz, J.S.; Gershon, A.S. Cardiovascular Outcomes and All-Cause Mortality in Patients with Obstructive Sleep Apnea and Chronic Obstructive Pulmonary Disease (Overlap Syndrome). *Ann. Am. Thorac. Soc.* **2019**, *16*, 71–81, doi:10.1513/ANNALSATS.201802-136OC.
62. Montgomery, S.T.; Mall, M.A.; Kicic, A.; Stick, S.M. Hypoxia and Sterile Inflammation in Cystic Fibrosis Airways: Mechanisms and Potential Therapies. *Eur. Respir. J.* **2017**, *49*, doi:10.1183/13993003.00903-2016.
63. Tuder, R.M.; Yun, J.H.; Bhunia, A.; Tuder, R.M.; Yun, J.H.; Bhunia, A.; Fijalkowska, I.; Bhunia, A. Hypoxia and Chronic Lung Disease. *J Mol Med* **2007**, *85*, 1317–1324, doi:10.1007/s00109-007-0280-4.
64. Lavie, L. Obstructive Sleep Apnoea Syndrome - An Oxidative Stress Disorder. *Sleep Med. Rev.* **2003**, *7*, 35–51, doi:10.1053/smr.2002.0261.

65. Lavie, L. Oxidative Stress in Obstructive Sleep Apnea and Intermittent Hypoxia--Revisited--the Bad Ugly and Good: Implications to the Heart and Brain. *Sleep Med. Rev.* **2015**, *20*, 27–45, doi:10.1016/J.SMRV.2014.07.003.
66. Lévy, P.; Kohler, M.; McNicholas, W.T.; Barbé, F.; McEvoy, R.D.; Somers, V.K.; Lavie, L.; Pépin, J.-L. Obstructive Sleep Apnoea Syndrome. *Nat. Rev. Dis. Primer* **2015**, *1*, 15015, doi:10.1038/nrdp.2015.15.
67. Lv, R.; Liu, X.; Zhang, Y.; Dong, N.; Wang, X.; He, Y.; Yue, H.; Yin, Q. Pathophysiological Mechanisms and Therapeutic Approaches in Obstructive Sleep Apnea Syndrome. *Signal Transduct. Target. Ther.* **2023**, *8*, 218, doi:10.1038/s41392-023-01496-3.
68. Leonard, M.O.; Kieran, N.E.; Howell, K.; Burne, M.J.; Varadarajan, R.; Dhakshinamoorthy, S.; Porter, A.G.; O'Farrelly, C.; Rabb, H.; Taylor, C.T.; et al. Reoxygenation-specific Activation of the Antioxidant Transcription Factor Nrf2 Mediates Cytoprotective Gene Expression in Ischemia-reperfusion Injury. *FASEB J.* **2006**, *20*, 2624–2626, doi:10.1096/fj.06-5097fje.
69. Benjafield, A.V.; Ayas, N.T.; Eastwood, P.R.; Heinzer, R.; Ip, M.S.M.; Morrell, M.J.; Nunez, C.M.; Patel, S.R.; Penzel, T.; Pépin, J.L.D.; et al. Estimation of the Global Prevalence and Burden of Obstructive Sleep Apnoea: A Literature-Based Analysis. *Lancet Respir. Med.* **2019**, *7*, 687–698, doi:10.1016/S2213-2600(19)30198-5.
70. Franklin, K.A.; Lindberg, E. Obstructive Sleep Apnea Is a Common Disorder in the Population-A Review on the Epidemiology of Sleep Apnea. *J. Thorac. Dis.* **2015**, *7*, 1311–1322, doi:10.3978/j.issn.2072-1439.2015.06.11.
71. Jordan, A.S.; McSharry, D.G.; Malhotra, A. Adult Obstructive Sleep Apnoea. *The Lancet* **2014**, *383*, 736–747, doi:10.1016/S0140-6736(13)60734-5.
72. Malhotra, A.; White, D.P. Obstructive Sleep Apnoea. *The Lancet* **2002**, *360*, 237–245, doi:10.1016/S0140-6736(02)09464-3.
73. Peracaula, M.; Torres, D.; Poyatos, P.; Luque, N.; Rojas, E.; Obrador, A.; Orriols, R.; Tura-Ceide, O. Endothelial Dysfunction and Cardiovascular Risk in Obstructive Sleep Apnea: A Review Article. *Life 2022 Vol 12 Page 537* **2022**, *12*, 537, doi:10.3390/LIFE12040537.
74. Rundo, J.V. Obstructive Sleep Apnea Basics. *Cleve. Clin. J. Med.* **2019**, *86*, doi:10.3949/ccjm.86.s1.02.
75. Frost & Sullivan *Hidden Health Crisis Costing America Billions Underdiagnosing and Undertreating Obstructive Sleep Apnea Draining Healthcare System*; American Academy of Sleep Medicine, 2016;
76. Maurer, J.T. Early Diagnosis of Sleep Related Breathing Disorders. *GMS Curr. Top. Otorhinolaryngol. Head Neck Surg.* **2008**, *7*, Doc03.
77. Guilleminault, C.; Tilkian, A.; Dement, W.C. The Sleep Apnea Syndromes. *Annu. Rev. Med.* **1976**, *27*, 465–484, doi:10.1146/annurev.me.27.020176.002341.
78. Ye, L.; Pien, G.W.; Ratcliffe, S.J.; Björnsdottir, E.; Sif Arnardottir, E.; Pack, A.I.; Benediksdottir, B.; Gislason, T.; Respir, E. The Different Clinical Faces of Obstructive Sleep Apnoea: A Cluster Analysis. *Eur. Respir. J.* **2014**, *44*, 1600–1607, doi:10.1183/09031936.00032314.
79. Senaratna, C.V.; Perret, J.L.; Lodge, C.J.; Lowe, A.J.; Campbell, B.E.; Matheson, M.C.; Hamilton, G.S.; Dharmage, S.C. Prevalence of Obstructive Sleep Apnea in the General Population: A Systematic Review. *Sleep Med. Rev.* **2017**, *34*, 70–81, doi:10.1016/j.smr.2016.07.002.
80. Lal, C.; Weaver, T.E.; Bae, C.J.; Strohl, K.P. Excessive Daytime Sleepiness in Obstructive Sleep Apnea Mechanisms and Clinical Management. *Ann. Am. Thorac. Soc.* **2021**, *18*, 757–768, doi:10.1513/ANNALSATS.202006-696FR/SUPPL_FILE/DISCLOSURES.PDF.
81. Riha, R.L. Defining Obstructive Sleep Apnoea Syndrome: A Failure of Semantic Rules. *Breathe* **2021**, *17*, 210082, doi:10.1183/20734735.0082-2021.

82. Zhang, W.; Si, L. Obstructive Sleep Apnea Syndrome (OSAS) and Hypertension: Pathogenic Mechanisms and Possible Therapeutic Approaches. *Ups. J. Med. Sci.* **2012**, *117*, 370–382, doi:10.3109/03009734.2012.707253.
83. Sateia, M.J. International Classification of Sleep Disorders-Third Edition. *Chest* **2014**, *146*, 1387–1394, doi:10.1378/chest.14-0970.
84. Goyal, M.; Johnson, J. Obstructive Sleep Apnea Diagnosis and Management. *Mo. Med.* **2017**, *114*, 120.
85. Kapur, V.K.; Auckley, D.H.; Chowdhuri, S.; Kuhlmann, D.C.; Mehra, R.; Ramar, K.; Harrod, C.G. Clinical Practice Guideline for Diagnostic Testing for Adult Obstructive Sleep Apnea: An American Academy of Sleep Medicine Clinical Practice Guideline. *J. Clin. Sleep Med. JCSM Off. Publ. Am. Acad. Sleep Med.* **2017**, *13*, 479–504, doi:10.5664/JCSM.6506.
86. Antic, N.A.; Catcheside, P.; Buchan, C.; Hensley, M.; Naughton, M.T.; Rowland, S.; Williamson, B.; Windler, S.; Doug McEvoy, R. EFFECTS OF CPAP ON DAYTIME FUNCTIONS The Effect of CPAP in Normalizing Daytime Sleepiness, Quality of Life, and Neurocognitive Function in Patients with Moderate to Severe OSA. *SLEEP* **2011**, *34*, 111–119.
87. Chang, H.P.; Chen, Y.F.; Du, J.K. Obstructive Sleep Apnea Treatment in Adults. *Kaohsiung J. Med. Sci.* **2020**, *36*, 7–12, doi:10.1002/KJM2.12130.
88. Oğuz, H.T. Contemporary Treatment Approaches to Obstructive Sleep Apnea Syndrome. In *Current Approaches in Orthodontics*; IntechOpen, 2019 ISBN 978-1-78985-182-3.
89. Weaver, T.E.; Grunstein, R.R. Adherence to Continuous Positive Airway Pressure Therapy: The Challenge to Effective Treatment. *Proc. Am. Thorac. Soc.* **2008**, *5*, 173–178, doi:10.1513/PATS.200708-119MG.
90. Chopra, S.; Polotsky, V.Y.; Jun, J.C. Sleep Apnea Research in Animals: Past, Present, and Future. *Am. J. Respir. Cell Mol. Biol.* **2016**, *54*, 299–305, doi:10.1165/RCMB.2015-0218TR.
91. Bunag, R. Myocardial Infarction. In *xPharm: The Comprehensive Pharmacology Reference*; Enna, S.J., Bylund, D.B., Eds.; Elsevier: New York, 2007; pp. 1–5 ISBN 978-0-08-055232-3.
92. Thygesen, K.; Alpert, J.S.; White, H.D.; null, null; et al. Universal Definition of Myocardial Infarction. *Circulation* **2007**, *116*, 2634–2653, doi:10.1161/CIRCULATIONAHA.107.187397.
93. Yellon, D.M.; Hausenloy, D.J. Myocardial Reperfusion Injury. *N. Engl. J. Med.* **2007**, *357*, 1121–1135, doi:10.1056/NEJMra071667.
94. Granger, D.N.; Kvietys, P.R. Reperfusion Injury and Reactive Oxygen Species: The Evolution of a Concept. *Redox Biol.* **2015**, *6*, 524–551, doi:10.1016/j.redox.2015.08.020.
95. Zuurbier, C.J.; Bertrand, L.; Beauloye, C.R.; Andreadou, I.; Ruiz-Meana, M.; Jespersen, N.R.; Kula-Alwar, D.; Prag, H.A.; Eric Botker, H.; Dambrova, M.; et al. Cardiac Metabolism as a Driver and Therapeutic Target of Myocardial Infarction. *J. Cell. Mol. Med.* **2020**, *24*, 5937–5954, doi:10.1111/jcmm.15180.
96. Granger, D.N. Ischemia-Reperfusion: Mechanisms of Microvascular Dysfunction and the Influence of Risk Factors for Cardiovascular Disease. *Microcirculation* **1999**, *6*, 167–178, doi:10.1111/j.1549-8719.1999.tb00099.x.
97. Agati, L. Microvascular Integrity after Reperfusion Therapy. *Am. Heart J.* **1999**, *138*, S76–S78, doi:10.1016/S0002-8703(99)70324-8.
98. Verma, S.; Fedak, P.W.M.; Weisel, R.D.; Butany, J.; Rao, V.; Maitland, A.; Li, R.-K.; Dhillon, B.; Yau, T.M. Fundamentals of Reperfusion Injury for the Clinical Cardiologist. *Circulation* **2002**, *105*, 2332–2336, doi:10.1161/01.CIR.0000016602.96363.36.

99. Peppard, P.E.; Young, T.; Palta, M.; Skatrud, J. Prospective Study of the Association between Sleep-Disordered Breathing and Hypertension. *N. Engl. J. Med.* **2000**, *342*, 1378–1384, doi:10.1056/NEJM200005113421901.
100. Coccagna, G.; Pollini, A.; Provini, F. Cardiovascular Disorders and Obstructive Sleep Apnea Syndrome. <http://dx.doi.org/10.1080/10641960600549090> **2009**, *28*, 217–224, doi:10.1080/10641960600549090.
101. Geissenberger, F.; Schwarz, F.; Probst, M.; Haberl, S.; Parkhe, A.; Faul, C.; von Lewinski, D.; Kroencke, T.; Schwaiblmair, M.; von Scheidt, W.; et al. Obstructive Sleep Apnea Is Associated with Pulmonary Artery Thrombus Load, Disease Severity, and Survival in Acute Pulmonary Embolism. *Clin. Res. Cardiol.* **2019**, *109*, 13–21, doi:doi:10.1007/s00392-019-01479-x.
102. Lippi, G.; Mattiuzzi, C.; Franchini, M. Sleep Apnea and Venous Thromboembolism: A Systematic Review. *Thromb. Haemost.* **2015**, *114*, 958–963, doi:10.1160/TH15-03-0188/ID/JR0188-6/BIB.
103. García-Ortega, A.; Mañas, E.; López-Reyes, R.; Selma, M.J.; García-Sánchez, A.; Oscullo, G.; Jiménez, D.; Martínez-García, M.Á. Obstructive Sleep Apnoea and Venous Thromboembolism: Pathophysiological Links and Clinical Implications. *Eur. Respir. J.* **2019**, *53*, doi:10.1183/13993003.00893-2018.
104. Marin, J.M.; Carrizo, S.J.; Vicente, E.; Agusti, A.G.N. Long-Term Cardiovascular Outcomes in Men with Obstructive Sleep Apnoea-Hypopnoea with or without Treatment with Continuous Positive Airway Pressure: An Observational Study. *Lancet* **2005**, *365*, 1046–1053, doi:10.1016/S0140-6736(05)74229-X.
105. D’Alessandro, R.; Magelli, C.; Gamberini, G.; Bacchelli, S.; Cristina, E.; Magnani, B.; Lugaresi, E. Snoring Every Night as a Risk Factor for Myocardial Infarction: A Case-Control Study. *Br. Med. J.* **1990**, *300*, 1557–1558, doi:10.1136/BMJ.300.6739.1557-A.
106. Hung, J.; Whitford, E.G.; Hillman, D.R.; Parsons, R.W. Association of Sleep Apnoea with Myocardial Infarction in Men. *The Lancet* **1990**, *336*, 261–264, doi:10.1016/0140-6736(90)91799-G.
107. Dewan, N.A.; Nieto, F.J.; Somers, V.K. Intermittent Hypoxemia and OSA. *Chest* **2015**, *147*, 266–274, doi:10.1378/chest.14-0500.
108. Franklin, K.A.; Sahlin, C.; Nilsson, J.B.; Näslund, U. Sleep Apnoea and Nocturnal Angina. *The Lancet* **1995**, *345*, 1085–1087, doi:10.1016/S0140-6736(95)90820-X.
109. Kuniyoshi, F.H.; Garcia-Touchard, A.; Gami, A.S.; Romero-Corral, A.; C, van der W.; Pusalavidyasagar, S.; Kara, T.; Caples, S.M.; Pressman, G.S.; Vasquez, E.C.; et al. Day-Night Variation of Acute Myocardial Infarction in Obstructive Sleep Apnea. *J. Am. Coll. Cardiol.* **2008**, *52*, doi:10.1016/j.jacc.2008.04.027.
110. McCord, J.M. Oxygen-Derived Free Radicals in Postischemic Tissue Injury. *N. Engl. J. Med.* **1985**, *312*, 159–163, doi:10.1056/NEJM198501173120305.
111. McCord, J.M. The Evolution of Free Radicals and Oxidative Stress. *Am. J. Med.* **2000**, *108*, 652–659, doi:10.1016/S0002-9343(00)00412-5.
112. Rahman, S.M.; Eichinger, C.D.; Hlady, V. Effects of Upstream Shear Forces on Priming of Platelets for Downstream Adhesion and Activation. *Acta Biomater.* **2018**, *73*, 228–235, doi:10.1016/j.actbio.2018.04.002.
113. Snippert, H.J.; van der Flier, L.G.; Sato, T.; van Es, J.H.; van den Born, M.; Kroon-Veenboer, C.; Barker, N.; Klein, A.M.; van Rheenen, J.; Simons, B.D.; et al. Intestinal Crypt Homeostasis Results from Neutral Competition between Symmetrically Dividing Lgr5 Stem Cells. *Cell* **2010**, *143*, 134–144, doi:10.1016/j.cell.2010.09.016.
114. Livet, J.; Weissman, T.A.; Kang, H.; Draft, R.W.; Lu, J.; Bennis, R.A.; Sanes, J.R.; Lichtman, J.W. Transgenic Strategies for Combinatorial Expression of Fluorescent Proteins in the Nervous System. *Nature* **2007**, *450*, 56–62, doi:10.1038/nature06293.

115. Tiedt, R.; Schomber, T.; Hao-Shen, H.; Skoda, R.C. Pf4-Cre Transgenic Mice Allow the Generation of Lineage-Restricted Gene Knockouts for Studying Megakaryocyte and Platelet Function in Vivo. *Blood* **2007**, *109*, 1503–1506, doi:10.1182/blood-2006-04-020362.
116. Faust, N.; Varas, F.; Kelly, L.M.; Heck, S.; Graf, T. Insertion of Enhanced Green Fluorescent Protein into the Lysozyme Gene Creates Mice with Green Fluorescent Granulocytes and Macrophages. *Blood* **2000**, *96*, 719–726.
117. Pinho, S.; Marchand, T.; Yang, E.; Wei, Q.; Nerlov, C.; Frenette, P.S. Lineage-Biased Hematopoietic Stem Cells Are Regulated by Distinct Niches. *Dev. Cell* **2018**, *44*, 634–641.e4, doi:10.1016/j.devcel.2018.01.016.
118. University of Zurich Pain Treatment with Buprenorphine in Mice.
119. Farré, R.; Montserrat, J.M.; Gozal, D.; Almendros, I.; Navajas, D. Intermittent Hypoxia Severity in Animal Models of Sleep Apnea. *Front. Physiol.* **2018**, *9*, doi:10.3389/FPHYS.2018.01556.
120. Farré, N.; Otero, J.; Falcones, B.; Torres, M.; Jorba, I.; Gozal, D.; Almendros, I.; Farré, R.; Navajas, D. Intermittent Hypoxia Mimicking Sleep Apnea Increases Passive Stiffness of Myocardial Extracellular Matrix. A Multiscale Study. *Front. Physiol.* **2018**, *9*, 1143, doi:10.3389/fphys.2018.01143.
121. Xu, Z.; Alloush, J.; Beck, E.; Weisleder, N. A Murine Model of Myocardial Ischemia-Reperfusion Injury through Ligation of the Left Anterior Descending Artery. *J. Vis. Exp.* **2014**, 51329, doi:10.3791/51329.
122. Surin, W.R.; Prakash, P.; Barthwal, M.K.; Dikshit, M. Optimization of Ferric Chloride Induced Thrombosis Model in Rats: Effect of Anti-Platelet and Anti-Coagulant Drugs. *J. Pharmacol. Toxicol. Methods* **2010**, *61*, 287–291, doi:10.1016/j.vascn.2009.11.002.
123. Petzold T; Zhang Z, Ballesteros I Saleh I Polzin A Thienel M Liu LUI Ain Q Weber C Kilani B Mertsch P Götschke J Cremer, E.V.; S Lorenz M Ishikawa-Ankerhold H Raatz E El-Nemr S Görlach A, F.W.; Marhuenda E Pircher J Stegner D Gieger C Schmidt-Supprian, S.K.; M Almendros I Kelm M Schulz C Hidalgo A Massberg S., G.F. Neutrophil “Plucking” on Megakaryocytes Drives Platelet Production and Boosts Cardiovascular Disease. *Immunity* **2022**, doi:doi:10.1016/j.immuni.2022.10.001.
124. Conchinha, N.V.; Sokol, L.; Teuwen, L.-A.; Veys, K.; Dumas, S.J.; Meta, E.; García-Caballero, M.; Geldhof, V.; Chen, R.; Treps, L.; et al. Protocols for Endothelial Cell Isolation from Mouse Tissues: Brain, Choroid, Lung, and Muscle. *STAR Protoc.* **2021**, *2*, 100508, doi:10.1016/j.xpro.2021.100508.
125. Van Wonderen, S.F.; Van Baarle, F.L.F.; De Bruin, S.; Peters, A.L.; De Korte, D.; Van Bruggen, R.; Vlaar, A.P.J. Biotinylated Platelets: A Promising Labeling Technique? *Transfus. Med. Rev.* **2023**, *37*, 150719, doi:10.1016/j.tmr.2023.01.001.
126. R&Dsystems *Proteome Profiler Mouse XL Cytokine Array Catalog #: ARY028*;
127. Liu, Y. Standardizing a Simpler, More Sensitive and Accurate Tail Bleeding Assay in Mice. *World J. Exp. Med.* **2012**, *2*, 30, doi:10.5493/wjem.v2.i2.30.
128. Rahangdale, S.; Yeh, S.Y.; Novack, V.; Stevenson, K.; Barnard, M.R.; Furman, M.I.; Frelinger, A.L.; Michelson, A.D.; Malhotra, A. The Influence of Intermittent Hypoxemia on Platelet Activation in Obese Patients with Obstructive Sleep Apnea. *J. Clin. Sleep Med.* **2011**, *07*, 172–178, doi:10.5664/jcsm.28105.
129. Krieger, A.C.; Anand, R.; Hernandez-Rosa, E.; Maidman, A.; Milrad, S.; DeGrazia, M.Q.; Choi, A.J.; Oromendia, C.; Marcus, A.J.; Drosopoulos, J.H.F. Increased Platelet Activation in Sleep Apnea Subjects with Intermittent Hypoxemia. *Sleep Breath. Schlaf Atm.* **2020**, *24*, 1537–1547, doi:10.1007/s11325-020-02021-4.
130. Günbey, E.; Karabulut, I.; Karabulut, H.; Zaim, M. Impact of Multilevel Surgical Treatment on Mean Platelet Volume in Patients With Obstructive Sleep Apnea

- Syndrome. *J. Craniofac. Surg.* **2015**, *26*, 1287–1289, doi:10.1097/SCS.0000000000001556.
131. Roshal, M.; Reyes Gil, M. Measurement of Platelet Count, Mean Platelet Volume, and Reticulated Platelets. In *Transfusion Medicine and Hemostasis*; Elsevier, 2019; pp. 811–815 ISBN 978-0-12-813726-0.
 132. Weinreich, G.; Wessendorf, T.E.; Erdmann, T.; Moebus, S.; Dragano, N.; Lehmann, N.; Stang, A.; Roggenbuck, U.; Bauer, M.; Jöckel, K.-H.; et al. Association of Obstructive Sleep Apnoea with Subclinical Coronary Atherosclerosis. *Atherosclerosis* **2013**, *231*, 191–197, doi:10.1016/j.atherosclerosis.2013.09.011.
 133. Reininger, A.J.; Bernlochner, I.; Penz, S.M.; Ravanat, C.; Smethurst, P.; Farndale, R.W.; Gachet, C.; Brandl, R.; Siess, W. A 2-Step Mechanism of Arterial Thrombus Formation Induced by Human Atherosclerotic Plaques. *J. Am. Coll. Cardiol.* **2010**, *55*, 1147–1158, doi:10.1016/j.jacc.2009.11.051.
 134. Ruggeri, Z.M. Platelets in Atherothrombosis. *Nat. Med.* **2002**, *8*, 1227–1234, doi:10.1038/nm1102-1227.
 135. Penz, S.; Reininger, A.; Toth, O.; Deckmyn, H.; Brandl, R.; Siess, W. Glycoprotein Iba Inhibition and ADP Receptor Antagonists, but Not Aspirin, Reduce Platelet Thrombus Formation in Flowing Blood Exposed to Atherosclerotic Plaques. *Thromb. Haemost.* **2007**, *97*, 435–443, doi:10.1160/TH06-07-0415.
 136. Kannan, M.; Ahmad, F.; Saxena, R. Platelet Activation Markers in Evaluation of Thrombotic Risk Factors in Various Clinical Settings. *Blood Rev.* **2019**, *37*, 100583, doi:10.1016/j.blre.2019.05.007.
 137. Gauer, J.S.; Ajjan, R.A.; Ariëns, R.A.S. Platelet–Neutrophil Interaction and Thromboinflammation in Diabetes: Considerations for Novel Therapeutic Approaches. *J. Am. Heart Assoc.* **2022**, *11*, e027071, doi:10.1161/JAHA.122.027071.
 138. Pilkauskaitė, G.; Miliauskas, S.; Sakalauskas, R. Reactive Oxygen Species Production in Peripheral Blood Neutrophils of Obstructive Sleep Apnea Patients. *Sci. World J.* **2013**, *2013*, doi:10.1155/2013/421763.
 139. Wachowicz, B.; Olas, B.; Zbikowska, H.M.; Buczyński, A. Generation of Reactive Oxygen Species in Blood Platelets. *Platelets* **2002**, *13*, 175–182, doi:10.1080/09533710022149395.
 140. Yamada, M.; Kubo, H.; Kobayashi, S.; Ishizawa, K.; He, M.; Suzuki, T.; Fujino, N.; Kunishima, H.; Hatta, M.; Nishimaki, K.; et al. The Increase in Surface CXCR4 Expression on Lung Extravascular Neutrophils and Its Effects on Neutrophils during Endotoxin-Induced Lung Injury. *Cell. Mol. Immunol.* **2011**, *8*, 305–314, doi:10.1038/cmi.2011.8.
 141. Bot, I.; Daissormont, I.T.M.N.; Zerneck, A.; Van Puijvelde, G.H.M.; Kramp, B.; De Jager, S.C.A.; Sluimer, J.C.; Manca, M.; Hérias, V.; Westra, M.M.; et al. CXCR4 Blockade Induces Atherosclerosis by Affecting Neutrophil Function. *J. Mol. Cell. Cardiol.* **2014**, *74*, 44–52, doi:10.1016/j.yjmcc.2014.04.021.
 142. Radermecker, C.; Sabatel, C.; Vanwinge, C.; Ruscitti, C.; Maréchal, P.; Perin, F.; Schyns, J.; Rocks, N.; Toussaint, M.; Cataldo, D.; et al. Locally Instructed CXCR4hi Neutrophils Trigger Environment-Driven Allergic Asthma through the Release of Neutrophil Extracellular Traps. *Nat. Immunol.* **2019**, *20*, 1444–1455, doi:10.1038/s41590-019-0496-9.
 143. Davis, E.M.; O'Donnell, C.P. Rodent Models of Sleep Apnea. *Respir. Physiol. Neurobiol.* **2013**, *188*, 355–361, doi:10.1016/J.RESP.2013.05.022.
 144. Li, L.; Ren, F.; Qi, C.; Xu, L.; Fang, Y.; Liang, M.; Feng, J.; Chen, B.; Ning, W.; Cao, J. Intermittent Hypoxia Promotes Melanoma Lung Metastasis via Oxidative Stress and Inflammation Responses in a Mouse Model of Obstructive Sleep Apnea. *Respir. Res.* **2018**, *19*, doi:10.1186/s12931-018-0727-x.

145. Lim, D.C.; Brady, D.C.; Po, P.; Chuang, L.P.; Marcondes, L.; Kim, E.Y.; Keenan, B.T.; Guo, X.; Maislin, G.; Galante, R.J.; et al. Simulating Obstructive Sleep Apnea Patients' Oxygenation Characteristics into a Mouse Model of Cyclical Intermittent Hypoxia. *J. Appl. Physiol.* **2015**, *118*, 544–557, doi:10.1152/JAPPLPHYSIOL.00629.2014.
146. Zhen, X.; Moya, E.A.; Gautane, M.; Zhao, H.; Lawrence, E.S.; Gu, W.; Barnes, L.A.; Yuan, J.X.J.; Jain, P.P.; Xiong, M.; et al. Combined Intermittent and Sustained Hypoxia Is a Novel and Deleterious Cardio-Metabolic Phenotype. *Sleep* **2022**, *45*, doi:10.1093/SLEEP/ZSAB290.
147. Jun, J.; Reinke, C.; Bedja, D.; Berkowitz, D.; Bevans-Fonti, S.; Li, J.; Barouch, L.A.; Gabrielson, K.; Polotsky, V.Y. EFFECT OF INTERMITTENT HYPOXIA ON ATHEROSCLEROSIS IN APOLIPROTEIN E-DEFICIENT MICE. *Atherosclerosis* **2010**, *209*, 381, doi:10.1016/J.ATHEROSCLEROSIS.2009.10.017.
148. Heazlewood, S.Y.; Williams, B.; Storan, M.J.; Nilsson, S.K. The Prospective Isolation of Viable, High Ploidy Megakaryocytes from Adult Murine Bone Marrow by Fluorescence Activated Cell Sorting. In *Stem Cell Niche*; Turksen, K., Ed.; Methods in Molecular Biology; Humana Press: Totowa, NJ, 2013; Vol. 1035, pp. 121–133 ISBN 978-1-62703-507-1.
149. Levine, R.; Hazzard, K.; Lamberg, J. The Significance of Megakaryocyte Size. *Blood* **1982**, *60*, 1122–1131, doi:10.1182/blood.V60.5.1122.1122.
150. Pariser, D.N.; Hilt, Z.T.; Ture, S.K.; Blick-Nitko, S.K.; Looney, M.R.; Cleary, S.J.; Roman-Pagan, E.; Saunders, J.; Georas, S.N.; Veazey, J.; et al. Lung Megakaryocytes Are Immune Modulatory Cells. *J. Clin. Invest.* **2021**, *131*, e137377, doi:10.1172/JCI137377.
151. Lefrançais, E.; Ortiz-Muñoz, G.; Caudrillier, A.; Mallavia, B.; Liu, F.; Sayah, D.M.; Thornton, E.E.; Headley, M.B.; David, T.; Coughlin, S.R.; et al. The Lung Is a Site of Platelet Biogenesis and a Reservoir for Haematopoietic Progenitors. *Nature* **2017**, *544*, 105–109, doi:10.1038/nature21706.
152. Yeung, A.K.; Villacorta-Martin, C.; Hon, S.; Rock, J.R.; Murphy, G.J. Lung Megakaryocytes Display Distinct Transcriptional and Phenotypic Properties. *Blood Adv.* **2020**, *4*, 6204–6217, doi:10.1182/bloodadvances.2020002843.
153. Asquith, N.L.; Carminita, E.; Camacho, V.; Rodriguez-Romera, A.; Stegner, D.; Freire, D.; Becker, I.C.; Machlus, K.R.; Khan, A.O.; Italiano, J.E. The Bone Marrow Is the Primary Site of Thrombopoiesis. *Blood* **2024**, *143*, 272–278, doi:10.1182/blood.2023020895.
154. Chong, D.L.W.; Rebeyrol, C.; José, R.J.; Williams, A.E.; Brown, J.S.; Scotton, C.J.; Porter, J.C. ICAM-1 and ICAM-2 Are Differentially Expressed and Up-Regulated on Inflamed Pulmonary Epithelium, but Neither ICAM-2 nor LFA-1: ICAM-1 Are Required for Neutrophil Migration Into the Airways In Vivo. *Front. Immunol.* **2021**, *12*, 691957, doi:10.3389/fimmu.2021.691957.
155. Carlson, J.T.; Rångemark, C.; Hedner, J.A. Attenuated Endothelium-Dependent Vascular Relaxation in Patients with Sleep Apnoea. *J. Hypertens.* **1996**, *14*, 577–584, doi:10.1097/00004872-199605000-00006.
156. Ursavaş, A.; Karadağ, M.; Rodoplu, E.; Yilmaztepe, A.; Oral, H.B.; Gözü, R.O. Circulating ICAM-1 and VCAM-1 Levels in Patients with Obstructive Sleep Apnea Syndrome. *Respiration* **2007**, *74*, 525–532, doi:10.1159/000097770.
157. Shreeniwas, R.; Koga, S.; Karakurum, M.; Pinsky, D.; Kaiser, E.; Brett, J.; Wolitzky, B.A.; Norton, C.; Plocinski, J.; Benjamin, W. Hypoxia-Mediated Induction of Endothelial Cell Interleukin-1 Alpha. An Autocrine Mechanism Promoting Expression of Leukocyte Adhesion Molecules on the Vessel Surface. *J. Clin. Invest.* **1992**, *90*, 2333–2339, doi:10.1172/JCI116122.
158. Lapidot, T.; Kollet, O. The Essential Roles of the Chemokine SDF-1 and Its Receptor CXCR4 in Human Stem Cell Homing and Repopulation of Transplanted Immune-

- Deficient NOD/SCID and NOD/SCID/B2mnull Mice. *Leukemia* **2002**, *16*, 1992–2003, doi:10.1038/sj.leu.2402684.
159. Visan, I. Aging Neutrophils. *Nat. Immunol.* **2015**, *16*, 1113–1113, doi:10.1038/ni.3304.
 160. Lefort, C.T.; Ley, K. Neutrophil Arrest by LFA-1 Activation. *Front. Immunol.* **2012**, *3*, 157, doi:10.3389/fimmu.2012.00157.
 161. Osher, S.; Eren, M.; Urich, D.; Weiss, I.M.; Gonzalez, A.; Soberanes, S.; Radigan, K.A.; Kwaan, H.C.; Vaughan, D.E.; Budinger, G.R.S.; et al. Intermittent Hypoxia And Elevated Plasminogen Activator Inhibitor-1 Accelerate Arterial Thrombosis. In Proceedings of the B63. EXPERIMENTAL MODELS IN PULMONARY HYPERTENSION I; American Thoracic Society, May 2012; pp. A3442–A3442.
 162. Drager, L.F.; Polotsky, V.Y.; O'Donnell, C.P.; Cravo, S.L.; Lorenzi-Filho, G.; Machado, B.H. Translational Approaches to Understanding Metabolic Dysfunction and Cardiovascular Consequences of Obstructive Sleep Apnea. <https://doi.org/10.1152/ajpheart.00094.2015> **2015**, doi:10.1152/ajpheart.00094.2015.
 163. Getz, T.M.; Piatt, R.; Petrich, B.G.; Monroe, D.; Mackman, N.; Bergmeier, W. Novel Mouse Hemostasis Model for Real-time Determination of Bleeding Time and Hemostatic Plug Composition. *J. Thromb. Haemost.* **2015**, *13*, 417–425, doi:10.1111/jth.12802.
 164. Domagała-Kulawik, J.; Osińska, I.; Piechuta, A.; Bielicki, P.; Skirecki, T. T, B, and NKT Cells in Systemic Inflammation in Obstructive Sleep Apnoea. *Mediators Inflamm.* **2015**, *2015*, 1–7, doi:10.1155/2015/161579.
 165. Klinker, M.W.; Lundy, S.K. Multiple Mechanisms of Immune Suppression by B Lymphocytes. *Mol. Med.* **2012**, *18*, 123–137, doi:10.2119/molmed.2011.00333.
 166. Ludwig, K.; Huppertz, T.; Radsak, M.; Gouveris, H. Cellular Immune Dysfunction in Obstructive Sleep Apnea. *Front. Surg.* **2022**, *9*, 890377, doi:10.3389/fsurg.2022.890377.
 167. Xie, H.; Yin, J.; Bai, Y.; Peng, H.; Zhou, X.; Bai, J. Differential Expression of Immune Markers in the Patients with Obstructive Sleep Apnea/Hypopnea Syndrome. *Eur. Arch. Otorhinolaryngol.* **2019**, *276*, 735–744, doi:10.1007/s00405-018-5219-6.
 168. Rolink, A.; Ten Boekel, E.; Melchers, F.; Fearon, D.T.; Krop, I.; Andersson, J. A Subpopulation of B220+ Cells in Murine Bone Marrow Does Not Express CD19 and Contains Natural Killer Cell Progenitors. *J. Exp. Med.* **1996**, *183*, 187–194, doi:10.1084/jem.183.1.187.
 169. Cao, M.T.; Sternbach, J.M.; Guilleminault, C. Continuous Positive Airway Pressure Therapy in Obstructive Sleep Apnea: Benefits and Alternatives. <http://dx.doi.org/10.1080/17476348.2017.1305893> **2017**, doi:10.1080/17476348.2017.1305893.
 170. Rosa, D.; Amigoni, C.; Rimoldi, E.; Ripa, P.; Ligorio, A.; Fracchiolla, M.; Lombardi, C.; Parati, G.; Perger, E. Obstructive Sleep Apnea and Adherence to Continuous Positive Airway Pressure (CPAP) Treatment: Let's Talk about Partners! *Healthcare* **2022**, *10*, 943, doi:10.3390/healthcare10050943.
 171. Hoffman, D.L.; Salter, J.D.; Brookes, P.S. Response of Mitochondrial Reactive Oxygen Species Generation to Steady-State Oxygen Tension: Implications for Hypoxic Cell Signaling. *Am. J. Physiol.-Heart Circ. Physiol.* **2007**, *292*, H101–H108, doi:10.1152/ajpheart.00699.2006.
 172. Xu, L.; Yang, Y.; Chen, J. The Role of Reactive Oxygen Species in Cognitive Impairment Associated with Sleep Apnea. *Exp. Ther. Med.* **2020**, *20*, 1–1, doi:10.3892/etm.2020.9132.
 173. Willson, J.A.; Arienti, S.; Sadiku, P.; Reyes, L.; Coelho, P.; Morrison, T.; Rinaldi, G.; Dockrell, D.H.; Whyte, M.K.B.; Walmsley, S.R. Neutrophil HIF-1 α Stabilization Is

- Augmented by Mitochondrial ROS Produced via the Glycerol 3-Phosphate Shuttle. *Blood* **2022**, *139*, 281–286, doi:10.1182/blood.2021011010.
174. Mochol, J.; Gawrys, J.; Gajecki, D.; Szahidewicz-Krupska, E.; Martynowicz, H.; Doroszko, A. Cardiovascular Disorders Triggered by Obstructive Sleep Apnea—A Focus on Endothelium and Blood Components. *Int. J. Mol. Sci.* **2021**, *22*, 5139, doi:10.3390/ijms22105139.
 175. Ziegler, M.; Wang, X.; Peter, K. Platelets in Cardiac Ischaemia/Reperfusion Injury: A Promising Therapeutic Target. *Cardiovasc. Res.* **2019**, *115*, 1178–1188, doi:10.1093/cvr/cvz070.
 176. Liehn, E.A.; Tuchscheerer, N.; Kanzler, I.; Drechsler, M.; Fraemohs, L.; Schuh, A.; Koenen, R.R.; Zander, S.; Soehnlein, O.; Hristov, M.; et al. Double-Edged Role of the CXCL12/CXCR4 Axis in Experimental Myocardial Infarction. *J. Am. Coll. Cardiol.* **2011**, *58*, 2415–2423, doi:10.1016/j.jacc.2011.08.033.
 177. Ma, Y. Role of Neutrophils in Cardiac Injury and Repair Following Myocardial Infarction. *Cells* **2021**, *10*, 1676, doi:10.3390/cells10071676.
 178. Moris, D.; Spartalis, M.; Spartalis, E.; Karachaliou, G.-S.; Karaolani, G.I.; Tsourouflis, G.; Tsilimigras, D.I.; Tzatzaki, E.; Theocharis, S. The Role of Reactive Oxygen Species in the Pathophysiology of Cardiovascular Diseases and the Clinical Significance of Myocardial Redox. *Ann. Transl. Med.* **2017**, *5*, 326–326, doi:10.21037/atm.2017.06.27.
 179. Arruda-Olson, A.M.; Reeder, G.S.; Bell, M.R.; Weston, S.A.; Roger, V.L. Neutrophilia Predicts Death and Heart Failure After Myocardial Infarction: A Community-Based Study. *Circ. Cardiovasc. Qual. Outcomes* **2009**, *2*, 656–662, doi:10.1161/CIRCOUTCOMES.108.831024.
 180. Grove, E.L.; Hvas, A.M.; Mortensen, S.B.; Larsen, S.B.; Kristensen, S.D. Effect of Platelet Turnover on Whole Blood Platelet Aggregation in Patients with Coronary Artery Disease. *J. Thromb. Haemost.* **2011**, *9*, 185–191, doi:10.1111/j.1538-7836.2010.04115.x.
 181. Guthikonda, S.; Alviar, C.L.; Vaduganathan, M.; Arian, M.; Tellez, A.; DeLao, T.; Granada, J.F.; Dong, J.F.; Kleiman, N.S.; Lev, E.I. Role of Reticulated Platelets and Platelet Size Heterogeneity on Platelet Activity after Dual Antiplatelet Therapy with Aspirin and Clopidogrel in Patients with Stable Coronary Artery Disease. *J. Am. Coll. Cardiol.* **2008**, *52*, doi:10.1016/j.jacc.2008.05.031.
 182. Gopal, P.; Gosker, H.R.; de. Theije, C.; Eurlings, I.M.; Sell, D.R.; Monnier, V.M.; Reynaert, N.L. Effect of Chronic Hypoxia on RAGE and Its Soluble Forms in Lungs and Plasma of Mice. *Biochim. Biophys. Acta* **2015**, *1852*, 992–1000, doi:10.1016/j.bbadis.2015.02.003.
 183. Pichiule, P.; Chavez, J.C.; Schmidt, A.M.; Vannucci, S.J. Hypoxia-Inducible Factor-1 Mediates Neuronal Expression of the Receptor for Advanced Glycation End Products Following Hypoxia/Ischemia *. *J. Biol. Chem.* **2007**, *282*, 36330–36340, doi:10.1074/jbc.M706407200.
 184. Martinez, C.-A.; Kerr, B.; Jin, C.; Cistulli, P.; Cook, K. Obstructive Sleep Apnea Activates HIF-1 in a Hypoxia Dose-Dependent Manner in HCT116 Colorectal Carcinoma Cells. *Int. J. Mol. Sci.* **2019**, *20*, 445, doi:10.3390/ijms20020445.
 185. Nanduri, J.; Vaddi, D.R.; Khan, S.A.; Wang, N.; Makarenko, V.; Semenza, G.L.; Prabhakar, N.R. HIF-1 α Activation by Intermittent Hypoxia Requires NADPH Oxidase Stimulation by Xanthine Oxidase. *PLOS ONE* **2015**, *10*, e0119762, doi:10.1371/journal.pone.0119762.
 186. Bucciarelli, L.G.; Kaneko, M.; Ananthakrishnan, R.; Harja, E.; Lee, L.K.; Hwang, Y.C.; Lerner, S.; Bakr, S.; Li, Q.; Lu, Y.; et al. Receptor for Advanced-Glycation End Products. *Circulation* **2006**, *113*, 1226–1234, doi:10.1161/CIRCULATIONAHA.105.575993.
 187. Van den Steen, P.E.; Dubois, B.; Nelissen, I.; Rudd, P.M.; Dwek, R.A.; Opdenakker, G. Biochemistry and Molecular Biology of Gelatinase B or Matrix Metalloproteinase-9

- (MMP-9). *Crit. Rev. Biochem. Mol. Biol.* **2002**, *37*, 375–536, doi:10.1080/10409230290771546.
188. Bergers, G.; Brekken, R.; McMahon, G.; Vu, T.H.; Itoh, T.; Tamaki, K.; Tanzawa, K.; Thorpe, P.; Itohara, S.; Werb, Z.; et al. Matrix Metalloproteinase-9 Triggers the Angiogenic Switch during Carcinogenesis. *Nat. Cell Biol.* **2000**, *2*, 737–744, doi:10.1038/35036374.
 189. Du, R.; Lu, K.V.; Petritsch, C.; Liu, P.; Ganss, R.; Passegué, E.; Song, H.; Vandenberg, S.; Johnson, R.S.; Werb, Z.; et al. HIF1alpha Induces the Recruitment of Bone Marrow-Derived Vascular Modulatory Cells to Regulate Tumor Angiogenesis and Invasion. *Cancer Cell* **2008**, *13*, 206–220, doi:10.1016/j.ccr.2008.01.034.
 190. Jin, H.; Aiyer, A.; Su, J.; Borgstrom, P.; Stupack, D.; Friedlander, M.; Varner, J. A Homing Mechanism for Bone Marrow-Derived Progenitor Cell Recruitment to the Neovasculature. *J. Clin. Invest.* **2006**, *116*, 652–662, doi:10.1172/JCI24751.
 191. Oladipupo, S.; Hu, S.; Kovalski, J.; Yao, J.; Santeford, A.; Sohn, R.E.; Shohet, R.; Maslov, K.; Wang, L.V.; Arbeit, J.M. VEGF Is Essential for Hypoxia-Inducible Factor-Mediated Neovascularization but Dispensable for Endothelial Sprouting. *Proc. Natl. Acad. Sci. U. S. A.* **2011**, *108*, 13264–13269, doi:10.1073/pnas.1101321108.
 192. Fan; Lu X Long H Li T Zhang Y . The Association of Hemocyte Profile and Obstructive Sleep Apnea. *J Clin Lab Anal* **2018**, *33* :e22680, doi:https://doi.org/10.1002/jcla.22680.
 193. Duksal, F. Association of Obstructive Sleep Apnea Syndrome with Hematological Parameters and Comorbid Diseases. <https://www.neurology-asia.org/system/index.php/neuro/article/view/677> **2022**, doi:https://www.neurology-asia.org/system/index.php/neuro/article/view/677.
 194. Varol, E.; Ozturk, O.; Yucel, H.; Gonca, T.; Has, M.; Dogan, A.; Akkaya, A. The Effects of Continuous Positive Airway Pressure Therapy on Mean Platelet Volume in Patients with Obstructive Sleep Apnea. <http://dx.doi.org/10.3109/09537104.2011.578182> **2011**, doi:10.3109/09537104.2011.578182.
 195. Bülbül, Y.; Aydin Özgür, E.; Örem, A. Platelet Indices in Obstructive Sleep Apnea: The Role of Mean Platelet Volume, Platelet Distribution Widht and Plateletcrit. *Tuberk. Ve Toraks* **2016**, *64*, 206–210, doi:10.5578/tt.29170.
 196. Martin, JohnF.; Bath, PhilipM.W.; Burr, MichaelL. Mean Platelet Volume and Myocardial Infarction. *The Lancet* **1992**, *339*, 1000–1001, doi:10.1016/0140-6736(92)91587-X.
 197. Panova-Noeva, M.; Schulz, A.; Hermanns, M.I.; Grossmann, V.; Pefani, E.; Spronk, H.M.H.; Laubert-Reh, D.; Binder, H.; Beutel, M.; Pfeiffer, N.; et al. Sex-Specific Differences in Genetic and Nongenetic Determinants of Mean Platelet Volume: Results from the Gutenberg Health Study. *Blood* **2016**, *127*, 251–259, doi:10.1182/blood-2015-07-660308.
 198. Noris, P.; Melazzini, F.; Balduini, C.L. New Roles for Mean Platelet Volume Measurement in the Clinical Practice? *Platelets* **2016**, *27*, 607–612, doi:10.1080/09537104.2016.1224828.
 199. Berndt, M.C.; Metharom, P.; Andrews, R.K. Primary Haemostasis: Newer Insights. *Haemophilia* **2014**, *20*, 15–22, doi:10.1111/hae.12427.
 200. Geiser, T.; Departments of Pulmonary Medicine; Laboratory for Thrombosis Research Bern Switzerland, U.H.; Buck, F.; Departments of Pulmonary Medicine; Meyer, B.J.; and, C.; Bassetti, C.; Neurology, and; Haeberli, A.; et al. In Vivo Platelet Activation Is Increased during Sleep in Patients with Obstructive Sleep Apnea Syndrome. *Respiration* **2023**, *69*, 229–234, doi:10.1159/000063625.
 201. Wright, H.P.; Scholar, G. Changes in the Adhesiveness of Blood Platelets Following Parturition and Surgical Operations. *J. Pathol. Bacteriol.* **1942**, *54*, 461–468, doi:10.1002/path.1700540408.

202. Hirsh, J.; Glynn, M.F.; Mustard, J.F. The Effect of Platelet Age on Platelet Adherence to Collagen. *J. Clin. Invest.* **1968**, *47*, 466–473, doi:10.1172/JCI105743.
203. Hille, L.; Lenz, M.; Vlachos, A.; Grüning, B.; Hein, L.; Neumann, F.; Nührenberg, T.G.; Trenk, D. Ultrastructural, Transcriptional, and Functional Differences between Human Reticulated and Non-reticulated Platelets. *J. Thromb. Haemost.* **2020**, *18*, 2034–2046, doi:10.1111/jth.14895.
204. Bongiovanni, D.; Santamaria, G.; Klug, M.; Santovito, D.; Felicetta, A.; Hristov, M.; Von Scheidt, M.; Aslani, M.; Cibella, J.; Weber, C.; et al. Transcriptome Analysis of Reticulated Platelets Reveals a Prothrombotic Profile. *Thromb. Haemost.* **2019**, *119*, 1795–1806, doi:10.1055/s-0039-1695009.
205. Hannawi, B.; Hannawi, Y.; Kleiman, N.S. Reticulated Platelets: Changing Focus from Basics to Outcomes. *Thromb. Haemost.* **2018**, *118*, 1517–1527, doi:10.1055/s-0038-1667338.
206. McBane, R.D.; Gonzalez, C.; Hodge, D.O.; Wysokinski, W.E. Propensity for Young Reticulated Platelet Recruitment into Arterial Thrombi. *J. Thromb. Thrombolysis* **2013**, *37*, 148–154, doi:doi:10.1007/s11239-013-0932-x.
207. Eleftheriadis, T.; Pissas, G.; Filippidis, G.; Liakopoulos, V.; Stefanidis, I. Reoxygenation Induces Reactive Oxygen Species Production and Ferroptosis in Renal Tubular Epithelial Cells by Activating Aryl Hydrocarbon Receptor. *Mol. Med. Rep.* **2021**, *23*, 1–11, doi:10.3892/MMR.2020.11679.
208. Neri, M.; Riezzo, I.; Pascale, N.; Pomara, C.; Turillazzi, E. Ischemia/Reperfusion Injury Following Acute Myocardial Infarction: A Critical Issue for Clinicians and Forensic Pathologists. *Mediators Inflamm.* **2017**, *2017*, 7018393, doi:10.1155/2017/7018393.
209. Richard, V.; Murry, C.; Jennings, R.; Reimer, K. Oxygen-Derived Free Radicals and Postischemic Myocardial Reperfusion: Therapeutic Implications. *Fundam. Clin. Pharmacol.* **1990**, *4*, 85–103, doi:10.1111/J.1472-8206.1990.TB01019.X.
210. Dean, R.T.; Wilcox, T. 2. Natural History of Sleep Apnea Possible Atherogenic Effects of Hypoxia During Obstructive Sleep Apnea. *Sleep* **1993**, *16*, 15–522.
211. Bolli, R.; Jeroudi, M.O.; Patel, B.S.; Aruoma, O.I.; Halliwell, B.; Lai, E.K.; Mccay, P.B. *Marked Reduction of Free Radical Generation and Contractile Dysfunction by Antioxidant Therapy Begun at the Time of Reperfusion Evidence That Myocardial "Stunning" Is a Manifestation of Reperfusion Injury*; 1989;
212. Zhou, T.; Chuang, C.C.; Zuo, L. Molecular Characterization of Reactive Oxygen Species in Myocardial Ischemia-Reperfusion Injury. *BioMed Res. Int.* **2015**, *2015*, doi:10.1155/2015/864946.
213. Song, J.; Sundar, K.M.; Robert, C.; Horvathova, M.; Kralova, B.; Divoky, V.; Ganz, T.; Prchal, J.T. Pathophysiology of Obstructive Sleep Apnea (OSA) - Blood Cells' Reactive Oxygen Species and Inflammation Prevent Polycythemia. *Blood* **2018**, *132*, 1028–1028, doi:10.1182/blood-2018-99-116658.
214. Schulz, R.; Mahmoudi, S.; Hattar, K.; Sibeli, U.; Olschewski, H.; Mayer, K.; Seeger, W.; Grimminger, F. Enhanced Release of Superoxide from Polymorphonuclear Neutrophils in Obstructive Sleep Apnea Impact of Continuous Positive Airway Pressure Therapy. *Am J Respir Crit Care Med* **2000**, *162*, 566–570.
215. Kircher, M.; Herhaus, P.; Schottelius, M.; Buck, A.K.; Werner, R.A.; Wester, H.-J.; Keller, U.; Lapa, C. CXCR4-Directed Theranostics in Oncology and Inflammation. *Ann. Nucl. Med.* **2018**, *32*, 503–511, doi:doi:10.1007/s12149-018-1290-8.
216. Wang, J.; Hossain, M.; Thanabalasuriar, A.; Gunzer, M.; Meininger, C.; Kubes, P. Visualizing the Function and Fate of Neutrophils in Sterile Injury and Repair. *Science* **2017**, *358*, 111–116, doi:10.1126/science.aam9690.

217. Kato, M.; Roberts-Thomson, P.; Phillips, B.G.; Haynes, W.G.; Winnicki, M.; Accurso, V.; Somers, V.K. Impairment of Endothelium-Dependent Vasodilation of Resistance Vessels in Patients with Obstructive Sleep Apnea. *Circulation* **2000**, *102*, 2607–2610, doi:10.1161/01.CIR.102.21.2607.
218. Rotenberg, B.W.; Murariu, D.; Pang, K.P. Trends in CPAP Adherence over Twenty Years of Data Collection: A Flattened Curve. *J. Otolaryngol. - Head Neck Surg.* **2016**, *45*, 1–9, doi:doi:10.1186/s40463-016-0156-0.
219. Zolotoff, C.; Bertoletti, L.; Gozal, D.; Mismetti, V.; Flandrin, P.; Roche, F.; Perek, N. Obstructive Sleep Apnea, Hypercoagulability, and the Blood–Brain Barrier. *J. Clin. Med.* **2021**, *10*, 3099, doi:10.3390/jcm10143099.
220. Hui, D.S.; Ko, F.W.; Fok, J.P.; Chan, M.C.; Li, T.S.; Tomlinson, B.; Cheng, G. The Effects of Nasal Continuous Positive Airway Pressure on Platelet Activation in Obstructive Sleep Apnea Syndrome. *Chest* **2004**, *125*, 1768–1775, doi:10.1378/chest.125.5.1768.
221. Oga, T.; Chin, K.; Tabuchi, A.; Kawato, M.; Morimoto, T.; Takahashi, K.; Handa, T.; Takahashi, K.; Taniguchi, R.; Kondo, H.; et al. Effects of Obstructive Sleep Apnea with Intermittent Hypoxia on Platelet Aggregability. *J. Atheroscler. Thromb.* **2009**, *16*, doi:10.5551/jat.2188.
222. Jurado-Gómez, B.; Fernandez-Marin, M.C.; Gómez-Chaparro, J.L.; Muñoz-Cabrera, L.; Lopez-Barea, J.; Perez-Jimenez, F.; Lopez-Miranda, J. Relationship of Oxidative Stress and Endothelial Dysfunction in Sleep Apnoea. **2011**, doi:10.1183/09031936.00027910.
223. Kim, Y.-S.; Kwak, J.W.; Lee, K.E.; Cho, H.S.; Lim, S.J.; Kim, K.S.; Yang, H.S.; Kim, H.J. Can Mitochondrial Dysfunction Be a Predictive Factor for Oxidative Stress in Patients with Obstructive Sleep Apnea? *Antioxid. Redox Signal.* **2014**, *21*, 1285–1288, doi:10.1089/ars.2014.5955.
224. Khan, S.A.; Nanduri, J.; Yuan, G.; Kinsman, B.; Kumar, G.K.; Joseph, J.; Kalyanaraman, B.; Prabhakar, N.R. NADPH Oxidase 2 Mediates Intermittent Hypoxia-Induced Mitochondrial Complex I Inhibition: Relevance to Blood Pressure Changes in Rats. *Antioxid. Redox Signal.* **2011**, *14*, 533–542, doi:10.1089/ars.2010.3213.
225. Buchner, N.J.; Sanner, B.M.; Borgel, J.; Rump, L.C. Continuous Positive Airway Pressure Treatment of Mild to Moderate Obstructive Sleep Apnea Reduces Cardiovascular Risk. *Httpsdoiorg101164rccm200611-1588OC* **2012**, doi:10.1164/rccm.200611-1588OC.
226. Bock, J.M.; Vungarala, S.; Karim, S.; Somers, V.K. Obstructive Sleep Apnea as a Cardiovascular Risk Factor—Beyond CPAP. *Can. J. Cardiol.* **2021**, *37*, 756–765, doi:10.1016/j.cjca.2021.01.027.
227. Picard, F.; Panagiotidou, P.; Weinig, L.; Steffen, M.; Tammen, A.-B.; Klein, R.M. Effect of CPAP Therapy on Nocturnal Blood Pressure Fluctuations, Nocturnal Blood Pressure, and Arterial Stiffness in Patients with Coexisting Cardiovascular Diseases and Obstructive Sleep Apnea. *Sleep Breath.* **2021**, *25*, 151–161, doi:10.1007/s11325-020-02075-4.
228. Jelic, S.; Padeletti, M.; Kawut, S.M.; Higgins, C.; Canfield, S.M.; Onat, D.; Colombo, P.C.; Basner, R.C.; Factor, P.; LeJemtel, T.H. Inflammation, Oxidative Stress, and Repair Capacity of the Vascular Endothelium in Obstructive Sleep Apnea. *Circulation* **2008**, *117*, 2270–2278, doi:10.1161/CIRCULATIONAHA.107.741512.
229. McEvoy, R.D.; Antic, N.A.; Heeley, E.; Luo, Y.; Ou, Q.; Zhang, X.; Mediano, O.; Chen, R.; Drager, L.F.; Liu, Z.; et al. CPAP for Prevention of Cardiovascular Events in Obstructive Sleep Apnea. *N. Engl. J. Med.* **2016**, *375*, 919–931, doi:10.1056/NEJMoa1606599.
230. Peker, Y.; Glantz, H.; Eulenburg, C.; Wegscheider, K.; Herlitz, J.; Thunström, E. Effect of Positive Airway Pressure on Cardiovascular Outcomes in Coronary Artery Disease Patients with Nonsleepy Obstructive Sleep Apnea. The RICCADSA Randomized Controlled Trial. *Am. J. Respir. Crit. Care Med.* **2016**, *194*, 613–620, doi:10.1164/rccm.201601-0088OC.

231. Hedner, J.; Ludger, G. *The Link between Sleep Apnea and Cardiovascular Disease Time to Target the Nonsleepy Sleep Apneics?*; 2001;
232. Barbé, F.; Mayoralas, L.R.; Duran, J.; Masa, J.F.; Maimó, A.; Montserrat, J.M.; Monasterio, C.; Bosch, M.; Lalaria, A.; Rubio, M.; et al. Treatment with Continuous Positive Airway Pressure Is Not Effective in Patients with Sleep Apnea but No Daytime Sleepiness: A Randomized, Controlled Trial. *Ann. Intern. Med.* **2001**, *134*, 1015–1023, doi:10.7326/0003-4819-134-11-200106050-00007.

Acknowledgment

I would like to express my sincere gratitude to my supervisor, PD Dr. med Tobias Petzold, for giving me the opportunity to join his Lab at LMU Hospital and for his continuous reinforcement to excel in every task and diligently meet deadlines throughout my Ph.D. journey. I was taught how to be independent and to do everything by myself. This thesis would have not been promising without his adamant guidance. I would also like to thank my TAC members, Prof. Sperandio and Prof. Markus Moser for their valuable input and comments on my project. I truly appreciate all the generous support and warm encouragement of Prof. Sperandio throughout my very stressful times by making my Ph.D. journey productive and motivating.

I would offer my deepest appreciation to Dr. Verena Kochan, my IRTG coordinator, and Dr. Antje Hentrich, the head of MMRS, because of their trusty integrity and selfless devotion to both my personal and academic progress. Thank you for answering my countless questions and inquiries wisely, for trusting me, and for being very understanding with me over the years.

It was a pleasure to be a member of IRTG914, DZHK, DGK, and AG19 groups. I am grateful for the many collaborations I had with different labs in Barcelona, Munich, and Düsseldorf. I am thankful for conducting my research in a thriving Lab and for meeting amazing colleagues (Badr, Ainee, Yifan, Afra, etc.) and vets. Special big thanks to my dearest technicians who saved me in my hardest times and time-limited experiments: Elisabeth, Cuong, Anna, Zeljka, Dominik, and Michael. I would like to also thank my Lab members for participating in this project especially Manuella Thienel for writing the ethical amendments in German, Zhe Zhang mainly for helping in intravital microscopy, CXCR4 ablation and LFA-1 experiments done in Barcelona, and the medical student Evan Maroulis for helping with carotid artery experiments and writing amendments in German. I would like to thank Dr.med. Pontus Mertsch and Dr.med. Dieter Munker at LMU-Innenstadt, who helped with recruiting OSA patients and taking blood samples.

My greatest acknowledgment goes to my wonderful friends (Kritika, Mya, Mirna, and Youmna) for their endless support and encouragement that empowered me to face stress, depression, and difficulties throughout my Ph.D. journey.

Lastly, I would like to dedicate my work to **every single member of my great family** for being there for me at all times, for believing in what I do, for all their prayers, and for their unconditional and infinite love. I am truly blessed to have you in my life. Sorry that to complete my Ph.D., I had to miss the moments that I should have otherwise been spending with you. You are my ultimate source of endless support and inspiration. Thank you for saving me from falling into a deep depression and for consistently encouraging me to persist until I reach my goals. Sylvester Stallone expresses it the best.

“You, me, or nobody is gonna hit as hard as life; but, it ain’t about how hard you hit. It’s about how hard you can get hit and keep moving forward. How much you can take and keep moving forward.”

- Sylvester Stallone (Rocky Balboa)

Affidavit

| | | | | |
|---|---|---|---|---|
|  | LUDWIG- MAXIMILIANS- UNIVERSITÄT MÜNCHEN | Promotionsbüro Medizinische Fakultät |  |  |
|---|---|---|---|---|

Affidavit

El Nemr, Shaza

Surname, first name

Marchioninistraße 15

Street

81377, München, Germany

Zip code, town, country

I hereby declare, that the submitted thesis entitled:

**" Investigating Neutrophil-driven Thrombopoiesis in Cardiovascular/Inflammatory Diseases:
Intermittent Hypoxia and Myocardial Infarction"**

.....
is my own work. I have only used the sources indicated and have not made unauthorised use of services of a third party. Where the work of others has been quoted or reproduced, the source is always given.

I further declare that the dissertation presented here has not been submitted in the same or similar form to any other institution for the purpose of obtaining an academic degree.

Munich, 25.07.2024

place, date

Shaza El Nemr

Signature doctoral candidate

Confirmation of congruency



LUDWIG-
MAXIMILIANS-
UNIVERSITÄT
MÜNCHEN

Promotionsbüro
Medizinische Fakultät



**Confirmation of congruency between printed and electronic version of
the doctoral thesis**

El Nemr, Shaza

—

Surname, first name

Marchioninistraße 15

Street

81377, München, Germany

Zip code, town, country

I hereby declare, that the submitted thesis entitled:

**" Investigating Neutrophil-driven Thrombopoiesis in Cardiovascular/Inflammatory Diseases:
Intermittent Hypoxia and Myocardial Infarction"**

is congruent with the printed version both in content and format.

Munich, 25.07.2024

place, date

Shaza El Nemr

Signature doctoral candidate